

UNIVERSIDAD NACIONAL DE COLOMBIA



Applications to the semiclassical propagator of the Wigner function

Dissertation

Author:

Edgar Arturo Gómez González
code: 183147

Thesis advisor:

Dr. Thomas Dittrich

FACULTY OF SCIENCE
DEPARTMENT OF PHYSICS
BOGOTÁ D.C, COLOMBIA
2010

*Dedicated to my parents, Elkin and Luz Amparo,
and my darling Diana.*

Abstract

This thesis is focused on semiclassical studies of Wigner propagator, more precisely, two semiclassical methods are considered, one based on van Vleck approach which leads to the concept of trajectory pairs in phase space, it is surprisingly accurate in significantly nonlinear system. The other corresponds to a uniform approximation for the Wigner propagator in the framework of phase-space path integrals. In this way, several difficulties as caustics in phase space and lack of normalization associated to the semiclassical propagator are overcome. This work also emphasizes on numerical applications to the semiclassical Wigner propagation. In order to test the performance of these semiclassical methods the wave packets dynamics and semiclassical propagation in presence of strong quantum effects are considered.

Acknowledgments

I would like to thank my thesis advisor, Dr. T. Dittrich, without whose support and encouragement completion of this dissertation would not have been possible.

I would like to express my thanks to Leonardo Pachón for many inspiring discussions and suggestions during my studies at the Universidad Nacional de Colombia. Moreover, I am much obliged to other members of the group (*Grupo de Caos y Complejidad*) for many discussions and their wonderful company both inside and outside of the office.

I am very grateful to the Volkswagen Foundation, Universidad Nacional de Colombia and ALECOL program of the German Academic Exchange Service DAAD, for their financial support during my research, also I thank for the hospitality extended to me by Technical University Kaiserslautern, where part of this work has been carried out. I would like to express my sincere thanks to Dr. H. J. Korsch for a lot of inspiring discussions and suggestions during my visit to his research group (*Theoretical Quantum Dynamic's group*), moreover extend my thanks to all members of this group.

I extend my sincere thanks to Luis Sandoval, Saravana Prakash and Cemal Engin by their collaboration and unquestioning help in many aspects and interesting discussions during my visit to Germany.

Last but not least, I would like to thank sincerely to my family, to Diana and her family too, for their lifelong encouragement and support of my studies and everything else they have done for me over the years. Without their help, I would not have been able to not only finish but even start the research leading to this thesis.

Edgar A. Gómez González

Contents

1	Introduction	1
1.0.1	The state of art of semiclassical propagation.	3
2	Quantum dynamics	5
2.1	Wigner function.	5
2.2	Moyal equation.	7
2.3	Properties of the Wigner function.	8
3	Wigner function propagator	11
3.1	Weyl propagator.	11
3.1.1	Properties: Weyl propagator.	11
3.2	Wigner propagator.	13
3.2.1	Properties: Wigner propagator.	14
3.2.2	Markovian properties of the Wigner propagator.	15
3.3	Exact Wigner propagator.	18
3.4	Models.	19
3.4.1	Morse Oscillator.	19
3.4.2	Quartic double well.	21
3.5	Autocorrelation functions.	21
3.6	Numerical applications.	23
4	Semiclassical Wigner function propagator	27
4.1	Semiclassical Wigner propagator from van Vleck's approach.	29
4.2	Algorithms for the semiclassical propagation.	31

4.2.1	Propagating delta functions.	31
4.2.2	Propagating smooth initial states.	32
4.2.3	Single time step.	33
4.3	Numerical applications.	34
4.3.1	Propagating stationary states	38
4.3.2	Propagating Schrödinger cats.	42
4.3.3	Propagation in the presence of classical chaos	43
4.4	Perturbation theory and the semiclassical propagator.	45
5	Midpoints distribution and Random numbers	49
5.1	Generating Random Numbers.	50
5.2	Computing the exact midpoints distribution: Algorithms.	50
5.2.1	Gaussian distributions.	51
5.2.2	Example: Gaussian state.	53
6	Wigner propagator from phase-space path integrals	55
6.1	Weyl propagator for small time step.	55
6.2	Semiclassical Limit.	57
6.3	Complex trajectories.	58
7	Semiclassical Wigner propagator from phase-space path integrals	61
7.1	Semiclassical Wigner propagator.	61
7.2	Analytical expression for the Wigner propagator.	64
7.2.1	Asymptotic limits $t \rightarrow 0$, $\hbar \rightarrow 0$	65
7.2.2	Harmonic oscillator.	66
7.2.3	Semiclassical Wigner propagator and the asymptotic limits.	67
7.2.4	Path-integral approach for weak cubic nonlinearity.	67
7.3	Numerical applications.	68
8	Semiclassical Wigner propagator and tunneling.	75
8.1	Semiclassical description of tunneling.	76
9	Conclusions and perspectives.	81

A Weyl Formalism.	83
B Simplified action for Wigner-van Vleck propagator.	89
C Box Müller Method.	93

List of Figures

1.1	Semiclassical Approximations: van Vleck-Gutzwiller (VVG), Herman-Kluk (HK), Frozen Gaussian Approx. (FGA), Thawed Gaussian Approx. (TGA), Cellular-Dynamics (CD), Integral-Expressions (IE), Coherent States propagator (K_{cs}), Coherent States propagator with mixed-boundary conditions (\bar{K}_{cs}), Wigner propagator (G_W), Wigner-van Vleck propagator (G_{WV}), Wigner-Path Integrals propagator (G_{WPI}).	3
3.1	Time evolution of the Wigner propagator for a Morse potential. The quantum calculations are shown as a sequence of times, $t = 0$ (panel a), 0.5072 (b), 1.0144 (c), 1.5216 (d), 2.0288 (e), 2.536 (f). The underlying classical trajectory has been launched at $\mathbf{r}_0 = (-0.1, 0)$. Parameter values are $D = 1$, $\alpha = 1.25$, $\hbar = 0.005$. Color code ranges from red (negative) through white (zero) through blue (positive).	24
3.2	Time evolution of an initial Wigner function (Gaussian state) in the Morse potential. The quantum calculations are shown as a sequence at times $t = 0$ (panel a), 0.5072 (b), 1.0144 (c), 1.5216 (d), 2.0288 (e), 2.536 (f). In panel a, some contour lines of the potential are shown superimposed. The underlying classical trajectory has been launched at $\mathbf{r}_0 = (-0.1, 0)$. Parameter values are $D = 1$, $\alpha = 1.25$, $\hbar = 0.005$	25
4.1	Berry's construction of chord rule in phase space: $A_j(\mathbf{r}'_j, t)$ corresponds to the symplectic area associated to \mathbf{r}'_j classical trajectory.	29
4.2	Symplectic areas entering in the semiclassical Wigner propagator. The $A_{j\pm}$ are the phases of the Weyl propagators and A_j is the area enclosed between the classical trajectories. The dashed line is the classical trajectory $\mathbf{r}^{cl}(\mathbf{r}', t)$, full line is the propagation path $\bar{\mathbf{r}}(\mathbf{r}', t)$ connecting the initial and final arguments of propagator.	30

- 4.3 Initial phase space points covering smooth initial distribution, An ensemble of random points \mathbf{r}'_j ($j = 1, 2, \dots, N$) serves as initial conditions for N classical trajectories, give rise to $(N(N - 1)/2)$ midpoint paths starting in the centers $\bar{\mathbf{r}}'_{jk} = (\mathbf{r}'_j + \mathbf{r}'_k)/2$ (red dots) and defines the support for the semiclassical Wigner propagator 33
- 4.4 Time evolution of the Wigner propagator in the Morse potential from semiclassical approximation at times, $t = 0$ (panel a), 0.5072 (b), 1.0144 (c), 1.5216 (d), 2.0288 (e), 2.536 (f). The underlying classical trajectory has been launched at $\mathbf{r}_0 = (-0.1, 0)$. Parameter values are $D = 1$, $\alpha = 1.25$, $\hbar = 0.005$. Color code ranges from red (negative) through white (zero) through blue (positive). . . . 35
- 4.5 Time evolution of an initial Wigner function (Gaussian state) in the Morse potential for the semiclassical approximation at times $t = 0$ (panel a), 0.5072 (b), 1.0144 (c), 1.5216 (d), 2.0288 (e), 2.536 (f). In panel a, some contour lines of the potential are shown superimposed. The underlying classical trajectory has been launched at $\mathbf{r}_0 = (-0.1, 0)$. Parameter values are $D = 1$, $\alpha = 1.25$, $\hbar = 0.005$ 36
- 4.6 Comparison of time-evolved Wigner initial state (black contour lines), from semiclassical Wigner van-Vleck propagator (panel a) and to the exact quantum calculation (panel b). 37
- 4.7 Autocorrelation function for a Gaussian initial state in a Morse potential, for the semiclassical Wigner propagator (dashed line, red color) as compared to an exact quantum result (full line, blue color), and classical calculation (dotted line, black color) for a time involving exactly four periods of the underlying classical trajectory. 37
- 4.8 Wigner representation of the ground state $n = 0$ (panel a) and the second excited state $n = 2$ (panel b) of the Morse potential (dotted contour lines), compare to the classical orbits at the corresponding eigenenergies E_n . Parameter values are $D = 1$, $\alpha = 1.25$, $\hbar = 0.005$ 39
- 4.9 Wigner representation of the second excited state of the Morse oscillator. (contours are represented as black dotted lines), compared to the classical orbit $\mathbf{r}_{E_2}^{\text{cl}}(t)$ at the corresponding eigenenergy E_2 (full line, red) and to midpoint paths $\bar{\mathbf{r}}_j(t) = [\mathbf{r}_{j-}^{\text{cl}}(t) + \mathbf{r}_{j+}^{\text{cl}}(t)]/2$ (\times -symbol, red) for pairs of classical trajectories $\mathbf{r}_{j\pm}^{\text{cl}}(t)$ (dashed lines, red), with common initial midpoint $\bar{\mathbf{r}}'_j = \mathbf{r}_{E_2}^{\text{cl}}(0)$ but increasing initial separation $\check{\mathbf{r}}'_j \equiv (\check{p}'_j, \check{q}'_j) = \mathbf{r}'_{j+} - \mathbf{r}'_{j-}$ with $\check{p}'_j = 0$ and $\check{q}'_j = 0.002, 0.2, 0.24, 0.26$ (see text). Parameter values are $D = 1$, $a = 1.25$, $\hbar = 0.005$ 39

- 4.10 Semiclassical Wigner-van Vleck propagator (panel a) and the corresponding quantum result (panel b) for the Morse potential at time $t = 1.5216$. They are compared to the classical orbit $\mathbf{r}_{E_2}^{cl}$ and the contours of the Wigner-eigenstate. The initial point $\mathbf{r}' = \mathbf{r}^{cl}(0)$ is the same as Fig. 4.9. Parameter values are $D = 1$, $\alpha = 1.25$, $\hbar = 0.005$ 40
- 4.11 Deviation of autocorrelation function from exact value 1 (quantum calculation) for second excited eigenstate in the Morse potential. The parameter values are the same as Fig. 4.9. 41
- 4.12 Cross section at $q = 0$ of the Wigner eigenfunction $W_2(\mathbf{r})$ at time $t = 10$. The quantum result (full line, blue) as compare to classical calculation (dotted line, black color) and the semiclassical Wigner van Vleck propagation (dashed line, red color). 41
- 4.13 Accuracy of the autocorrelation function for the ground state $W_0(\mathbf{r})$ of the Morse oscillator (equivalent to the norm conservation) propagated with the semiclassical approximation to the Wigner propagator (dashed line, red color), a deterministic flow along Wigner trajectories (full line, green color), and the classical Liouville's propagator (dotted line, black color, data taken from Ref. [LS82]), at discrete times running from $t = 0$ through 2 by steps of 0.1. The values stated are the deviations from the exact value 1. Parameter values are $D = 0.15$, $a = 1$, $\hbar = 1.0$ 42
- 4.14 Schrödinger-cat states time-evolved in the Morse potential at time $t = 0.3$. The exact quantum calculation (panel a) as compare to semiclassical propagation from Wigner van Vleck propagator (panel a). Parameter values are $m = 0.5$, $D = 1$, $\alpha = 1.25$, $\hbar = 0.005$. The initial midpoint and separation of the Schrödinger-cat are $(q_0, p_0) = (0.3, 0)$, $d = 1$, respectively. 43
- 4.15 Autocorrelation function for two coupled Morse potentials (4.24) at $c = 0.3$. Parameter values are $m = 0.5$, $D = 1$, $a = 1.25$, $\hbar = 0.125$, the initial centroid is $(q_{10}, p_{10}, q_{20}, p_{20}) = (0.5, -0.3, 0.4322, 0)$, corresponding to a total energy $E = 0.5$. Inset: Poincaré surface of section at $p_2 = 0$ of the corresponding classical dynamics. Different initial conditions encoded by colors. The blue circle is the contour of the initial Gaussian enclosing a Planck cell. 44

- 4.16 Different versions of the Wigner propagator for a harmonic oscillator in the regime of weak anharmonicity as a function of final phase-space coordinates (q'', p'') at time $\tau = \pi/3$. Wigner propagator from phase-space path integrals approach (Eq. (X)) (panel a), uniform approximation for short times (Eq. 4.34) (b), exact quantum calculation (Eq. (3.30)) (c), semiclassical approximation based on van Vleck approach (Eq. (4.32) (d)), and the contributions to Eq. (Eq. (4.32) corresponding to hyperbolic (cosine term) (e), and elliptic trajectory pairs (sine term (f)). Parameters values are $\hbar = 0.01$, $\epsilon = 0.2$, $m = 1$, $\omega = 1$. The underlying classical trajectory (full line, red) has been launched at $(0, -0.1)$ 48
- 6.1 Phase space representation of the quartic double well (dashed lines, black). A typical midpoint trajectory based on complex trajectory pairs, the initial point is $(q', p') = (5, 0)$ and $\mathbf{r}'_{\pm} = (5, \pm 0.1)$, $\tilde{\mathbf{R}} = (5, 0.1)$ at time $t = 10$, (full line, red, panel a). Final coordinates of one hundred midpoint trajectories (dots, red, panel b) launched from right side (dot, blue) for the same initial conditions as panel a, except for $\tilde{\mathbf{R}}$ where the values have been choose randomness. Parameter values are $m = 1$, $\Delta = 1$ 60
- 7.1 Time evolution of the Wigner propagator in the Morse potential from semiclassical approximation at times, $t = 0$ (panel a), 0.5072 (b), 1.0144 (c), 1.5216 (d), 2.0288 (e), 2.536 (f). The underlying classical trajectory has been launched at $\mathbf{r}_0 = (-0.1, 0)$. Parameter values are $D = 1$, $\alpha = 1.25$, $\hbar = 0.005$. Color code ranges from red (negative) through white (zero) through blue (positive). . . . 70
- 7.2 Time evolution of an initial Wigner function (Gaussian state) in the Morse potential for the semiclassical approximation based on path integrals at times $t = 0$ (panel a), 0.5072 (b), 1.0144 (c), 1.5216 (d), 2.0288 (e), 2.536 (f). In panel a, some contour lines of the potential are shown superimposed. The underlying classical trajectory has been launched at $\mathbf{r}_0 = (-0.1, 0)$. Parameter values are $D = 1$, $\alpha = 1.25$, $\hbar = 0.005$ 71
- 7.3 Time-evolved quantum spot from semiclassical Wigner-van Vleck propagator Eq. (??) (panel a) as compared with semiclassical approximation for Wigner propagator based on phase-space path integrals Eq. (7.11) (panel b) at time $t = 10$. The classical trajectory underlying with initial point $(q', p') = (-0.1, 0)$ is superimposed. Parameter values are $D = 1$, $\alpha = 1.25$, $\hbar = 0.005$ 72
- 7.4 Autocorrelation function for an initial Gaussian state in the Morse potential, the semiclassical Wigner propagator based on phase-space path integrals (dashed line, red color) compared with the exact quantum result (full line, blue color) and classical calculations (dotted line, black color). Parameter values are $m = 0.5$, $D = 1$, $\alpha = 1.25$, $\hbar = 0.005$ 72

- 7.5 Time evolution of the Wigner propagator in the semiclassical approximation based on phase-space path integration as a function of final phase-space coordinates (q'', p'') for a potential with constant cubic anharmonicity $\sigma(t) = \text{const}$ at times $t = \pi/18$ (panel a), $t = \pi/3$ (b), $t = \pi$ (c), $t = 2\pi - 0.3$ (d). The underlying classical trajectory has been launched at $(q', p') = (0, -0.1)$. Parameters value are $m = 1$, $\omega = 1$, $\hbar = 1$, $\epsilon = 0.2$. Color code ranges from red (negative) through white (zero) through blue (positive). 73
- 8.1 Semiclassical description of coherent tunneling in terms of trajectory pairs, in the framework of the Wigner van Vleck propagator. A wave packet initially prepared near the right minimum of a double-well potential (blue patch) can be transported along a non-classical midpoint path $\bar{\mathbf{r}}(t)$ (dashed red line) into the opposite well if the two classical orbits $\mathbf{r}_{\pm}^{\text{cl}}(t)$ (full red lines) underlying this path through $\bar{\mathbf{r}}(t) = (\mathbf{r}_{-}^{\text{cl}}(t) + \mathbf{r}_{+}^{\text{cl}}(t))/2$ are sufficiently separated initially, e.g., $\mathbf{r}_{+}^{\text{cl}}$ on the same side but above the barrier, $\mathbf{r}_{-}^{\text{cl}}$ within the opposite well. Other contours of the potential and the separatrix are indicated by black curves. 76
- 8.2 Time evolution of initial Gaussian state in the quartic double well (contour lines in panel a) from semiclassical Wigner propagator at times $t = 0$ (panel a), $t = 3$ (b), $t = 6$ (c), $t = 9$ (d), $t = 12$ (e), $t = 15$ (f). The full red line is the classical trajectory the initial state $(q_0, p_0) = (0, 2)$. Parameter values are $m = 1$, $\Delta = 6$ 78
- 8.3 Time-evolved semiclassical propagator of the Wigner function (panel a) and the corresponding exact quantum propagator (panel b) for the quartic double well at time $t = 15$ with energy $E = 1.0026$. Parameter values are $m = 1$, $\Delta = 6$ 79
- 8.4 Autocorrelation function for a Gaussian initial state in a quartic double well at an energy $E = 1.0026$ above the barrier top, the semiclassical approximation based on Wigner van Vleck propagator (dashed line, red color) as compare to an exact quantum result (full line, blue color) and classical calculation (dotted line, black color). The initial Gaussian state is $(q_0, p_0) = (0, 2)$. The inset shows non-conservation norm along time evolution, where N denotes the integral of the Wigner function over all phase space. Parameter values are $m = 1$, $\Delta = 6$ 79
- 8.5 Time-evolved state, initially prepared as Gaussian state at time $t = 5$ in the quartic double well, semiclassical approximation based on Wigner van Vleck propagator (panel a) and the corresponding exact quantum calculation (panel b) with energy $E = -0.958$. Parameter values are $m = 1$, $\Delta = 6$ 80

- 8.6 Autocorrelation function for a Gaussian initial state in a quartic double well at an energy $E = -0.958$ below the barrier top, the semiclassical approximation based on Wigner van Vleck propagator (dashed line, red color) as compare to exact quantum result (full line, blue color) and the classical calculation (dotted line, black color). The initial Gaussian state is $(q_0, p_0) = (2, 0)$. Parameter values are $m = 1, \Delta = 6$ 80

List of Tables

- 2.1 Comparison between classical and quantum mechanics (Hilbert-space and phase-space representations). First line corresponds to usual product of two observables. Brackets (P : Poisson. M : Moyal) are shown in the second line. Evolution equations in Heisenberg and Schrödinger representations are presented in third line and fourth line respectively. Fifth line shows the expressions for mean value of an observable. Sixth line is the representation for a pure state 6

Chapter 1

Introduction

One of the most exciting areas of physics is semiclassical physics. Since decades, it has been considered as the borderline between classical and quantum world. In general, semiclassical physics is dedicated to develop theoretical tools to understand the features of classical behavior that emerge into quantum scale and related phenomena. Perhaps, the first attempt on semiclassical study began with WKB theory, later it has been extended to chaotic systems with the EBK-approximation. In fact, those studies established the relevance and ability of semiclassical approximations as a bridge between both theories. For instance, the discovery of the so-called Gutzwiller trace formula [Gut91, Gut43] that relates the quantum energy levels with purely classical quantities of the system. On the other hand, semiclassical methods in time-domain have been successfully applied to study chaotic billiards [Lib30] also other quantum studies have provided a strong evidence of localization in the semiclassical limit [Kap98]. In recent years, attention has focussed on semiclassical approximations continue to grow rapidly, and it is not only in theoretical aspects but also have plagued practically all branches of physics. Their possible applications are renewed constantly by numerical simulations and experimental realizations, which confirms many of those theoretical predictions. Particularly, in the context of quantum chaos several achievements have been obtained by a direct observation of quantum phenomena in the semiclassical domain as chaos-assisted tunneling [DASR74], dynamical tunnelling and localization [WKH*et. al.*52, P*Set. al.*01] with cold atoms.

In connection with semiclassical description of quantum evolution, a lot of important contributions have been obtained in the past. More precisely, van Vleck [Vle78], Maslov [Mas72, Mas81] and Herman-Kluk [HK84] contributions are considered as pioneers in the treatment to semiclassical propagation in terms of classical trajectories. However, only with the advent of the Feynman's path integrals a lot of attention was focused on study of time evolution of the quantum system by time propagators and its semiclassical approximations. In order to understand, how the propagator's formalism is introduced for quantum evolution, let us consider the kernel or propagator $K(\mathbf{q}'', t; \mathbf{q}', 0)$ which is defined in terms of time evolution operator $\hat{U}(t) = \exp(-i\hat{H}t/\hbar)$, for example, the projection on coordinate representation

reads,

$$K(\mathbf{q}'', t; \mathbf{q}', 0) = \langle \mathbf{q}'' | \hat{U}(t) | \mathbf{q}' \rangle. \quad (1.1)$$

Where \hat{H} is the Hamiltonian function of the system, and t corresponds to the propagation time. Thus, the wave function evolve in time from an initial state $\psi(\mathbf{q}', 0)$ following the rule,

$$\psi(\mathbf{q}'', t) = \int_{-\infty}^{\infty} K(\mathbf{q}'', t; \mathbf{q}', 0) \psi(\mathbf{q}', 0) d\mathbf{q}'. \quad (1.2)$$

In principle, the integral representation depicts a simple route to perform the time evolution of an initial state, moreover it allows us formulate differents semiclassical approximations to the exact quantum evolution. However, serious difficulties emerge from those approximations, that are inherent to the representation considered and compromise the ability of the method for capturing quantum features. Indeed, several difficulties were manifested long time ago in the well-known van Vleck-Gutzwiller propagator (VVG).

- *The search root problem:* In position representation, for each pair of coordinates $\mathbf{q}', \mathbf{q}''$ apparently requires to identify the classical trajectories connecting those two points at time t . But, this trajectories are specified as solutions to the Hamilton's equation, *i.e.*, by initial conditions $(\mathbf{q}', \mathbf{p}')$. Therefore, there are special boundary conditions on trajectories that contribute to the propagator. This procedure requires a search of trajectories that fullfill the boundary conditions, even much more difficult for chaotic systems, due to the extreme sensitivity to the classical trajectories.
- *The caustics problem:* The amplitude becomes infinity in singular points, that are called focal points or caustics. Hence, this behavior degrades the approximation and impose serious difficulties to the numerical convergence.

Despite of this, the semiclassical van Vleck-Gutzwiller approach should not be underestimated due to it has served *(i)* as the basis for many semiclassical methods, mainly in position and momentum representations [VM07, BHW01, GC06], *(ii)* important studies about semiclassical description of global phase (Maslov indices) due to caustics [LR87, SLS78, CB94], *(iii)* it has motivated a lot of others approximations that aim to avoid those disadvantages in order to obtain a better performance of semiclassical methods. In fact, the most familiar semiclassical approaches to the quantum propagator are the primitive Cellular-Dynamics (CD), Herman-Kluk (HK) propagator and the so-called Frozen and Thawed Gaussian Approximations (FGA, TGA) and the semiclassical coherents state propagator via path integrals.

The semiclassical propagation scenario might seems to be a broad range and very complicated due to the large number of semiclassical approaches, that in principle have been formulated independently from each others. However, it is not completely true when those methods are considered from a general point of view, namely, *(i)* most of them are based on approximations up to second order in the framework of Gaussian approach. *(ii)* The contribution to the propagation is given in terms of purely classical quantities, *i.e.*, the phases as classical

actions and the amplitudes as stability matrices along of classical trajectories. A number of authors have reported the relationship between some of them [GJ94, Gro99, Kay05]. As well as they have been pointed out by K. Kay in seminal works [Kay94a, Kay94b] from a novel formulation called Integral-Expressions (IE) to the semiclassical propagator. Basically, this approach corresponds to an integral over initial conditions in phase space, together with the *principle of equivalence of the stationary phase method* leads to the well-known semiclassical propagators. More precisely, the Fig. 1.1 shows a schematic description of hierarchy between most of those semiclassical propagators and their representation (see in the left hand side on the figure)

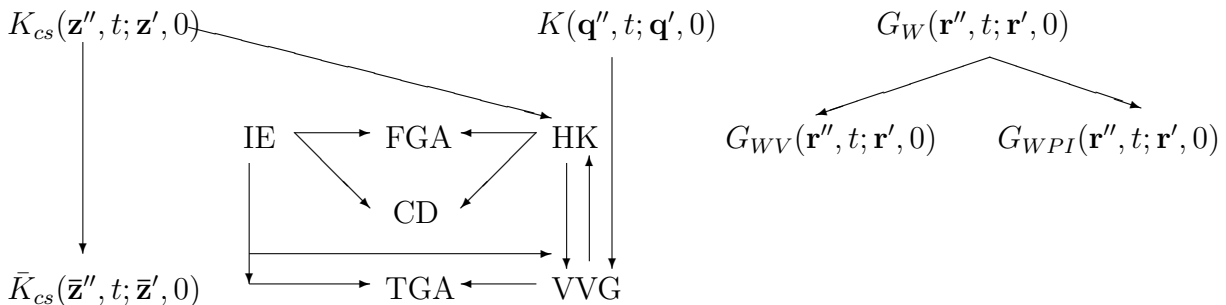


Figure 1.1: Semiclassical Approximations: van Vleck-Gutzwiller (VVG), Herman-Kluk (HK), Frozen Gaussian Approx. (FGA), Thawed Gaussian Approx. (TGA), Cellular-Dynamics (CD), Integral-Expressions (IE), Coherent States propagator (K_{cs}), Coherent States propagator with mixed-boundary conditions (\bar{K}_{cs}), Wigner propagator (G_W), Wigner-van Vleck propagator (G_{WV}), Wigner-Path Integrals propagator (G_{WPI}).

In practice, the performance of those methods are quite different when are capturing the important quantum features, it has been pointed out by number of publications in the framework of semiclassical propagation. For example, see [Gro26, Gro99, TW04, Kay05] and references therein.

1.0.1 The state of art of semiclassical propagation.

In the context of semiclassical propagation and its applications to quantum systems, there exists a vast literature on the same issue. Indeed, the semiclassical methods are an important tool for calculating the dynamics of atoms and molecules, and the popularity of such methods over the past years is evident, in fact, the number of applications grow rapidly in different areas of the physics. However, the performance of the semiclassical approximations have been compromised due to the underlying difficulties in the those approaches that are based directly on classical trajectories. In practice, the semiclassical propagation has to face mainly with the search root problem, caustics along of time evolution, poor convergence of methods and the inefficiency for capturing quantum features. In order to obtain a better performance of the semiclassical approximations and with the intention to avoid most complications it has

been derived a number of semiclassical propagators by considering different representations. Indeed, the most popular propagators are shown in the Fig. 1.1. At the same time, the figure illustrates the current state of the semiclassical propagation in terms of propagators. On the other hand, it is well-known that the semiclassical IVR treatments are considered as favorite approaches due to they can express the quantities to be determined for a given system in terms of classical trajectories, thus initial value representation methods (IVR-method) specify the classical trajectories in the most natural way, *i.e.*, in terms of their initial values. For example, the classical trajectories that need to be run in order to calculate the dynamical evolution of a system can be determined immediately by sampling the phase space occupied by the initial state. In practice, the IVR-methods took advantage of this, therefore they allow an straightforward adaptation of Monte-Carlo Metropolis algorithms for semiclassical propagation.

Since decades, a vast variety of semiclassical methods and their applications in the context of semiclassical propagation have been considered, certainly, a little that is known to date about semiclassical Wigner propagation, and much less as a description in terms of IVR representation. Likely, it is due to the lack of studies about quantum dynamics in phase space in the framework of Wigner-Weyl formalism which is related to the Moyal equation that governs the time evolution of the Wigner functions. However, recent studies [TDS03] in this direction has shown the route to explore in deep the time evolution of quantum systems from Wigner representation, more precisely in terms of semiclassical approximations to Wigner propagator. Therefore, the doors would remain opened for all kinds of research directly in phase space, starting with these semiclassical approximations and enabling new approaches and generalizations. The Fig. 1.1 shows at the right hand side, the schematic description of hierarchy of Wigner propagator and its semiclassical approximations. Indeed, we can be sure that the scenario of semiclassical Wigner propagation is just beginning.

This work has been organized as follows: The chapter two presents a review of the quantum dynamics in phase space, more precisely, an introduction to the mathematical formalism for the Wigner function and its properties. The chapter three describes an integral representation for time evolution to the Wigner function in terms of the Weyl propagator. Followed by a description of the exact Wigner propagator, moreover it discuss the first part of numerical applications. The chapter four describes the semiclassical Wigner-van Vleck propagator and the corresponding numerical applications. The chapter five discusses suitable numerical algorithms for semiclassical propagation of initial states. The chapter six introduces the phase-space path integral formalism. The next chapter we considers the semiclassical approximation to the Wigner propagator based on phase-space path integrals, so it is shown how under this approach it is possible to include a high order in approximation. Similarly, as in the preceding chapters the corresponding numerical application are considered. In this way, it is compared the performance of the semiclassical approximations to quantum approach. The last chapter is dedicated to study the tunneling phenomenon from semiclassical Wigner propagator.

Chapter 2

Quantum dynamics

The present chapter review the main properties of the Wigner function as well as the mathematical formalism about of quantum dynamics in phase space, which brings out clearly the differences and similarities between classical and quantum mechanics.

2.1 Wigner function.

The Wigner distribution function, a pioneer work was introduced in 1932 by E. P. Wigner [Wig49], in which he showed the possibility to describe the quantum systems in terms of distribution functions in phase space. Following his ideas, numerous physical applications have been found, for example, the Wigner function has been useful for describing quantum transport [JVLH32], nuclear physics, decoherence, quantum computation and quantum chaos. It is also plays a important role in signal processing and mathematics. Perhaps, the most important contribution in order to develop the complete theory of quantum mechanics in phase space was presented in a early work developed by J. E. Moyal in [Moy99], followed by important contributions in which the mathematical foundations were established [Wey27, Wey31, Gro05]. Additionally, various aspects of the phase-space formalism for quantum mechanics have been developed by several authors. More extensive list of literature on this subject can be found in excellent reviews [RFO21, RFO45, MH21, Lee47]. Besides the Wigner function others phase-space functions have been considered in the literature. In particular, the Husimi distribution (sometimes called Q-function) [Kan13] and the Glauber-Sudarshan P-function [Gla66, Sud77] have found extensive applications in quantum optics. Moreover, the quantum phenomena becomes transparent when it is viewed from phase space description and many experiments have been confirmed that the distribution functions are useful tool and brings out striking properties of the quantum states [Sch01, CZC05, Sch96]. However, we focus on Weyl-Wigner formalism (see Appendix A) due to that in this framework the Wigner function takes a complete mathematical operativity and many important properties arise in contrast to others distribution functions in phase space.

In fact, there is not a simple coincidence between quantum mechanics in phase space and the statistical classical mechanics, because the Wigner distribution function was proposed in such a way that from mathematical point of view, both theories shared special features. Thus, its formalism takes into account all requirements of the quantum mechanics. For example, the Heisenberg's uncertainty principle is manifested in phase space as a restriction on the size occupied by the quantum state. Furthermore, it is the representation of quantum mechanics in phase space which is the most symmetrical of all, because it relates correctly the operators in a Hilbert space with distributions functions in phase space. The table 2.1 shows a comparison between classical, Hilbert and phase-space representations of quantum mechanics.

Classical Mechanics	Quantum mechanics: Hilbert space	Quantum mechanics: Phase space
$A(q, p)B(q, p)$	$\hat{A}\hat{B}$	$A(q, p) \star B(q, p) \quad \star := \exp\left\{\frac{i\hbar}{2}(\overleftarrow{\partial}_q \overrightarrow{\partial}_p - \overleftarrow{\partial}_p \overrightarrow{\partial}_q)\right\} \quad \S$
$\{A(q, p), B(q, p)\}_P = A(q, p)(\overleftarrow{\partial}_q \overrightarrow{\partial}_p - \overleftarrow{\partial}_p \overrightarrow{\partial}_q)B(q, p)$	$[\hat{A}, \hat{B}] = \hat{A}\hat{B} - \hat{B}\hat{A}$	$\{A(q, p), B(q, p)\}_M = \frac{2}{\hbar} A(q, p) \sin\left\{\frac{\hbar}{2}(\overleftarrow{\partial}_q \overrightarrow{\partial}_p - \overleftarrow{\partial}_p \overrightarrow{\partial}_q)\right\} B(q, p)$
$\partial_t A = \{A, H\}_P$	$\partial_t \hat{A} = \frac{1}{i\hbar}[\hat{A}, \hat{H}]$	$\partial_t A = \{A, H\}_M$
$\partial_t \rho = \{H, \rho\}_P$	$\partial_t \hat{\rho} = \frac{1}{i\hbar}[\hat{H}, \hat{\rho}]$	$\partial_t W = \{H, W\}_M$
$\bar{A} = \int_{-\infty}^{\infty} A(q, p)\rho(q, p)dqdp$	$\bar{A} = Tr(\hat{A}\hat{\rho})$	$\bar{A} = \int_{-\infty}^{\infty} A(q, p)W(q, p)dqdp$
$\rho(q, p) = \delta(q - q(t))\delta(p - p(t))$	$\hat{\rho} = \psi\rangle\langle\psi $	$W(q, p) = \frac{1}{2\pi\hbar} \int_{-\infty}^{\infty} e^{-\frac{ipy}{\hbar}} \psi(q + \frac{y}{2})\psi^*(q - \frac{y}{2})dy$

§ The symbol \star is called star product.

Table 2.1: Comparison between classical and quantum mechanics (Hilbert-space and phase-space representations). First line corresponds to usual product of two observables. Brackets (P : Poisson. M : Moyal) are shown in the second line. Evolution equations in Heisenberg and Schrödinger representations are presented in third line and fourth line respectively. Fifth line shows the expressions for mean value of an observable. Sixth line is the representation for a pure state

A look into the representation of quantum mechanics in phase space resembles the classical mechanics. For example, the description of a state in classical mechanics is given by a classical distribution function, but this state in quantum mechanics is represented by the Wigner function. Also, the classical dynamics is governed by Poisson bracket in contrast to quantum case where the dynamics is given in terms of Moyal equation (see section 2.2). According to the correspondence principle, the classical world should emerge from the quantum world whenever Planck's constant \hbar is negligible, however, sometimes these similarities can be more evident or apparently contradictory as it pointed out by M. Berry in[Ber01].

The semiclassical physics has not only theoretical interest, but also technological too, in consequence a number of research groups have focused on to study the links between classical and quantum physics

Lets start considering the density operator $\hat{\rho}$ which contains all physical information of the quantum system, in this sense, it can be depicted as a pure or mixed state, in order to introduce a formal definition of the Wigner function, we consider the Weyl transform of the density operator,

$$W(p, q) = T_W \left[\frac{\hat{\rho}}{2\pi\hbar} \right]. \quad (2.1)$$

For an arbitrary operator \hat{A} the Weyl transform is defined as:

$$T_W[\hat{A}](p, q) = \int_{-\infty}^{\infty} \exp\left\{ -\frac{i}{\hbar}py \right\} \langle q + \frac{y}{2} | \hat{A} | q - \frac{y}{2} \rangle dy. \quad (2.2)$$

While considering the density operator represents a pure state $\hat{\rho} = |\psi\rangle\langle\psi|$, we obtain well-known expression for the Wigner function,

$$W(q, p) = \frac{1}{2\pi\hbar} \int_{-\infty}^{\infty} \exp\left\{ -\frac{i}{\hbar}py \right\} \psi(q + y/2) \psi^*(q - y/2) dy. \quad (2.3)$$

The previous expressions for the Wigner function were obtained in terms of position representation, but the momentum representation can also be used for this purpose. Thus, this formalism has an evident symmetry between canonical variables in phase space as it is the case of classical mechanics.

2.2 Moyal equation.

Quantum dynamics studies at the beginning with J. E. Moyal [Moy99] proposed an alternative for the time evolution of the Wigner functions. Basically, they are governed by a partial differential equation involving the classical Hamiltonian besides canonical variables in phase space. We show the connection between Schrödinger's picture and the Moyal equation: First, we operate on both sides of Eq. (2.3) with $\partial/\partial t$. When this operator acts on the wave function (or its conjugate) in the integrand, we use the Schrödinger time-dependent equation to replace the terms $\partial\psi/\partial t$ by $(-i/\hbar)\hat{H}\psi$. After integrating by parts, we have that the terms $-\nabla^2\psi$ lead to the terms $(-p/m)\partial W/\partial q$. In addition to this, the potential energy takes the form as $[U(q + y/2) - U(q - y/2)]$, and it will be expanded around the point q in a Taylor series. Finally, after some algebraic manipulations, it is straightforward to obtain the so-called *Moyal's equation*,

$$\frac{\partial W}{\partial t} = -\frac{p}{m} \frac{\partial W}{\partial q} + \frac{\partial U}{\partial q} \frac{\partial W}{\partial p} + \sum_{k=1}^{\infty} \frac{(-\hbar^2/4)^k}{(2k+1)!} \frac{\partial^{2k+1} U}{\partial q^{2k+1}} \frac{\partial^{2k+1} W}{\partial p^{2k+1}}. \quad (2.4)$$

Indeed, this equation suggests a link between classical and quantum mechanics, in particular, if the "quantum terms" involving explicitly \hbar vanishes, the Wigner function corresponds to

the classical distribution W_{cl} which is non-negative at every point in phase space, and the dynamics is reduced formally to the *Liouville equation*,

$$\frac{\partial W_{cl}}{\partial t} = -\frac{p}{m} \frac{\partial W_{cl}}{\partial q} + \frac{\partial U}{\partial q} \frac{\partial W_{cl}}{\partial p}. \quad (2.5)$$

The Moyal equation is exact, but it has infinity number of quantum contributions represented as powers of \hbar . In fact, there are no easy task to perform analytical solutions or numerical methods in which those all quantum contributions can be included. However, a lot of work has been addressed on time evolution of the Wigner function based on this approach [Fai81, Eft33, TAO79]. In order to surmount these difficulties some authors have explored semiclassical approaches to the Moyal equation, however, a relevant discussion about time evolution of Wigner function were considered long time ago by E. Heller in a seminal work [Hel89, EJM48]. He argued that the semiclassical propagation of the Wigner function fail and it cannot be possible due to quantum interferences. However, recent studies in the context of semiclassical approximations in phase space have shown that we must be careful in the semiclassical limit as was point out by T. Dittrich *et al.* [TDS03], where he solved the Heller's objections.

2.3 Properties of the Wigner function.

In order to present self-contained the Wigner formalism in phase space, this section is dedicated to review the main properties of the Wigner function, for more details see [Sch01] and references therein.

- The hermiticity of the density operator guarantees the real-valuedness for the Wigner function, *i.e.* $W(q, p) \in \text{Re}$.
- The Wigner function is normalized in phase space, $|W(q, p)| \leq \frac{1}{\pi\hbar}$, the equal sign holds only for pure state.
- The correct probability distributions are obtained by projecting on position or momentum representation the Wigner function.

$$\int_{-\infty}^{\infty} W(q, p) dp = |\psi(q)|^2,$$

$$\int_{-\infty}^{\infty} W(q, p) dq = |\psi(p)|^2.$$

- Lets be two density operators $\hat{\rho}_1$ and $\hat{\rho}_2$ then the trace operation in phase space reads,

$$\text{Tr}(\hat{\rho}_1 \hat{\rho}_2) = 2\pi\hbar \int_{-\infty}^{\infty} W_{\psi_1}(q, p) W_{\psi_2}(q, p) dp dq,$$

if these density operators are associated to pure states ¹ we have,

$$|\langle \psi_1 | \psi_2 \rangle|^2 = 2\pi\hbar \int_{-\infty}^{\infty} W_{\psi_1}(q, p) W_{\psi_2}(q, p) dp dq,$$

in consequence of the previous property, if we have orthogonal states ψ_1, ψ_2 the Wigner functions are orthogonal too, therefore we have the following property

$$\int_{-\infty}^{\infty} W_{\psi_1}(q, p) W_{\psi_2}(q, p) dp dq = 0.$$

Moreover, this condition enforces that the Wigner functions $W_{\psi_1}(q, p)$ or $W_{\psi_2}(q, p)$ must take negative values in phase space. This is the fact why sometimes it is called a *quasi-distribution* probability. Concerning to the features associated to the negativity of the Wigner functions, several authors have addressed and discussed the quantum implications of that, see for example [SEC04, Ken96].

- The size of the Wigner function is bounded, lets consider two density operators $\hat{\rho} = \hat{\rho}_1 = \hat{\rho}_2$, then by the trace property in phase space we have,

$$Tr(\hat{\rho}^2) \leq 1,$$

where the equal sign holds for pure states. Thus, it is straightforward shows that

$$2\pi\hbar \leq \frac{1}{\int_{-\infty}^{\infty} W(q, p)^2 dp dq}.$$

The previous equation shows that for a pure state the Wigner function occupy an area in phase space given by $2\pi\hbar$, whereas for mixed states the corresponding area is larger.

- The Wigner function has the following momentum properties,

$$\begin{aligned} \int_{-\infty}^{\infty} \int_{-\infty}^{\infty} q^n W_{\psi}(q, p) dq dp &= \int_{-\infty}^{\infty} q^n |\psi(q)|^2 dq, \\ \int_{-\infty}^{\infty} \int_{-\infty}^{\infty} p^n W_{\psi}(q, p) dq dp &= \int_{-\infty}^{\infty} p^n |\psi(p)|^2 dp. \end{aligned}$$

- The multiplication property is expressed in phase space in terms of the Wigner function: Lets be $\phi(q), \varphi(q)$ two functions in position representation which follows $\psi(q) = \phi(q)\varphi(q)$ then,

$$W_{\psi}(q, p) = \int_{-\infty}^{\infty} W_{\phi}(q, \bar{p}) W_{\varphi}(q, p - \bar{p}) d\bar{p}. \quad (2.6)$$

¹This notation indicates that the Wigner functions is:

$$W_{\psi}(q, p) = \frac{1}{2\pi\hbar} \int_{-\infty}^{\infty} \exp\left\{-\frac{i}{\hbar}py\right\} \psi\left(q + \frac{y}{2}\right) \psi^*\left(q - \frac{y}{2}\right) dy.$$

- The convolutive property can be expressed in phase space in terms of the Wigner function: Lets be $\phi(q)$, $\varphi(q)$ two functions in position representation which follows $\psi(q) = \int_{-\infty}^{\infty} \phi(q - \bar{q})\varphi(\bar{q})d\bar{q}$ then,

$$W^\psi(q, p) = \int_{-\infty}^{\infty} W^\phi(\bar{q}, p)W^\varphi(q - \bar{q}, p)d\bar{q}. \quad (2.7)$$

Chapter 3

Wigner function propagator

In this chapter we focus on quantum dynamics directly from Weyl-Wigner formalism, in this way, the Wigner function propagator emerges as an integral representation in phase space. In addition to this, important properties related to the propagator and numerical applications for corresponding quantum approach are shown.

3.1 Weyl propagator.

The Weyl-Wigner formalism provides us powerful mathematical tools, in which it is possible to give a correct representation in phase space to the quantum mechanics. As per discussion in the previous chapter, the Wigner function was introduced as Weyl transform of the density operator. In the same way, the Weyl propagator can be introduced as Weyl transform of the unitary evolution operator $\hat{U}(t, t_0)$ as follows,

$$U_W(\mathbf{r}, t, t_0) = \int_{-\infty}^{\infty} \exp\left\{-\frac{i}{\hbar} \mathbf{p} \cdot \mathbf{y}\right\} \left\langle \mathbf{q} + \frac{\mathbf{y}}{2} \left| \hat{U}(t, t_0) \right| \mathbf{q} - \frac{\mathbf{y}}{2} \right\rangle d\mathbf{y}^f. \quad (3.1)$$

Where the quantum propagator in position representation is given by the matrix element,

$$K(\mathbf{q}'', t; \mathbf{q}', t_0) = \langle \mathbf{q}'' | \hat{U}(t, t_0) | \mathbf{q}' \rangle. \quad (3.2)$$

Although, this object is called propagator and comes from evolution operator, it cannot be related to any temporal transformation in phase space. In fact, this object depends on only one coordinate in phase space in contrast to the Wigner propagator that is considered as a kernel of time evolution of the Wigner functions.

3.1.1 Properties: Weyl propagator.

The Weyl propagator has important properties which arise as a direct consequence of its relationship with the unitary evolution operator as follows:

Proposition: If the time $t = t_0$, then, $U_W(\mathbf{r}, t_0, t_0) = 1$.

Proof: Fixing the time $t = t_0$, we have that $\hat{U}(t_0, t_0) = \hat{I}$, then the Eq. (3.1) reads,

$$\begin{aligned}
U_W(\mathbf{r}, t_0, t_0) &= \int_{-\infty}^{\infty} \exp\left\{-\frac{i}{\hbar}\mathbf{p} \cdot \mathbf{y}\right\} \langle \mathbf{q} + \frac{\mathbf{y}}{2} | \hat{U}(t_0, t_0) | \mathbf{q} - \frac{\mathbf{y}}{2} \rangle d\mathbf{y}^f, \\
&= \int_{-\infty}^{\infty} \exp\left\{-\frac{i}{\hbar}\mathbf{p} \cdot \mathbf{y}\right\} \langle \mathbf{q} + \frac{\mathbf{y}}{2} | \hat{I} | \mathbf{q} - \frac{\mathbf{y}}{2} \rangle d\mathbf{y}^f, \\
&= \int_{-\infty}^{\infty} \exp\left\{-\frac{i}{\hbar}\mathbf{p} \cdot \mathbf{y}\right\} \delta(\mathbf{y}) d\mathbf{y}^f, \\
&= 1.
\end{aligned} \tag{3.3}$$

Proposition: The Weyl propagator follows the property $U_W(\mathbf{r}, -t, t_0) = U_W^*(\mathbf{r}, t, t_0)$.

Proof: By considering the Eq. (3.1) and changing $t \rightarrow -t$, together with the property of the evolution operator $\hat{U}(-t, t_0) = \hat{U}^\dagger(t, t_0)$, it is straightforward shows that:

$$\begin{aligned}
U_W(\mathbf{r}, -t, t_0) &= \int_{-\infty}^{\infty} \exp\left\{-\frac{i}{\hbar}\mathbf{p} \cdot \mathbf{y}\right\} \langle \mathbf{q} + \frac{\mathbf{y}}{2} | \hat{U}(-t, t_0) | \mathbf{q} - \frac{\mathbf{y}}{2} \rangle d\mathbf{y}^f, \\
&= \int_{-\infty}^{\infty} \exp\left\{-\frac{i}{\hbar}\mathbf{p} \cdot \mathbf{y}\right\} \langle \mathbf{q} + \frac{\mathbf{y}}{2} | \hat{U}^\dagger(t, t_0) | \mathbf{q} - \frac{\mathbf{y}}{2} \rangle d\mathbf{y}^f, \\
&= \int_{-\infty}^{\infty} \exp\left\{\frac{i}{\hbar}\mathbf{p} \cdot \mathbf{y}\right\} \langle \mathbf{q} + \frac{\mathbf{y}}{2} | \hat{U}(t, t_0) | \mathbf{q} - \frac{\mathbf{y}}{2} \rangle^* d\mathbf{y}^f, \\
&= U_W^*(\mathbf{r}, t, t_0).
\end{aligned}$$

Proposition: The Weyl propagator follows the property

$$Tr[\hat{U}(t, t_0)] = (2\pi\hbar)^{-2f} \int_{-\infty}^{\infty} U_W(\mathbf{r}, t, t_1) U_W(\mathbf{r}, t_1, t_0) d\mathbf{r}^{2f}.$$

Proof: If the time evolution is considered by two time steps with $t > t_1 > t_0$ the evolution operator can be represented as $\hat{U}(t, t_0) = \hat{U}(t, t_1) \hat{U}(t_1, t_0)$. In addition to this, by considering the trace operation in the Weyl formalism together with $A = \hat{U}(t, t_1)$, $B = \hat{U}(t_1, t_0)$ it is straightforward shows, (see appendix A)

$$\begin{aligned}
Tr[\hat{U}(t, t_0)] &= Tr[\hat{U}(t, t_1) \hat{U}(t_1, t_0)], \\
&= (2\pi\hbar)^{-2f} \int_{-\infty}^{\infty} U_W(\mathbf{r}, t, t_1) U_W(\mathbf{r}, t_1, t_0) d\mathbf{r}^{2f}.
\end{aligned} \tag{3.4}$$

Proposition: The Weyl propagator follows the property

$$Tr[\hat{U}(t, t_0)] = (2\pi\hbar)^{-f} \int_{-\infty}^{\infty} U_W(\mathbf{r}, t, t_0) d\mathbf{r}^{2f}. \tag{3.5}$$

Proof: By considering the previous proposition with $t_1 = t_0$ and taking into account that $A = \hat{U}(t, t_0)$, $B = \hat{I}$. It can be easily proved.

Proposition: The Weyl propagator follows the property

$$1 = \int_{-\infty}^{\infty} \exp\left\{\frac{i}{\hbar}\Delta_3(\mathbf{r}, \mathbf{r}_2, \mathbf{r}_1)\right\} U_W(\mathbf{r}_1, t, t_0) U_W^*(\mathbf{r}_2, t, t_0) d\mathbf{r}_1^{2f} d\mathbf{r}_2^{2f}. \quad (3.6)$$

Proof: The prove is straightforward by considering the Weyl transform for two operators (see appendix A), moreover taking into account that the identity for unitary evolution operator is $\hat{U}(t, t_0)\hat{U}^\dagger(t, t_0) = \hat{I}$.

3.2 Wigner propagator.

The density matrix operator plays an important role in the context of quantum dynamics, more precisely, this operator can describes pure or mixed quantum states, and their time evolution is based on *von Neumann equation*. In fact, we can write down the solution to this equation as follows,

$$\hat{\rho}(t) = \hat{U}(t, t_0)\hat{\rho}(t_0)\hat{U}^\dagger(t, t_0). \quad (3.7)$$

The Wigner function propagator is formally derive by considering the Weyl transform to the Eq. (3.7). In order to avoid losing the focus with this lengthly algebra here, in the appendix A the Weyl transform for two and three operators has been shown explicitly. Therefore, we here present the result as an integral representation to the time evolution of Wigner function,

$$W(\mathbf{r}'', t) = \int_{-\infty}^{\infty} G_W(\mathbf{r}'', t; \mathbf{r}', 0) W(\mathbf{r}', 0) d\mathbf{r}'^{2f}. \quad (3.8)$$

We assume that $t_0 = 0$ as the initial time. Thus, the propagator of the Wigner function $G_W(\mathbf{r}'', t; \mathbf{r}', 0)$ relates two phase-space points at time t . Clearly, this object defines a space-time traslation in phase space. Explicitly, the propagator is depicted in terms of Weyl propagator, see Eq. (3.1).

$$\begin{aligned} G_W(\mathbf{r}'', t; \mathbf{r}', 0) &= \frac{1}{(\pi\hbar)^2} \int_{-\infty}^{\infty} U_W(\mathbf{r}_1, t) U_W^*(\mathbf{r}_2, t) \exp\left\{-\frac{2i}{\hbar}(\mathbf{r}_2 \wedge \mathbf{r}'' + \mathbf{r}_1 \wedge \mathbf{r}')\right\} \\ &\times \delta(\mathbf{r}_2 - \mathbf{r}'' + \mathbf{r}_1 - \mathbf{r}') d\mathbf{r}_1^{2f} d\mathbf{r}_2^{2f}. \end{aligned} \quad (3.9)$$

Although, unusual, and perhaps more complicated, we introduce a new set of variables,

$$\mathbf{r}_\pm = (\mathbf{r}' + \mathbf{r}'' \pm \mathbf{R})/2. \quad (3.10)$$

Thus, the Wigner propagator is rewritten as a convoluted expression in terms of Weyl propagators,

$$\begin{aligned} G_W(\mathbf{r}'', t; \mathbf{r}', 0) &= \frac{1}{(2\pi\hbar)^{2f}} \int_{-\infty}^{\infty} U_W(\mathbf{r}_+, t) U_W^*(\mathbf{r}_-, t) \\ &\times \exp\left\{-\frac{i}{\hbar}(\mathbf{R} \wedge (\mathbf{r}'' - \mathbf{r}'))\right\} d\mathbf{R}^{2f}. \end{aligned} \quad (3.11)$$

This equation corresponds to the general representation for the Wigner propagator, which will be considered in the next chapter as starting point for the semiclassical approximations.

3.2.1 Properties: Wigner propagator.

At this point, the Wigner propagator is the object associated to time evolution of the Wigner functions. Thus, there are important properties that emerges as a result of the unitary evolution and hermiticity in quantum mechanics. Moreover, the temporal concatenation of the time evolution operator introduces Markovian properties for the propagator, as a result of this, a kind of phase-space path integrals is derived.

Proposition: The Wigner propagator $G_W(\mathbf{r}'', t; \mathbf{r}', 0)$ is a real function.

Proof: This property can be seen in an indirect form, by construction the Wigner function is real (see section 2.3), then for holding real-valuedness of this function, it implies that $G_W(\mathbf{r}'', t; \mathbf{r}', 0)$ also should be real.

Other way to prove this property is by considering the Eq. (3.11). Then we have,

$$\begin{aligned}
G_W(\mathbf{r}'', t; \mathbf{r}', 0) &= \frac{1}{(2\pi\hbar)^{2f}} \int_{-\infty}^{\infty} U_W\left(\frac{\mathbf{r}' + \mathbf{r}'' - \mathbf{R}}{2}, t\right) U_W^*\left(\frac{\mathbf{r}' + \mathbf{r}'' + \mathbf{R}}{2}, t\right), \\
&\times \exp\left\{\frac{i}{\hbar}(\mathbf{R} \wedge (\mathbf{r}'' - \mathbf{r}'))\right\} d\mathbf{R}^{2f}, \\
&= \frac{1}{(2\pi\hbar)^{2f}} \int_{-\infty}^{\infty} U_W^*\left(\frac{\mathbf{r}' + \mathbf{r}'' + \mathbf{R}}{2}, t\right) U_W\left(\frac{\mathbf{r}' + \mathbf{r}'' - \mathbf{R}}{2}, t\right), \\
&\times \exp\left\{-\frac{i}{\hbar}(\mathbf{R} \wedge (\mathbf{r}'' - \mathbf{r}'))\right\} d\mathbf{R}^{2f}, \\
&= G_W^*(\mathbf{r}'', t; \mathbf{r}', 0).
\end{aligned} \tag{3.12}$$

Proposition: For a time $t = 0$, then $G_W(\mathbf{r}'', 0; \mathbf{r}', 0) = \delta(\mathbf{r}'' - \mathbf{r}')$.

Proof: By considering the Eq (3.3) and Eq. (3.11), it is straightforward shows that,

$$\begin{aligned}
G_W(\mathbf{r}'', 0; \mathbf{r}', 0) &= \frac{1}{(2\pi\hbar)^{2f}} \int_{-\infty}^{\infty} \exp\left\{-\frac{i}{\hbar}(\mathbf{R} \wedge (\mathbf{r}'' - \mathbf{r}'))\right\} d\mathbf{R}^{2f}, \\
&= \delta(\mathbf{r}'' - \mathbf{r}').
\end{aligned} \tag{3.13}$$

Proposition: If the time $t = t_0$, then $G_W(\mathbf{r}'', t_0; \mathbf{r}', t_0) = \delta(\mathbf{r}'' - \mathbf{r}')$.

Proof: By considering the Eq. (3.18) and the trace operation in Weyl formalism (see appendix A), it is straightforward shows that,

$$\begin{aligned}
G_W(\mathbf{r}'', t_0; \mathbf{r}', t_0) &= Tr[\hat{T}(\mathbf{r}'')\hat{U}(t_0, t_0)\hat{T}(\mathbf{r}')\hat{U}^\dagger(t_0, t_0)], \\
&= Tr[\hat{T}(\mathbf{r}'')\hat{T}(\mathbf{r}')], \\
&= \delta(\mathbf{r}'' - \mathbf{r}').
\end{aligned} \tag{3.14}$$

Proposition: The Wigner propagator has an orthogonal property under integration on final phase-space coordinates *i.e.*, $\int_{-\infty}^{\infty} G_W(\mathbf{r}, t; \mathbf{r}'', t_0) G_W(\mathbf{r}, t; \mathbf{r}', t_0) d\mathbf{r}^{2f} = \delta(\mathbf{r}'' - \mathbf{r}')$.

Proof: By considering the trace operation in Weyl formalism (see appendix A) we have,

$$\begin{aligned}
\delta(\mathbf{r}'' - \mathbf{r}') &= \int_{-\infty}^{\infty} G_W(\mathbf{r}, t; \mathbf{r}', t_0) G_W(\mathbf{r}, t; \mathbf{r}'', t_0) d\mathbf{r}^{2f}, \\
&= \int_{-\infty}^{\infty} Tr[\hat{T}(\mathbf{r}) \hat{U}(t, t_0) \hat{T}(\mathbf{r}') \hat{U}^\dagger(t, t_0)] \\
&\quad \times Tr[\hat{T}(\mathbf{r}) \hat{U}(t, t_0) \hat{T}(\mathbf{r}'') \hat{U}^\dagger(t, t_0)] d\mathbf{r}^{2f}, \\
&= Tr[\hat{U}(t, t_0) \hat{T}(\mathbf{r}) \hat{T}(\mathbf{r}'') \hat{U}^\dagger(t, t_0)] d\mathbf{r}^{2f}, \\
&= Tr[\hat{T}(\mathbf{r}'') \hat{T}(\mathbf{r}')] d\mathbf{r}^{2f}, \\
&= \delta(\mathbf{r}'' - \mathbf{r}').
\end{aligned} \tag{3.15}$$

Proposition: The Wigner propagator has an orthogonal property under integration on initial phase-space coordinates *i.e.*, $\int_{-\infty}^{\infty} G_W(\mathbf{r}'', t; \mathbf{r}_0, t_0) G_W(\mathbf{r}', t; \mathbf{r}_0, t_0) d\mathbf{r}_0^{2f} = \delta(\mathbf{r}'' - \mathbf{r}')$.

Proof: The proof reads similar to the previous proposition.

$$\delta(\mathbf{r}'' - \mathbf{r}') = \int_{-\infty}^{\infty} G_W(\mathbf{r}'', t; \mathbf{r}_0, t_0) G_W(\mathbf{r}', t; \mathbf{r}_0, t_0) d\mathbf{r}_0^{2f}. \tag{3.16}$$

3.2.2 Markovian properties of the Wigner propagator.

In quantum mechanics, the state of the quantum system is associated to the wave function $|\psi(t)\rangle$ which change in time according to the Schrödinger equation. Moreover, the quantum dynamics can be considered in the framework of evolution operator which defines a unitary group of the form $\hat{U}(t, t_0) = \exp(-\frac{i}{\hbar} \hat{H}(t - t_0))$ where \hat{H} is a hermitian operator depending on momentum and position operators. Thus, the time evolution of a state follows the rule,

$$|\psi(t)\rangle = \hat{U}(t, t_0) |\psi(t_0)\rangle, \tag{3.17}$$

with an initial condition,

$$\hat{U}(t_0, t_0) = \hat{I}. \tag{3.18}$$

Also, the time evolution operator is solution to the Schrödinger equation,

$$i\hbar \frac{d\hat{U}(t, t_0)}{dt} = \hat{H}(t) \hat{U}(t, t_0). \tag{3.19}$$

In general, for time-dependent Hamiltonian the solution to this equation can be formally solved, so that

$$\hat{U}(t, t_0) = \hat{T} \exp\left(-\frac{i}{\hbar} \int_{t_0}^t \hat{H}(t') dt'\right). \tag{3.20}$$

Similarly, by considering the Hermitian adjoint of $\hat{U}(t, t_0)$ in the Eq. (3.19), the solution is given by,

$$\hat{U}^\dagger(t, t_0) = \hat{T}^r \exp\left(-\frac{i}{\hbar} \int_{t_0}^t \hat{H}(t') dt'\right). \quad (3.21)$$

where \hat{T} indicates the time-ordered product, and \hat{T}^r denotes the reverse time-ordered product,

$$\hat{T}\hat{H}(t')\hat{H}(t'') = \begin{cases} H(t')H(t''), & \text{If } t' > t'' \\ H(t'')H(t'), & \text{If } t'' > t'. \end{cases} \quad (3.22)$$

In order to show relevant properties of the Wigner propagator, the Eq. (3.7) is considered again, it corresponds to the density matrix evolved in time by the evolution operator. In this way, the propagator reads (see appendix A),

$$G_W(\mathbf{r}'', t; \mathbf{r}', t_0) = \text{Tr}[\hat{T}(\mathbf{r}'')\hat{U}(t, t_0)\hat{T}(\mathbf{r}')\hat{U}^\dagger(t, t_0)]. \quad (3.23)$$

When the Hamiltonian operator is time-dependent, two forms can be distinguished for time evolution operator $\hat{U}(t, t_0)$ and $\hat{U}^\dagger(t, t_0)$, these are given in the Eq. (3.20) and Eq. (3.21). If $t > t_1 > t_0$ then,

$$\begin{aligned} \hat{U}(t, t_0) &= \hat{U}(t, t_1)\hat{U}(t_1, t_0), \\ \hat{U}^\dagger(t, t_0) &= \hat{U}^\dagger(t, t_0)\hat{U}^\dagger(t, t_1). \end{aligned} \quad (3.24)$$

After replacing the Eq. (3.24) into (3.23) we have,

$$\begin{aligned} G_W(\mathbf{r}'', t; \mathbf{r}', t_0) &= \text{Tr}[\hat{U}^\dagger(t, t_1)\hat{T}(\mathbf{r}'')\hat{U}(t, t_1)\hat{U}(t_1, t_0)\hat{T}(\mathbf{r}')\hat{U}^\dagger(t, t_0)], \\ &= \int_{-\infty}^{\infty} \text{Tr}[\hat{T}(\mathbf{r}_1)\hat{U}(t, t_1)\hat{T}(\mathbf{r}'')\hat{U}(t, t_1)] \\ &\times \text{Tr}[\hat{T}(\mathbf{r}_1)\hat{U}^\dagger(t_1, t_0)\hat{T}(\mathbf{r}')\hat{U}^\dagger(t_1, t_0)] d\mathbf{r}_1^{2f}, \\ &= \int_{-\infty}^{\infty} G_W(\mathbf{r}'', t; \mathbf{r}_1, t_1)G_W(\mathbf{r}_1, t_1; \mathbf{r}', t_0) d\mathbf{r}_1^{2f}. \end{aligned} \quad (3.25)$$

The previous equation corresponds to the concatenation property along of time evolution, in fact, it is well-known in the context of Markovian processes as Chapman-Kolmogorov property. Assuming that the full time evolution of the Wigner function is divided in a small time steps, similarly to Feynman's construction, it can be formulated as phase-space path integrals representation in phase space for the Wigner propagator, more precisely, the full time propagation from \mathbf{r}' at time t_0 as initial phase-space point to \mathbf{r}'' at time t is represented in terms of contribution at small time steps $t = t_n > t_{n-1} > t_{n-2} \cdots > t_0$. Moreover, fixing $\mathbf{q}''_n = \mathbf{q}''$ and $\mathbf{p}''_n = \mathbf{p}''$, the concatenation property allows us write down an equation for full time propagation as,

$$G_W(\mathbf{r}'', t; \mathbf{r}', t_0) = \frac{1}{(2\pi\hbar)^f} \int_{-\infty}^{\infty} \prod_{k=1}^{n-1} d\mathbf{r}_k G_W(\mathbf{r}_{j+1}, t_{j+1}; \mathbf{r}_j, t_j). \quad (3.26)$$

In this way, the Wigner function evolves in time by means of phase-space path integrals,

$$W(\mathbf{r}'', t) = \frac{1}{(2\pi\hbar)^f} \lim_{n \rightarrow \infty} \int_{-\infty}^{\infty} \prod_{k=1}^{n-1} d\mathbf{r}_k^{2f} \prod_{j=0}^{n-1} G_W(\mathbf{r}_{j+1}, t_{j+1}; \mathbf{r}_j, t_j) W(\mathbf{r}_0, t_0) d\mathbf{r}_0^{2f}. \quad (3.27)$$

Here, note that the Wigner function behaves as a probability which follows a Markovian process in phase space.

3.3 Exact Wigner propagator.

It is well-known in quantum mechanics, most of the quantum systems cannot be solved in terms of exact solutions, even for one dimensional cases, and only few quantum systems are solvable in analytical form. However, nowadays the numerical methods are considered broadly and serves as strong supporting tools for theoretical studies. Particularly, quantum calculations of the eigenstates and its corresponding eigenvalues can be calculated with extreme accuracy by different methods. In the framework of the Wigner propagator, the full energy spectrum of the quantum system plays an important role. Namely, time evolution of the Wigner function is governed by the exact propagator which takes into account the Wigner eigenstates associated to the system as follows:

Lets start considering the Weyl propagator in terms of the Wigner functions,

$$\begin{aligned}
U_W(\mathbf{r}, t) &= \int_{-\infty}^{\infty} \exp\left\{-\frac{i}{\hbar}\mathbf{p} \cdot \mathbf{y}\right\} \langle \mathbf{q} + \frac{\mathbf{y}}{2} | \hat{U}(t) | \mathbf{q} - \frac{\mathbf{y}}{2} \rangle d\mathbf{y}^f, \\
&= \sum_{nm} \int_{-\infty}^{\infty} \exp\left\{-\frac{i}{\hbar}\mathbf{p} \cdot \mathbf{y}\right\} \langle \mathbf{q} + \frac{\mathbf{y}}{2} | n \rangle \langle n | \hat{U}(t) | m \rangle \langle m | \mathbf{q} - \frac{\mathbf{y}}{2} \rangle d\mathbf{y}^f, \\
&= \sum_n \exp\left\{-\frac{iE_n t}{\hbar}\right\} \int_{-\infty}^{\infty} \exp\left\{-\frac{i}{\hbar}\mathbf{p} \cdot \mathbf{y}\right\} \langle \mathbf{q} + \frac{\mathbf{y}}{2} | n \rangle \langle n | \mathbf{q} - \frac{\mathbf{y}}{2} \rangle d\mathbf{y}^f, \\
&= (2\pi\hbar)^f \sum_n \exp\left\{-\frac{iE_n t}{\hbar}\right\} W_{nn}(\mathbf{r}). \tag{3.28}
\end{aligned}$$

Here, we introduced the nons-diagonal Wigner eigenstates which involves the n, m indices.

$$W_{nm}(\mathbf{r}) = \frac{1}{(2\pi\hbar)^f} \int_{-\infty}^{\infty} \exp\left\{-\frac{i}{\hbar}\mathbf{p} \cdot \mathbf{y}\right\} \psi_n\left(\mathbf{q} + \frac{\mathbf{y}}{2}\right) \psi_m^*\left(\mathbf{q} - \frac{\mathbf{y}}{2}\right) d\mathbf{y}^f. \tag{3.29}$$

Is worthy of mentioning that, the Eq. (3.28) for Weyl propagator takes into account only the diagonal contributions of the Wigner eigenstates *i.e.* setting $n = m$. The next step consist of replacing the Eq. (3.28), and Eq. (3.10) into Eq. (3.11) together with Eq. (), Therefore, we obtain an expression for the Wigner propagator,

$$\begin{aligned}
G_W(\mathbf{r}'', t; \mathbf{r}', 0) &= \frac{1}{(2\pi\hbar)^{2f}} \int_{-\infty}^{\infty} U_W\left(\frac{\mathbf{r}' + \mathbf{r}'' - \mathbf{R}}{2}, t\right) U_W^*\left(\frac{\mathbf{r}' + \mathbf{r}'' + \mathbf{R}}{2}, t\right) \\
&\quad \times \exp\left\{-\frac{i}{\hbar}(\mathbf{R} \wedge (\mathbf{r}'' - \mathbf{r}'))\right\} d\mathbf{R}^{2f}, \\
&= \frac{1}{(2\pi\hbar)^{2f}} \int_{-\infty}^{\infty} \sum_{nm} \exp\left\{-\frac{i\Delta_{nm}t}{\hbar}\right\} W_{nm}\left(\frac{\mathbf{r}' + \mathbf{r}'' - \mathbf{R}}{2}\right) W_{nm}^*\left(\frac{\mathbf{r}' + \mathbf{r}'' + \mathbf{R}}{2}\right) \\
&\quad \times \exp\left\{-\frac{i}{\hbar}(\mathbf{R} \wedge (\mathbf{r}'' - \mathbf{r}'))\right\} d\mathbf{R}^{2f}, \\
&= \frac{1}{(2\pi\hbar)^{2f}} \sum_{nm} \exp\left\{-\frac{i\Delta_{nm}t}{\hbar}\right\} \int_{-\infty}^{\infty} \exp\left\{-\frac{i}{\hbar}(\mathbf{R} \wedge (\mathbf{r}'' - \mathbf{r}'))\right\} d\mathbf{R}^{2f} \\
&\quad \times \int_{-\infty}^{\infty} \exp\left\{-\frac{i}{\hbar}\mathbf{p}_+ \cdot \mathbf{y}_+\right\} \langle \mathbf{q}_+ + \frac{\mathbf{y}_+}{2} | n \rangle \langle n | \mathbf{q}_+ - \frac{\mathbf{y}_+}{2} \rangle d\mathbf{y}_+^f \\
&\quad \times \int_{-\infty}^{\infty} \exp\left\{-\frac{i}{\hbar}\mathbf{p}_- \cdot \mathbf{y}_-\right\} \langle \mathbf{q}_- + \frac{\mathbf{y}_-}{2} | m \rangle \langle m | \mathbf{q}_- - \frac{\mathbf{y}_-}{2} \rangle d\mathbf{y}_-^f, \\
&\quad \text{After algebraic manipulations, and performing the integral over } d\mathbf{R}^{2f}. \\
&= (2\pi\hbar)^f \sum_{nm} \exp\left\{-\frac{i\Delta_{nm}t}{\hbar}\right\} W_{nm}^*(\mathbf{r}') W_{nm}(\mathbf{r}''). \tag{3.30}
\end{aligned}$$

The Wigner propagator involves both diagonal and non-diagonal Wigner eigenstates. Moreover, $\Delta_{nm} = E_n - E_m$ involves the full energy spectrum of the quantum system.

3.4 Models.

3.4.1 Morse Oscillator.

In 1929 P. M. Morse in his early work [Mor57] suggested a potential function given by $U(r) = D(1 - e^{-\alpha r})^2$ in order to incorporate the non-linearity effects for interactions between molecules, it was initially applied successfully to the study of non-rotating diatomic molecules, and surprisingly, it was capable to fit experimental curves with good agreement for a large range of molecular systems, besides of the correct energy spectrum. Today the Morse potential remains considered as benchmark for more complex systems and there are large amount of applications in the literature where the Morse oscillator has been applied together with Wigner function, for example, in theory of photodissociation, atom-diatom collision processes [HWL61] and among problems in ordinary quantum theory, nuclear physics, chemical physics, and quantum field theory [PC45]. On the other hand, the importance of this potential is not only in a quantum level, but also in the context of the semiclassical physics. There are many applications where the Morse potential plays an important role, in particular, it is considered as a challenger for any semiclassical approximation that desire

reproduce all quantum features as long as are possible. So, we address our work on this potential in order to test our semiclassical approximations to the Wigner propagator. In follows we will discuss the Wigner propagator in terms of non-diagonal Wigner functions. Lets start considering the time-independent Schrödinger equation for one dimensional Morse potential:

$$-\frac{\hbar^2}{2m} \frac{d^2\psi}{dx^2} + V_{Morse}\psi = E_n\psi, \quad (3.31)$$

where the potential function reads,

$$V_{Morse} = D(1 - e^{-\alpha x})^2. \quad (3.32)$$

This equation can be easily rewritten in terms of dimensionless parameter, which is defined by $\lambda = \frac{\sqrt{2mD}}{\alpha\hbar}$, where \hbar is the Planck's constant, m the mass of the oscillator, the parameters D , and α are related to the depth and width of the potential well, respectively. There is no difficult to recognized that this equation corresponds to Ricatti equation, and the the solutions are given by,

$$\psi_n(x) = N(\lambda, n)\xi^{\lambda-n-1/2}e^{\xi/2}L_n^{2\lambda-2n-1}(\xi), \quad (3.33)$$

Where ξ and $N(\lambda, n)$ are defined as an auxiliary function and the normalization constant, respectively.

$$\xi(\lambda, x) = 2\lambda e^{-\alpha x}, \quad (3.34)$$

$$N(\lambda, n) = \sqrt{\frac{(2\lambda - 2n - 1)\Gamma(n + 1)}{\Gamma(2\lambda - n)}}. \quad (3.35)$$

The Gamma function with real argument is defined by the symbol $\Gamma(x)$. The eigenfunctions given by Eq. (3.33) are associated with the energy spectrum as follows,

$$E_n = \frac{2}{\lambda} \left[(n + 1/2) - \frac{1}{2\lambda} (n + 1/2)^2 \right], \quad (3.36)$$

with $n = 1, 2, \dots, \text{int}(\lambda - 1/2)$. Finally, the corresponding Wigner functions can be expressed in an analytical form by replacing the Eq. (3.33) into Eq. (2.3), then, after straightforward manipulations, the non-diagonal Wigner function reads,

$$W_{nm}(q, p) = \frac{2}{\pi\hbar} N(\lambda, n)N(\lambda, m)\xi^{2\lambda-n-m-1} \times \sum_{r=0}^n \sum_{s=0}^m b(\lambda, n, r)b(\lambda, m, s)\xi^{r+s}K_\nu(\xi), \quad (3.37)$$

where the function $K_\nu(\xi)$ is the modified Bessel function of third kind and complex order $\nu = s - r + 2ip/\hbar$, also, for binomial coefficients we abbreviate

$$b(\lambda, n, j) = \frac{(-1)^j}{j!} \frac{\Gamma(2\lambda - n)}{\Gamma(2\lambda - 2n + j)\Gamma(n - j + 1)}. \quad (3.38)$$

Perhaps, the most useful feature of the Wigner description is that it allows a direct comparison of quantum and classical dynamics. This has been stimulated several theoretical studies [MH17, Sta09], particularly with the diagonal representation ($n = m$) of Wigner functions [JPD35] in a Morse oscillator. Similarly, it has been derived the Wigner functions for radial Coulomb potential by considering a Langer transformation, see reference [Sta09].

3.4.2 Quartic double well.

The quartic double-well potential always attracted a lot of attention, and its relevance has been extended in almost all the branches of physics. For example, this simple model can be found in the description of important phenomena in quantum optics, chaos, mesoscopic systems and quantum transport. Moreover, it is the standard model for the study quantum manifestations as the coherent tunneling across the barriers.

In view of our numerical applications about semiclassical propagation of Wigner function, we here introduce the model and notation that will be consider in the following chapters. The quartic double well potential is defined as:

$$V(x) = -\frac{m\omega^2 x^2}{4} + \frac{m^2\omega^4 x^4}{64E_b}, \quad (3.39)$$

where ω is the oscillation frequency near the minima at $x_{\pm} = \pm\sqrt{8E_b/m\omega^2}$ and E_b is their depth. In natural units $q = \sqrt{m\omega/\hbar}x$ and $\tau = \omega t$, the full Hamiltonian of the system reads

$$H(p, q) = \frac{p^2}{2} - \frac{q^2}{4} + \frac{q^4}{64\Delta}. \quad (3.40)$$

The dimensionless barrier height $\Delta = E_b/\hbar\omega$ is the only relevant parameter measures approximately the number of tunneling doublets, *i.e.*, half the number of eigenstates below the barrier top.

3.5 Autocorrelation functions.

The propagation of localized initial states has been established as one of the most relevant test for semiclassical approximations. In this context, the autocorrelation function is a straightforward measure of efficiency associated with the propagation methods. In practice, it provides a robust and easy measure of performance of the semiclassical approximations along on time evolution of wave packets [Hel23, Gro26, Gro99, TW04]. The overlap $C_{\psi}(t) = \langle\psi(t)|\psi(0)\rangle$ for a given initial state $|\psi\rangle$ upon squaring translates into an expression in terms of the Wigner representation $W_{\psi}(\mathbf{r})$ of that state,

$$|C(t)|^2 = (2\pi\hbar)^f \int_{-\infty}^{\infty} W_{\psi}(\mathbf{r}, 0)W_{\psi}(\mathbf{r}, t)d\mathbf{r}^{2f}. \quad (3.41)$$

or involving the Wigner propagator explicitly,

$$|C(t)|^2 = (2\pi\hbar)^f \int_{-\infty}^{\infty} \int_{-\infty}^{\infty} W_{\psi}(\mathbf{r}'', 0) G_W(\mathbf{r}'', t; \mathbf{r}', 0) W_{\psi}(\mathbf{r}', 0) d\mathbf{r}''^{2f} d\mathbf{r}'^{2f}. \quad (3.42)$$

A fact well-known in the Wigner representation, is that the Wigner function can take negative values in phase space, therefore it cannot be associated to a probability distribution function. However, the Gaussian states are the only admissible Wigner functions which are positive defined, and therefore can be interpreted in the same way as a probability distribution function like in classical mechanics. In order to fix the notation about the initial wave packets that will be considered for numerical applications, let's assume that the wave-packet in configuration-space is given by

$$\psi(\mathbf{q}) = (\pi\hbar)^{-f/4} \exp\left\{ -\frac{|\mathbf{q} - \mathbf{q}_0|^2}{2\hbar} + \frac{i}{\hbar} \mathbf{p}_0 \cdot (\mathbf{q} - \mathbf{q}_0) \right\}. \quad (3.43)$$

Then, the corresponding Wigner function explicitly reads,

$$W(\mathbf{r}, 0) = (\pi\hbar)^{-f} \exp\left\{ -\frac{|\mathbf{r} - \mathbf{r}_0|^2}{\hbar} \right\}, \quad (3.44)$$

in a f -dimensional space.

3.6 Numerical applications.

We begin with the numerical applications for wave-packet dynamics in terms of Wigner function propagator, more precisely, the time evolution of localized initial states is performed by means of Eq. (3.8) together with Eq. (3.30), the last one corresponds to the kernel of propagation from quantum approach. Our numerical studies are focussed on dynamics of an initial wave packet evolving in a Morse potential directly in to phase space.

In relation to the quantum calculations for propagation of this state, we take an advantage of exact mixed Wigner eigenfunctions (see Eq. (3.37)). Therefore, the quantum Wigner propagator translates into a straightforward numerical algorithm in terms of eigenfunctions of the quantum system. In follows, the Fig. 3.1 shows the naked propagator evolving in a Morse potential, in this way, the underlying quantum features emerge in phase space representation.

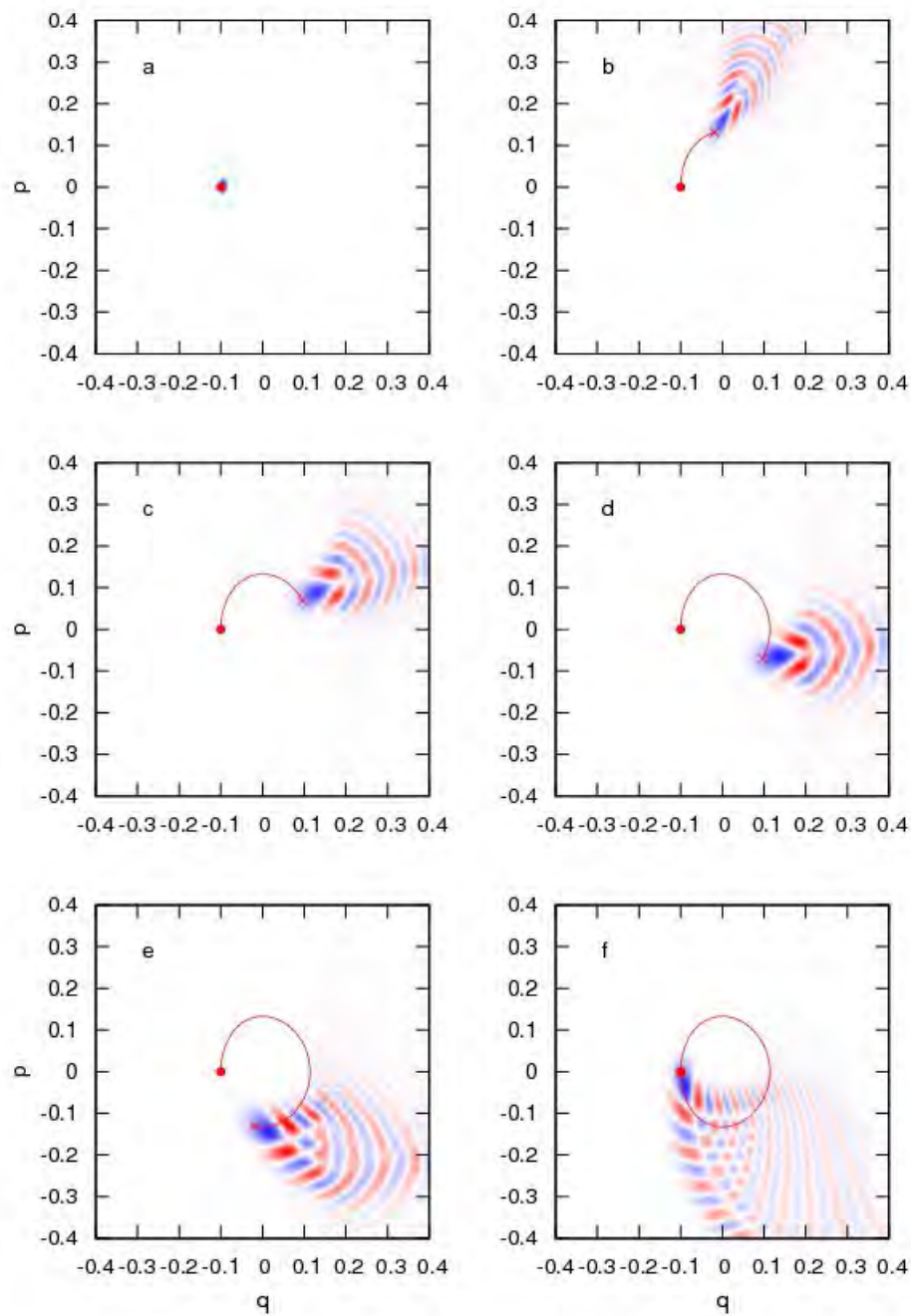


Figure 3.1: Time evolution of the Wigner propagator for a Morse potential. The quantum calculations are shown as a sequence of times, $t = 0$ (panel a), 0.5072 (b), 1.0144 (c), 1.5216 (d), 2.0288 (e), 2.536 (f). The underlying classical trajectory has been launched at $\mathbf{r}_0 = (-0.1, 0)$. Parameter values are $D = 1$, $\alpha = 1.25$, $\hbar = 0.005$. Color code ranges from red (negative) through white (zero) through blue (positive).

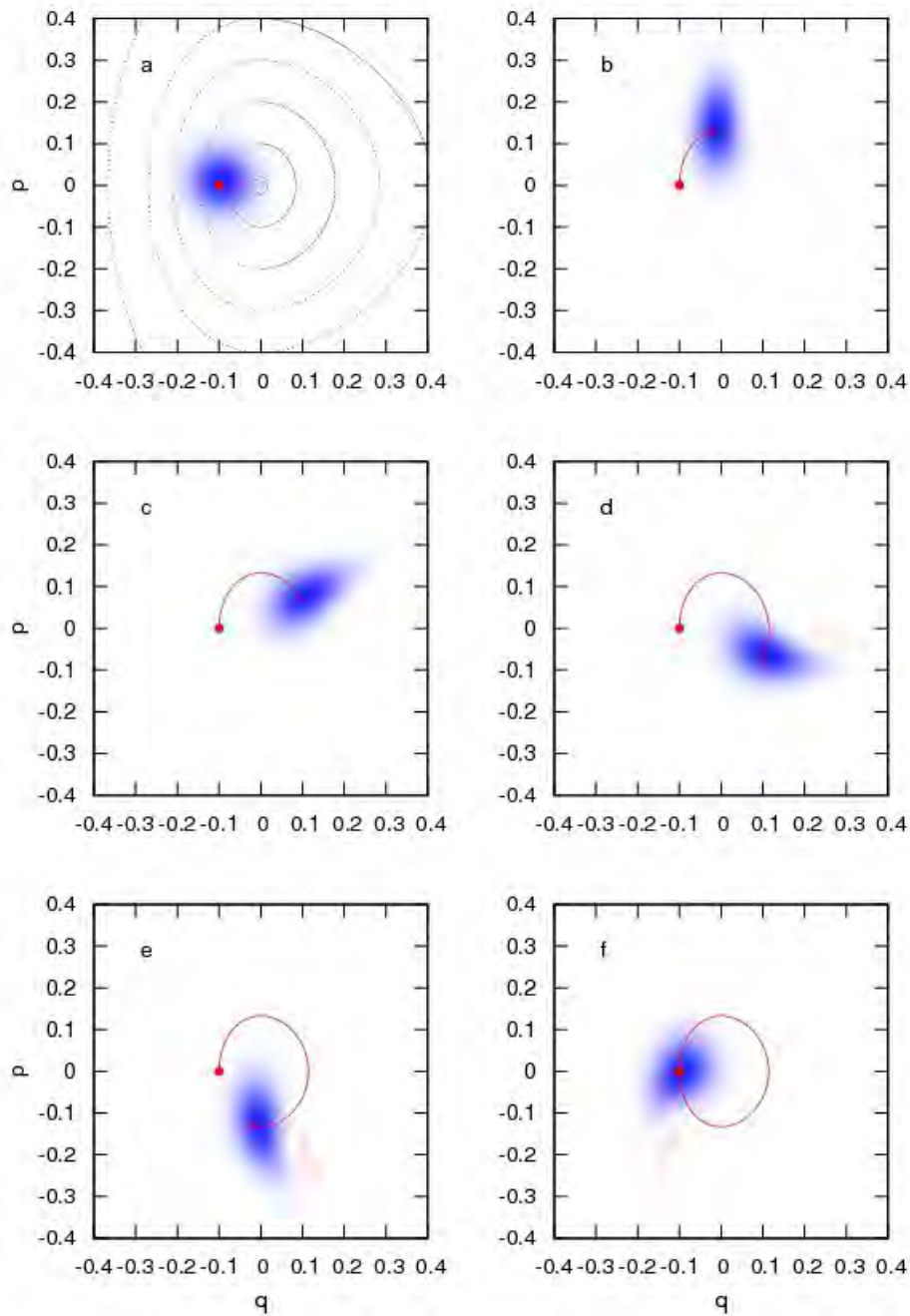


Figure 3.2: Time evolution of an initial Wigner function (Gaussian state) in the Morse potential. The quantum calculations are shown as a sequence at times $t = 0$ (panel a), 0.5072 (b), 1.0144 (c), 1.5216 (d), 2.0288 (e), 2.536 (f). In panel a, some contour lines of the potential are shown superimposed. The underlying classical trajectory has been launched at $\mathbf{r}_0 = (-0.1, 0)$. Parameter values are $D = 1$, $\alpha = 1.25$, $\hbar = 0.005$.

Chapter 4

Semiclassical Wigner function propagator

In this chapter we shall consider the semiclassical approximation to the Wigner function propagator based on van Vleck propagator in configuration space. Particularly, this approach leads to the concept of trajectory pairs in phase space, together with an initial value representation for the Wigner function propagator. We propose efficient algorithms in order to perform the semiclassical propagation of localized initial states, and the corresponding numerical applications are discussed.

The semiclassical treatments to quantum time evolution basically consist of replacing the quantum propagator with a particular semiclassical approximation, in fact, this is the standard way in the framework of semiclassical propagation, and it has been clearly discussed in different representations of quantum mechanics, (see chapter 1). Perhaps, the van Vleck-Gutzwiller propagator [Vle78], is being the oldest and most explored semiclassical approximation, this can be derived either by solving the Schrödinger-type equation asymptotically [Lit 7] in a similar manner to WKB treatment of time-dependent wave function or by applying the stationary phase method to the Feynman's path integrals [RPF65, Sch81a]. In effect, the van Vleck-Gutzwiller propagator in configuration space is written as:

$$K_{sc}(\mathbf{q}'', t; \mathbf{q}', 0) = \sum_j \left(\frac{1}{2\pi i \hbar} \right)^{\frac{f}{2}} \left| \frac{\partial R_j(\mathbf{q}'', \mathbf{q}')}{\partial q'_n \partial q''_m} \right|^{\frac{1}{2}} \exp \left\{ \frac{i}{\hbar} R_j(\mathbf{q}'', \mathbf{q}') - i\mu_j \frac{\pi}{2} \right\}. \quad (4.1)$$

Herein, f denotes the number of degrees of freedom for the classical system, and the sum over j -index takes into account all contribution of classical trajectories that are originated from \mathbf{q}' position at time 0 and end up in a position \mathbf{q}'' at time t , moreover the principal Hamilton function is defined as $R(\mathbf{q}'', \mathbf{q}')$. Additionally, the amplitude is represented in terms of stability matrix $\mathbf{M}(\mathbf{r}, t) = \partial R(\mathbf{q}'', \mathbf{q}') / \partial q'_n \partial q''_m$ which contains f -derivatives relating the final position with respect to initial momentum, and μ_j is so-called Morse index, it is an integer number that has to be taken into account when the trajectory encounters a caustic,

i.e. whereas the amplitude becomes singular.

In order to obtain the semiclassical representation for Weyl propagator, we followed a previous work [Viv00, San05]. We started by replacing the Eq. (4.1) into Eq. (3.1). As a result of this the Weyl propagator takes the form,

$$\begin{aligned} U_W(\mathbf{r}, t) &= \int_{-\infty}^{\infty} \exp\left\{-\frac{i}{\hbar}\mathbf{p} \cdot \mathbf{y}\right\} K_{sc}\left(\mathbf{q}'' + \frac{\mathbf{y}}{2}, t; \mathbf{q}' - \frac{\mathbf{y}}{2}, 0\right) d\mathbf{y}^f, \\ &= \sum_j \left(\frac{1}{2\pi i \hbar}\right)^{\frac{f}{2}} \left|\frac{\partial R_j(\mathbf{q}'', \mathbf{q}')}{\partial q'_n \partial q''_m}\right|^{\frac{1}{2}} \int_{-\infty}^{\infty} \exp\left\{\frac{i}{\hbar}(R_j(\mathbf{q}'', \mathbf{q}') - \mathbf{p} \cdot \mathbf{y})\right\} d\mathbf{y}^f. \end{aligned} \quad (4.2)$$

Note that we have dropped out the Morse index due to they do not make sense in phase space, *i.e.*, they appears in position or momentum representation only. By introducing a convenient transformation in position coordinate as $\mathbf{q}' = \mathbf{q} - \mathbf{y}/2$ and $\mathbf{q}'' = \mathbf{q} + \mathbf{y}/2$, easily is shown that $\mathbf{q} = (\mathbf{q}' + \mathbf{q}'')/2$. On the other hand, the semiclassical limit of phase factor associated to this integral is highly oscillating as is known in the framework of semiclassical approximations. In order to overcome this difficulty we regarded the main contribution given by the stationary points, more precisely, the stationary phase method imposes an additional restriction over momentum, $\mathbf{p} = (\mathbf{p}' + \mathbf{p}'')/2$. Thus we have,

$$\mathbf{r}_j = \frac{\mathbf{r}'_j + \mathbf{r}''_j}{2}. \quad (4.3)$$

In addition to this, the previous equation stand out the concept of *chord rule* in phase space which have introduced by M. Berry in [Ber19, Ber37]. Basically, it corresponds to the symplectic area enclosed by the classical trajectory starting from \mathbf{r}'_j and ending at \mathbf{r}''_j in phase-space, then coming back in straight line through of \mathbf{r}_j . It is illustrated in the Fig. 4. On the other hand, the amplitude factor in the van Vleck propagator can be written in terms of stability matrix elements [Ber19]. Therefore, the contribution associated to each trajectory is,

$$\frac{2^f}{\sqrt{|\det(\mathbf{M}(\mathbf{r}_j, t) + \mathbf{I})|}}. \quad (4.4)$$

Note that j -index denotes an arbitrary classical trajectory. We proceed putting all together and, after that the Weyl propagator reads,

$$U_W(\mathbf{r}, t) = 2^f \sum_j \frac{\exp\left\{\frac{i}{\hbar}S_j(\mathbf{r}, t)\right\}}{\sqrt{|\det(\mathbf{M}(\mathbf{r}_j, t) + \mathbf{I})|}}, \quad (4.5)$$

where the action has defined as $S_j(\mathbf{r}, t) = A_j(\mathbf{r}, t) - H_j(\mathbf{r}, t)t$ with $A_j(\mathbf{r}, t)$ denoting the symplectic area, and $H_j(\mathbf{r}, t)$ the Hamiltonian of the system.

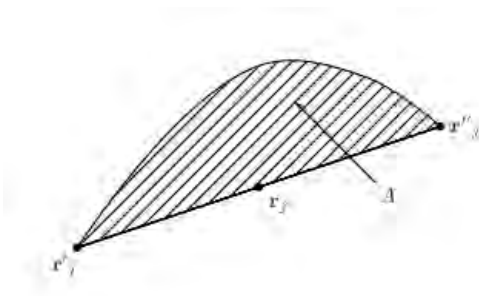


Figure 4.1: Berry's construction of chord rule in phase space: $A_j(\mathbf{r}'_j, t)$ corresponds to the symplectic area associated to \mathbf{r}'_j classical trajectory.

4.1 Semiclassical Wigner propagator from van Vleck's approach.

In order to obtain a semiclassical approximation to the Wigner function propagator, we must consider the previous representation for Weyl propagator, to be precise, we have replaced the Eq. (4.5) into Eq. (3.11), then we get

$$\begin{aligned}
 G_{WV}(\mathbf{r}'', t; \mathbf{r}', 0) &= \sum_{j\pm} \frac{1}{(\pi\hbar)^{2f}} \int_{-\infty}^{\infty} \exp\left\{ -\frac{i}{\hbar} (\mathbf{R} \wedge (\mathbf{r}'' - \mathbf{r}')) \right\} \\
 &\times \frac{\exp\left\{ \frac{i}{\hbar} (S_{j+}(\mathbf{r}_+, t) - S_{j-}(\mathbf{r}_-, t)) \right\}}{\sqrt{|\det(\mathbf{M}(\mathbf{r}_{j+}, t) + \mathbf{I})| |\det(\mathbf{M}(\mathbf{r}_{j-}, t) + \mathbf{I})|}} d\mathbf{R}^{2f}.
 \end{aligned} \tag{4.6}$$

The phase factor can be expressed in terms of \mathbf{r}_{\pm} coordinates (see Eq. 3.10) as follows,

$$\hbar\Phi(\mathbf{R}, \mathbf{r}'', \mathbf{r}') = \mathbf{R} \wedge (\mathbf{r}'' - \mathbf{r}') - \left(A_j(\mathbf{r}_+, t) - H_j(\mathbf{r}_+, t)t - A_j(\mathbf{r}_-, t) + H_j(\mathbf{r}_-, t)t \right). \tag{4.7}$$

According to the procedure involved in the stationary phase method, we must consider up to second order in approximation to phase factor. Therefore, the first variation with respect to \mathbf{R} -variable leads to the following constrain,

$$\nabla_{\mathbf{R}} \left(\mathbf{r}'' - \mathbf{r}' + S_{j+} \left(\frac{\mathbf{r}_{j+} + \mathbf{r}_{j-} + \mathbf{R}}{2}, t \right) - S_{j-} \left(\frac{\mathbf{r}_{j+} + \mathbf{r}_{j-} - \mathbf{R}}{2}, t \right) \right) = 0. \tag{4.8}$$

$$\mathbf{r}'' - \mathbf{r}' = \frac{\mathbf{r}'_{j+} - \mathbf{r}'_{j-} + \mathbf{r}''_{j+} - \mathbf{r}''_{j-}}{2}, \tag{4.9}$$

Now the contribution to the propagation is given in terms of classical trajectories, labeled as $j\pm$, moreover, the chord rule associated to each trajectory implies that,

$$\mathbf{r}' + \mathbf{r}'' \pm \mathbf{R} = \mathbf{r}'_{j\pm} + \mathbf{r}''_{j\pm}. \tag{4.10}$$

So, taking into account the Eqs. (4.9) and Eq. (4.10) is not hard to show that,

$$\begin{aligned}\mathbf{r}' &= (\mathbf{r}'_{j+} + \mathbf{r}'_{j-})/2, \\ \mathbf{r}'' &= (\mathbf{r}''_{j+} + \mathbf{r}''_{j-})/2.\end{aligned}\quad (4.11)$$

Thus, the semiclassical Wigner propagation is given by non-local contribution of trajectory pairs \mathbf{r}_{\pm} in such a way that initial and final phase-space points are localized in between of those trajectory pairs. This situation is shown below, see Fig. 4.2. On the other hand, the

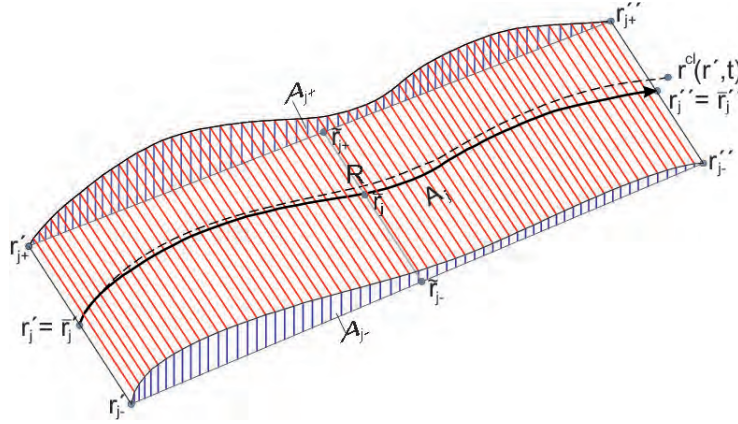


Figure 4.2: Symplectic areas entering in the semiclassical Wigner propagator. The $A_{j\pm}$ are the phases of the Weyl propagators and A_j is the area enclosed between the classical trajectories. The dashed line is the classical trajectory $\mathbf{r}^{cl}(\mathbf{r}', t)$, full line is the propagation path $\bar{\mathbf{r}}(\mathbf{r}', t)$ connecting the initial and final arguments of propagator.

first and second variations are evaluated at the stationary points,

$$\begin{aligned}\frac{\partial(\hbar\Phi(\mathbf{R}, \mathbf{r}'', \mathbf{r}'))}{\partial\mathbf{R}} &= 0, \\ \frac{\partial^2(\hbar\Phi(\mathbf{R}, \mathbf{r}'', \mathbf{r}'))}{\partial\mathbf{R}^2} &= \mathbf{J} \frac{\mathbf{M}(\mathbf{r}_{j-}, t) - \mathbf{M}(\mathbf{r}_{j+}, t)}{(\mathbf{M}(\mathbf{r}_{j+}, t) + \mathbf{I})(\mathbf{M}(\mathbf{r}_{j-}, t) + \mathbf{I})}.\end{aligned}\quad (4.12)$$

Now, we rewrite explicitly the Eq. (4.6), it will form into,

$$\begin{aligned}G_{WV}(\mathbf{r}'', t; \mathbf{r}', 0) &= \sum_{j\pm} \frac{1}{(\pi\hbar)^{2f}} \int_{-\infty}^{\infty} \exp\left\{-\frac{i}{\hbar}(S_{j\pm}(\mathbf{r}'', \mathbf{r}', t))\right\} \\ &\times \frac{\exp\left\{\frac{i}{\hbar}\left(\frac{\mathbf{R}^t}{2} \cdot \frac{\partial^2(\hbar\Phi(\mathbf{R}, \mathbf{r}'', \mathbf{r}'))}{\partial\mathbf{R}^2} \cdot \mathbf{R}\right)\right\}}{\sqrt{|\det(\mathbf{M}(\mathbf{r}_{j+}, t) + \mathbf{I})| |\det(\mathbf{M}(\mathbf{r}_{j-}, t) + \mathbf{I})|}} d\mathbf{R}^{2f}.\end{aligned}\quad (4.13)$$

Herein \mathbf{I} is a $2f \times 2f$ -dimensional unity matrix, and the full action associated to trajectory pairs have defined as,

$$S_{j\pm}(\mathbf{r}'', \mathbf{r}', t) = \frac{1}{2}(\mathbf{r}'_{j+} - \mathbf{r}'_{j-} + \mathbf{r}''_{j+} - \mathbf{r}''_{j-}) \wedge (\mathbf{r}'' - \mathbf{r}') + S_{j+} - S_{j-}.\quad (4.14)$$

Moreover, S_{j+} , S_{j-} are the classical actions along each trajectory. Finally, the Gaussian integration over \mathbf{R} -variable can be performed easily, furthermore, by taking into account that the contributions relate pairs of trajectories, the semiclassical Wigner-van Vleck propagator is,

$$G_{WV}(\mathbf{r}'', t; \mathbf{r}', 0) = \frac{4^f}{(2\pi\hbar)^f} \sum_{j\pm} \frac{2 \cos(S_{j\pm}(\mathbf{r}'', \mathbf{r}', t)/\hbar - f\frac{\pi}{2})}{\sqrt{|\det(\mathbf{M}(\mathbf{r}_{j+}, t) - \mathbf{M}(\mathbf{r}_{j-}, t))|}}. \quad (4.15)$$

It is worthy of mentioning that, the extra term appearing in the argument of the cosine function is associated with f -degrees of freedom, that come from the Gaussian integration.

4.2 Algorithms for the semiclassical propagation.

The initial value representation of semiclassical treatments has several advantages, in principle, IVR-methods depict the classical trajectories in a convenient form, *i.e.* the trajectories can be immediately determined by sampling the phase space occupied by the initial state. In fact, the semiclassical Wigner propagator takes advantage of this sampling schema and it can be integrated readily to Monte-Carlo Metropolis methods. In follows, we describe an algorithm that computes the contribution of these trajectory pairs efficiently for performing the semiclassical propagation in phase space.

4.2.1 Propagating delta functions.

Although delta function cannot represent an admissible state in phase space, it plays an important role in the context of Wigner function propagator. Namely, this is the simplest function that can be propagated, at the same time, it gives an origin to the concept of quantum-spot which is no more than the naked propagator evolved in phase space. This approach shows important quantum features along of time evolution of the propagator, and it allows a direct comparison without reference to an initial state. The algorithm for propagating delta functions comprises the following steps:

1. Define a local grid *e.g.* in polar coordinates around the initial point \mathbf{r}' , identifying trajectory pairs (satellites) $\mathbf{r}'_{j+}, \mathbf{r}'_{j-}$ with \mathbf{r}' in their middle.
2. Propagate trajectory pairs $\mathbf{r}_{j\pm}$ classically, then keeping track the symplectic area A_j between them.
3. Find the quantities of interest for the propagator, those are the amplitude and phase of each trajectory pair, then associate them to the final midpoints $\bar{\mathbf{r}}_j = \frac{\mathbf{r}''_{j+}, \mathbf{r}''_{j-}}{2}$, which corresponds to the deformed cone projected onto phase space.
4. Superpose the contributions of the two surfaces, after smoothing the amplitude and phase over $\bar{\mathbf{r}}_j$ within each of them.

4.2.2 Propagating smooth initial states.

In order to propagate a physically admissible initial state, the procedure must be different from previous algorithm. In fact, it is not appropriate to define an initial environment of "satellites" separately for each initial point in a distributed set according to the initial Wigner function, the algorithm is much more efficient to first define a set of N satellites and then find their $N_{pairs} = N(N-1)/2$ midpoints, then apply the above procedure to each N_{pairs} pairs, in this way $O(N^2)$ data points for the initial distribution can be calculated by propagating only N trajectories. There are various factors that has to be taken into account in order to choose the N points for the initial distribution. (i) The phase space extension of the initial state in dimensionless units, (ii) the closeness of the classical limit. The algorithm for propagating an admissible initial function comprises the following steps:

1. *Initial condition:* Define a set of the initial points \mathbf{r}'_j ($j = 1, 2, \dots, N$). it can be done in two ways: (i) Generate a swarm of N random phase-space points \mathbf{r}'_j covering approximately the same phase space region as the initial Wigner function $W_0(\mathbf{r}', t')$, then attach a weight factor to the trajectories from the midpoints $\bar{\mathbf{r}}_{jk} = (\mathbf{r}'_j + \mathbf{r}'_k)/2$, where $k = 1, 2, \dots, N$ and $j = 1, 2, \dots, k-1$. The Fig. 4.3 shows an illustrative representation of this situation, gray color depicts the area occupied by the initial state in phase space, after the contribution a swarm, we have a dense set of midpoints which covers the state. It is denoted by the symbol \otimes (red color). (ii) Depending on the initial state, find the exact distribution $W_{sat}(\mathbf{r}, t')$ that entails $W_0(\bar{\mathbf{r}}, t')$ as the distribution of its midpoints *i.e.*, it is self-convolution, and generates the \mathbf{r}'_j according to $W_{sat}(\mathbf{r}', t')$.

There is important comment about Monte Carlo-Metropolis methods and their possibilities to use them in this framework. In general, those schemes for sampling the phase space will also work and they can be adopted as an alternative method. However, an additional computational effort must be taken into account.

2. *Propagation:* Propagate all N satellite points \mathbf{r}'_j along the classical trajectories, keeping track of their respective stability matrices $\mathbf{M}(\mathbf{r}'_j, t')$ and their N_{pair} actions S_{jk} .
3. *Evaluation of the final state:* Find the value of the Wigner propagator $G_{WV}(\bar{\mathbf{r}}''_{jk}, t; \bar{\mathbf{r}}'_{jk}, 0)$ at each of the final midpoints $\bar{\mathbf{r}}''_{jk} = \frac{\bar{\mathbf{r}}'_j + \bar{\mathbf{r}}'_k}{2}$. Calculate a coarse-grained final distribution as an average over these data points, possibly taking into account the weight $W_0(\bar{\mathbf{r}}', 0)$ attached in 1. to each midpoint.

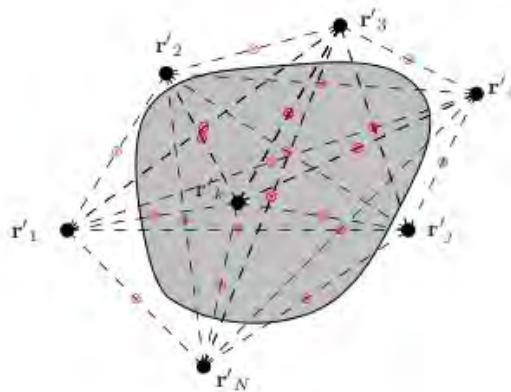


Figure 4.3: Initial phase space points covering smooth initial distribution, An ensemble of random points \mathbf{r}'_j ($j = 1, 2, \dots, N$) serves as initial conditions for N classical trajectories, give rise to $(N(N - 1)/2)$ midpoint paths starting in the centers $\bar{\mathbf{r}}'_{jk} = (\mathbf{r}'_j + \mathbf{r}'_k)/2$ (red dots) and defines the support for the semiclassical Wigner propagator

4.2.3 Single time step.

The propagation is accomplished numerically, as a sequence of L discrete steps $t_l \rightarrow t_{l+1}$, $l = 0, 1, 2 \dots L - 1$, $t_l = t + \Delta t$, $\Delta t = (t - t')/L$ the input required to perform a single time step $t_l \rightarrow t_{l+1} = lt + \Delta t$ comprises:

1. The classical trajectories and their coordinates in phase space $\mathbf{r}_j(t_l)$ $j = 1, 2 \dots N$.

2. The Hamiltonian forces,

$$\dot{\mathbf{r}}_j(t_l) = \mathbf{J}^t \nabla H(\mathbf{r}_j(t_l)), \quad (4.16)$$

3. The stability matrices along of the classical trajectories,

$$\dot{\mathbf{M}}(t_l) = \mathbf{M}(t_l) \mathbf{J}^t \frac{\partial^2 H(\mathbf{r}_j(t_l))}{\partial \mathbf{r}_j^2(t_l)}. \quad (4.17)$$

These stability matrices describes the linear response of the systems to the small variations of the initial conditions \mathbf{r}' .

The propagation is achieved considering the following steps,

- The increment of N trajectories $\Delta \mathbf{r}_j(t_l) = \mathbf{J}^t \nabla H(\mathbf{r}_j(t_l))$,
- The increment of N stability matrices.

$$\Delta \mathbf{M}(t_l) = \mathbf{M}(t_l) \mathbf{J}^t \frac{\partial^2 H(\mathbf{r}_j(t_l))}{\partial \mathbf{r}_j^2(t_l)} \Delta t. \quad (4.18)$$

- The increments of the N_{pair} actions $k = 1, 2 \dots N$ $j = 1, 2 \dots k - 1$

$$\Delta S_{jk}(\mathbf{r}'', \mathbf{r}') = (\mathbf{r}_k(t_l) - \mathbf{r}_j(t_l)) \wedge (\Delta \mathbf{r}_k(t_l) + \Delta \mathbf{r}_j(t_l)) / 2 - (H(\mathbf{r}_k(t_l)) - H(\mathbf{r}_j(t_l))) \Delta t. \quad (4.19)$$

- Finally the Wigner function at t_{l+1} is evaluated as a coarse-grained of its values at N_{pair} of $\bar{\mathbf{r}}''_{jk}$ then,

$$W(\bar{\mathbf{r}}_{j,k}, t_{l+1}) = \frac{4^f}{(2\pi\hbar)^f} \frac{2 \cos(S_{jk\pm}(t_{l+1})/\hbar - f\frac{\pi}{2})}{\sqrt{|\det(\mathbf{M}(\mathbf{r}_j, t_{l+1}) - \mathbf{M}(\mathbf{r}_k, t_{l+1}))|}}, \quad (4.20)$$

as a weight average over the data points contained in a given phase space bin α .

$$W(\mathbf{r}_\alpha, t_{l+1}) = \sum_{\bar{\mathbf{r}}_{j,k} \in \alpha} W(\bar{\mathbf{r}}_{j,k}, t_{l+1}) W_0(\bar{\mathbf{r}}_{j,k}). \quad (4.21)$$

4.3 Numerical applications.

In this section, we shall consider different numerical applications to the semiclassical Wigner propagator. Particularly, we are interested in aspects concerning to the performance of the semiclassical approximation in the context of wave packet dynamics, moreover, to study the advantages or its possible faults in the semiclassical propagation of non-classical states. Lets start considering the time evolution of localized initial state in a Morse potential, more precisely, for the purpose of comparison, we follows the same procedure described in the chapter 3 involving the exact Wigner propagator. Indeed, the parameter values for localized initial state and the Morse potential are the same as previously. The Fig. 4.4 shows the time evolution of naked Wigner van Vleck propagator, from this point of view important quantum features in phase space are revealed, more precisely, the nodelines structure that appears in the quantum-spot of the Fig 3.1 are reproduced qualitatively, *i.e.* the deformation of the quantum-spot along of time evolution are quiet similar. Moreover, the semiclassical approximation defines an area in phase space where the two trajectory pairs can contribute to each phase space point. also, the structure formed and its boundaries originate caustics in phase space where the two trajectory pairs collapse into one.

The Fig. 4.5 shows several snapshots of the semiclassical propagation based on Wigner van Vleck propagator, evidently the approximation based on trajectory pairs reproduce at least qualitatively the deformation of the wave packet along of time evolution, and it captures those features that are manifested in phase space, like the oscillatory fringes where the distribution takes negative values. In fact, the droplet shape of the distribution can be explained in terms of the underlying structure associated to the propagator, more precisely, it is shown in the Fig. 4.6 where is considered the time-evolved Gaussian state, it is depicted by contour lines, and superimposed the Wigner propagator from semiclassical (panel a) and quantum calculations (panel b). On the other hand, the performance of the semiclassical approximation is more evident in the autocorrelation function. It is shown in the Fig. 4.7 for semiclassical, classical and quantum calculations. here the accuracy of the semiclassical method is impressive.

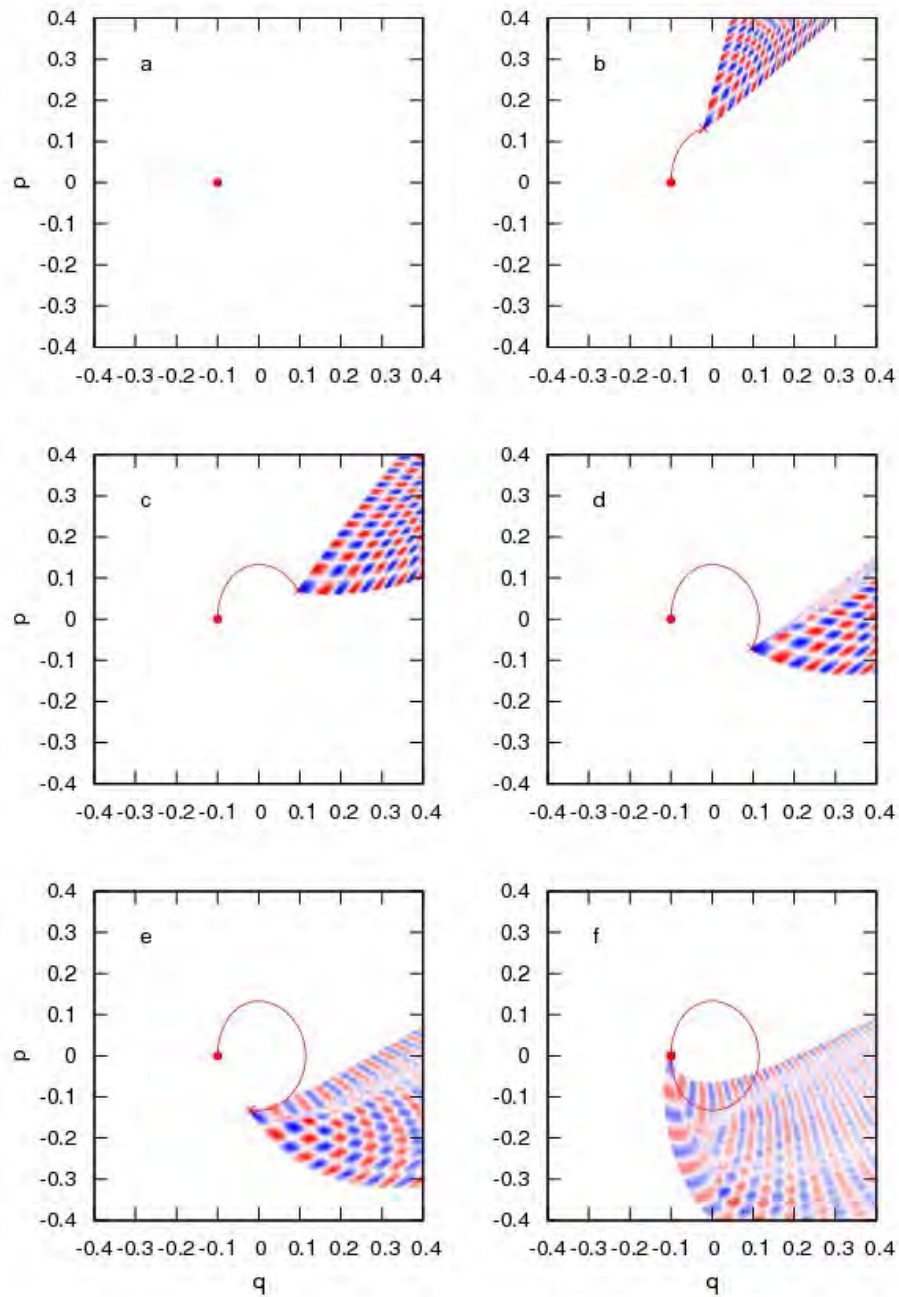


Figure 4.4: Time evolution of the Wigner propagator in the Morse potential from semi-classical approximation at times, $t = 0$ (panel a), 0.5072 (b), 1.0144 (c), 1.5216 (d), 2.0288 (e), 2.536 (f). The underlying classical trajectory has been launched at $\mathbf{r}_0 = (-0.1, 0)$. Parameter values are $D = 1$, $\alpha = 1.25$, $\hbar = 0.005$. Color code ranges from red (negative) through white (zero) through blue (positive).

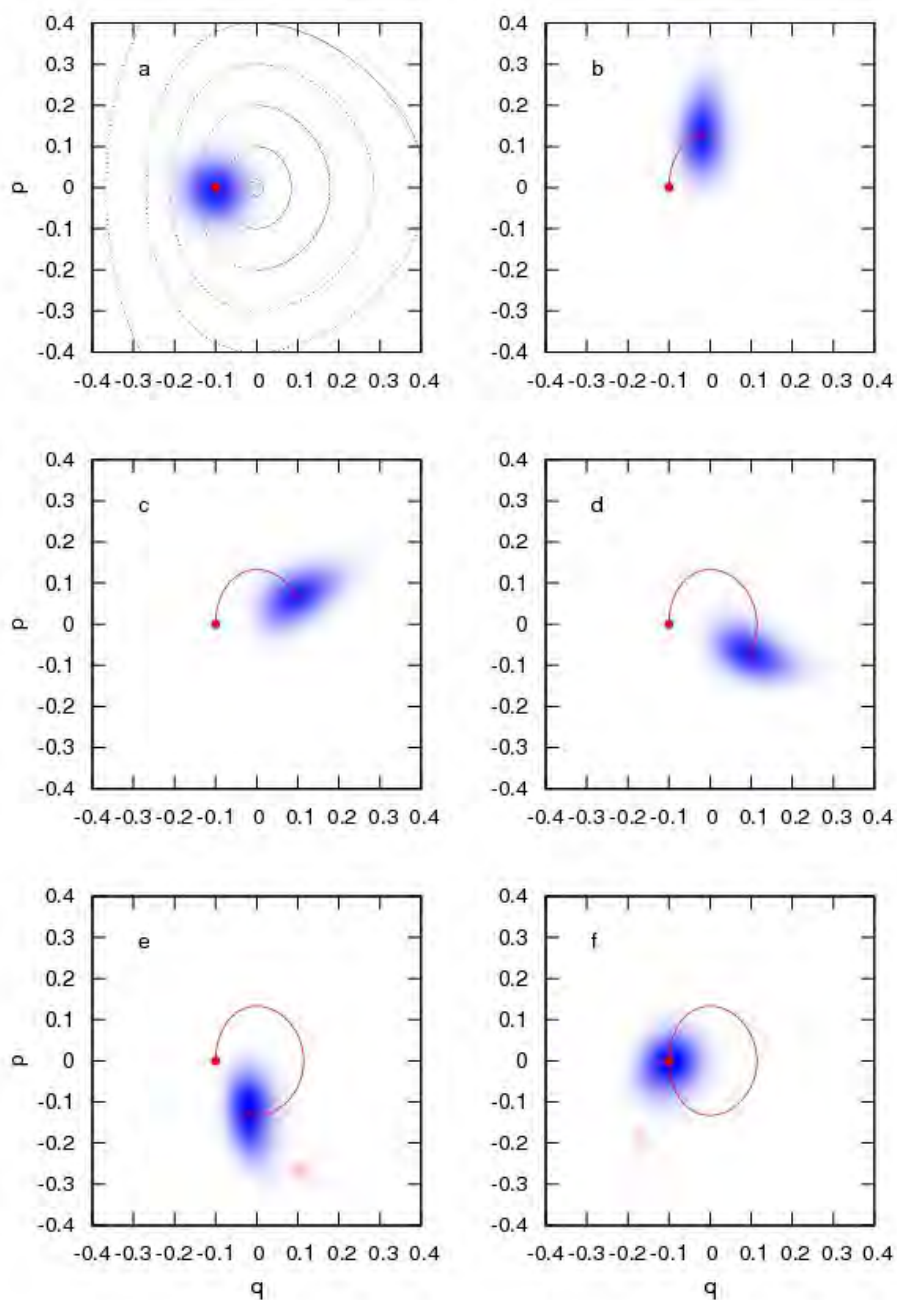


Figure 4.5: Time evolution of an initial Wigner function (Gaussian state) in the Morse potential for the semiclassical approximation at times $t = 0$ (panel a), 0.5072 (b), 1.0144 (c), 1.5216 (d), 2.0288 (e), 2.536 (f). In panel a, some contour lines of the potential are shown superimposed. The underlying classical trajectory has been launched at $\mathbf{r}_0 = (-0.1, 0)$. Parameter values are $D = 1$, $\alpha = 1.25$, $\hbar = 0.005$.

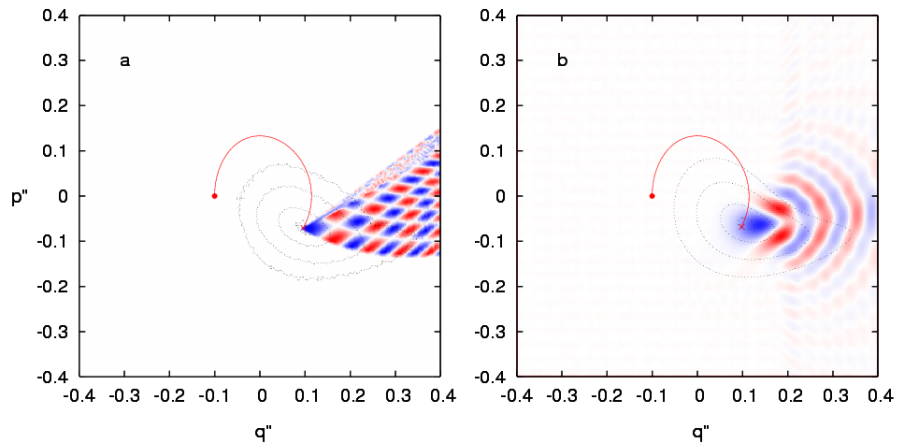


Figure 4.6: Comparison of time-evolved Wigner initial state (black contour lines), from semiclassical Wigner van-Vleck propagator (panel a) and to the exact quantum calculation (panel b).

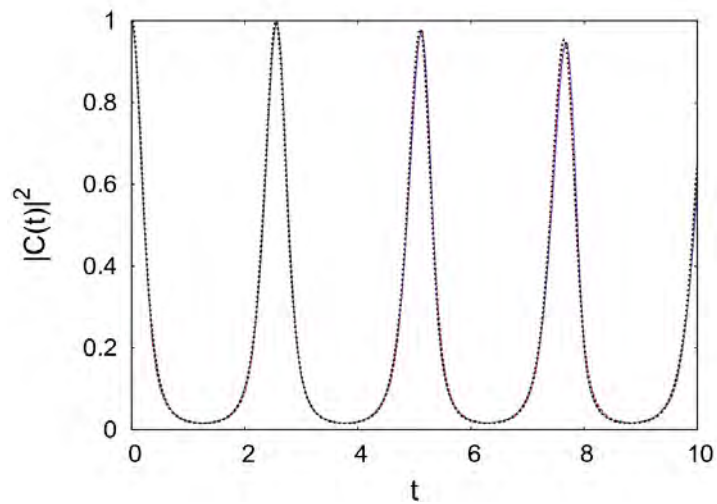


Figure 4.7: Autocorrelation function for a Gaussian initial state in a Morse potential, for the semiclassical Wigner propagator (dashed line, red color) as compared to an exact quantum result (full line, blue color), and classical calculation (dotted line, black color) for a time involving exactly four periods of the underlying classical trajectory.

4.3.1 Propagating stationary states

As it is well-known in basic quantum mechanics that, the time evolution of eigenstates are invariant in time, and therefore not much attention has been paid to this. However, an interesting discussion was presented in a remarkable work by Lee and Scully [LS82] in relation to the semiclassical propagation of Wigner eigenstates. Particularly, they introduced the concept of Wigner or quantum trajectories that are a kind of trajectory that governs fully the quantum evolution in phase space. Even though these trajectories are not well-defined in terms of classical mechanics, they have been considered by several authors [Lee95, Raz19, Tra11] as an alternative method for semiclassical propagation of Wigner functions. We confront the ideas exposed by Lee and Scully with the semiclassical Wigner van vleck propagator. Furthermore, we present convincing arguments; why the concept of flow in phase space along of Wigner trajectory is misleading.

In follows, we present briefly the Scully's ideas for suggesting that the Wigner trajectories are plausible for semiclassical propagation of Wigner functions. Namely, *(i)* if a quantum system is prepared in one of its energy eigenstates, it should be remain in the same eigenstate throughout. In terms of the Wigner function, it means that each phase-space point should move in such a way that the Wigner function does not change in time. *(ii)* The phase-space flow along of classical trajectories cannot reproduce the quantum dynamics, therefore those trajectories are quantum, in sense that they follows the full quantum evolution given by the Moyal equation. Moreover, they argued that for the case of Wigner eigenstate, those Wigner trajectories are manifested along of surfaces on which the Wigner function takes the same value, *i.e.* the equi-Wigner surfaces. In order to illustrate this situation, the Fig. 4.8 shows the ground and second excited eigenstate for Morse oscillator, the same figure some contours (dotted lines) and the classical trajectory (full line, red) are shown. Particularly, we have chosen the classical trajectory at energy E which has the same eigenenergy E_n where the Wigner eigenstate is strongly localized.

We find that in both cases the classical trajectory follows the "Wigner trajectory", more precisely, the corresponding contour at this energy, but is observed a large for excited eigenstates. One of the main characteristics of semiclassical approaches is that they represent a significant improvement to the simple classical propagation, the Fig. 4.9 illustrates how to achieve it by propagating along the midpoints of non-identical trajectory pairs. In practice, we consider an initial phase-space point \mathbf{r}' at energy E_2 for a given Wigner contour, then we increase the initial separation $\check{\mathbf{r}}'_j = \mathbf{r}'_{j+} - \mathbf{r}'_{j-}$ for several trajectory pairs launched in $\mathbf{r}'_{j\pm}$. Although the midpoint paths $\bar{\mathbf{r}}_j(t) = [\mathbf{r}_{j-}^{\text{cl}}(t) + \mathbf{r}_{j+}^{\text{cl}}(t)]/2$ (denoted by \times -symbol) move towards the Wigner contour with increasing $\check{\mathbf{r}}'$, they do not approach asymptotically. As is shown in figure, the increasing of separation the midpoint path moves far away from the contour, indicating that it does play no particular role for the quantum propagation in phase space.

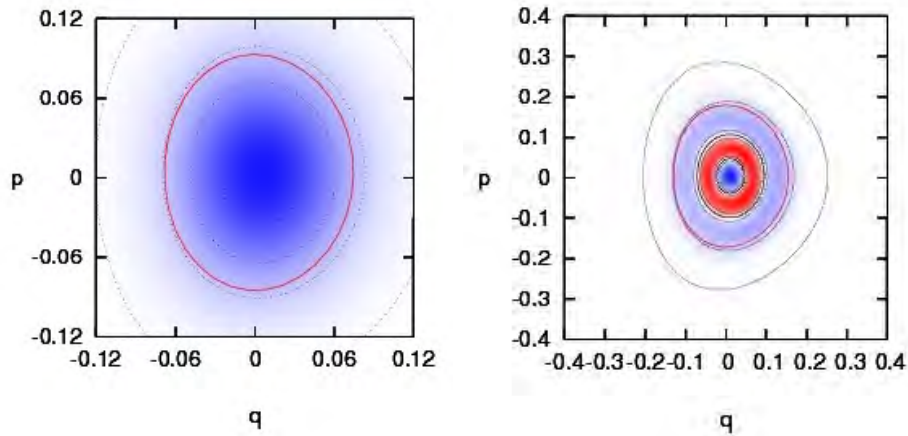


Figure 4.8: Wigner representation of the ground state $n = 0$ (panel a) and the second excited state $n = 2$ (panel b) of the Morse potential (dotted contour lines), compare to the classical orbits at the corresponding eigenenergies E_n . Parameter values are $D = 1$, $\alpha = 1.25$, $\hbar = 0.005$.

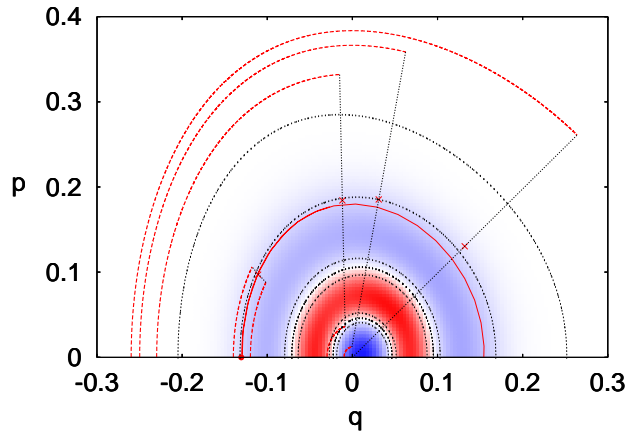


Figure 4.9: Wigner representation of the second excited state of the Morse oscillator. (contours are represented as black dotted lines), compared to the classical orbit $\mathbf{r}_{E_2}^{\text{cl}}(t)$ at the corresponding eigenenergy E_2 (full line, red) and to midpoint paths $\bar{\mathbf{r}}_j(t) = [\mathbf{r}_{j-}^{\text{cl}}(t) + \mathbf{r}_{j+}^{\text{cl}}(t)]/2$ (\times -symbol, red) for pairs of classical trajectories $\mathbf{r}_{j\pm}^{\text{cl}}(t)$ (dashed lines, red), with common initial midpoint $\bar{\mathbf{r}}_j = \mathbf{r}_{E_2}^{\text{cl}}(0)$ but increasing initial separation $\bar{\mathbf{r}}'_j \equiv (\bar{p}'_j, \bar{q}'_j) = \mathbf{r}'_{j+} - \mathbf{r}'_{j-}$ with $\bar{p}'_j = 0$ and $\bar{q}'_j = 0.002, 0.2, 0.24, 0.26$ (see text). Parameter values are $D = 1$, $a = 1.25$, $\hbar = 0.005$.

On the other hand, from theoretical point of view, in principle, we cannot talk about trajectories in sense of quantum mechanics. However, the discussion presented by Lee and Scully insinuates the existence of a deterministic flow that moves along the contour lines of the Wigner eigenstate, but a critical point emerges in relation to classical flow around of these Wigner trajectories, and how it maintains invariant the phase-space flow. If it is considered that this flow in phase space would flows in terms of classical propagator, it cannot completely be true, because, only the classical trajectories can do that, then it could be a smother propagator that nevertheless leaves invariant the Wigner eigenstate. Therefore, the semiclassical Wigner propagation cannot be reduce to a deterministic phase-space flow along classical or Wigner trajectories. The Fig. 4.10 shows the quantum-spot for semiclassical Wigner propagator and quantum result, indeed, the propagator appears as a smooth distribution that cannot be replaced by a delta function on the classical trajectory or Wigner co

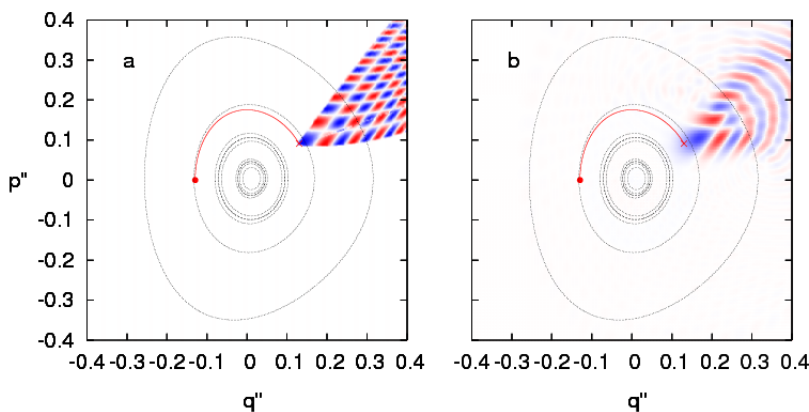


Figure 4.10: Semiclassical Wigner-van Vleck propagator (panel a) and the corresponding quantum result (panel b) for the Morse potential at time $t = 1.5216$. They are compared to the classical orbit $\mathbf{r}_{E_2}^{cl}$ and the contours of the Wigner-eigenstate. The initial point $\mathbf{r}' = \mathbf{r}^{cl}(0)$ is the same as Fig. 4.9. Parameter values are $D = 1$, $\alpha = 1.25$, $\hbar = 0.005$.

In order to illustrate the performance of the semiclassical Wigner van Vleck propagator for time evolution of Wigner eigenstates, we consider a more demanding test by propagating the second excited eigenstate in the Morse potential. In the Fig. 4.11 shows the deviation of the autocorrelation function from quantum result, *i.e.* $1 - |C(t)|^2$, in relation to this, the Fig. 4.12 shows a superposition of a cross section of the Wigner eigenstate $W_2(\mathbf{r})$ at time $t = 0$.

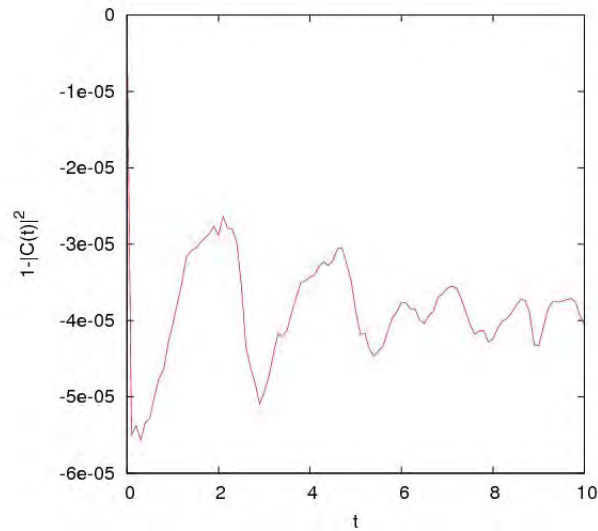


Figure 4.11: Deviation of autocorrelation function from exact value 1 (quantum calculation) for second excited eigenstate in the Morse potential. The parameter values are the same as Fig. 4.9.

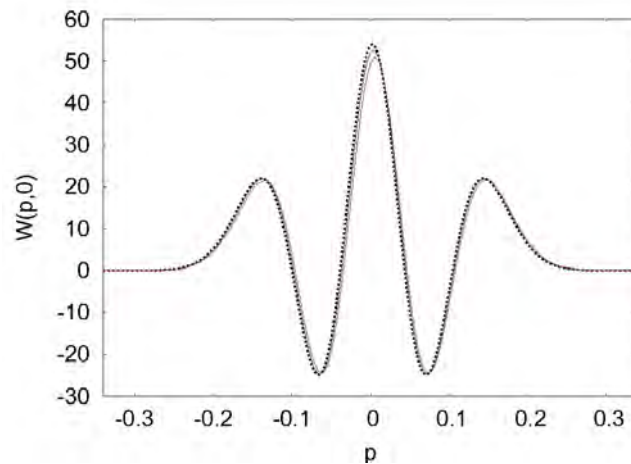


Figure 4.12: Cross section at $q = 0$ of the Wigner eigenfunction $W_2(\mathbf{r})$ at time $t = 10$. The quantum result (full line, blue) as compare to classical calculation (dotted line, black color) and the semiclassical Wigner van Vleck propagation (dashed line, red color).

As a complementary test for our semiclassical Wigner propagator, we take advantage of the fact that, the reference [LS82] is based on a study of the Morse oscillator from Wigner trajectories, In follows we consider this model for comparison purposes, more precisely, we find that our semiclassical approximation describes the time evolution of Wigner eigenstates with high accuracy in terms of autocorrelation function, much better than Wigner trajec-

jectories approach. In order to illustrate this, we are monitoring the autocorrelation function for the same case as was considered in the previous reference. The Fig. 4.13 compares our semiclassical Wigner propagation method with Wigner trajectories and classical propagation, respectively. Evidently, the semiclassical propagation by trajectory pairs represents an improvement to the classical propagation in phase space.

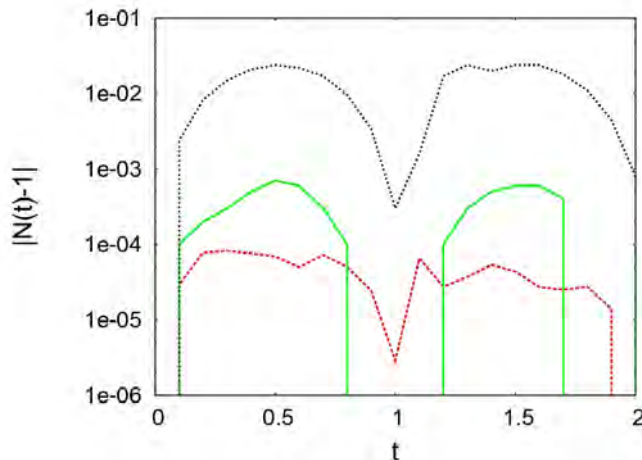


Figure 4.13: Accuracy of the autocorrelation function for the ground state $W_0(\mathbf{r})$ of the Morse oscillator (equivalent to the norm conservation) propagated with the semiclassical approximation to the Wigner propagator (dashed line, red color), a deterministic flow along Wigner trajectories (full line, green color), and the classical Liouville's propagator (dotted line, black color, data taken from Ref. [LS82]), at discrete times running from $t = 0$ through 2 by steps of 0.1. The values stated are the deviations from the exact value 1. Parameter values are $D = 0.15$, $a = 1$, $\hbar = 1.0$.

4.3.2 Propagating Schrödinger cats.

The time evolution of Wigner function has been considered long time ago, in fact, one of the most representatives studies about semiclassical Wigner propagation was presented by E. Heller in his seminal 1976 paper [Hel89]. Basically he argued that the semiclassical propagation of Wigner functions fails due to those off-diagonal terms of the density matrix, more precisely, those terms are manifested in the Wigner representation as cross terms that encodes the quantum coherences. It is well-known in the scientific community that the quantum coherences are a pure quantum manifestation and it has no classical analogue, therefore their propagation is not a simple task [LM07], and much less for those semiclassical approaches based on classical trajectories. In order to perform our semiclassical Wigner propagation method. We here consider the propagation of Schrödinger cats prepared as a superposition of two coherent states given by Eq. (3.43) with variable separation d initially

in position. In the Wigner representation the Schrödinger cat reads,

$$W_{\text{cat}}(\mathbf{r}) = W_-(\mathbf{r}) + W_+(\mathbf{r}) + W_{\times}(\mathbf{r}), \quad (4.22)$$

where $\mathbf{r}_{\pm} = \mathbf{r}_0 \pm (0, d)$ and those terms are defined as follows,

$$\begin{aligned} W_{\pm}(\mathbf{r}) &= \exp\{-[p_{\pm}^2 + \gamma^2 q_{\pm}^2]/\gamma\hbar\}/\pi, \\ W_{\times}(\mathbf{r}) &= \exp\{-[(p - p_0)^2 + \gamma^2(q - q_0)^2]/\gamma\hbar\} \\ &\quad \times \cos(2(p - p_0)d/\hbar). \end{aligned} \quad (4.23)$$

The Fig. 4.14 shows the time-evolved Schrödinger cat for a time $t = 0.3$, the semiclassical Wigner propagator reproduces the interference pattern associated to the quantum coherences, besides of Gaussian envelopes. Is worthy of mentioning that, the quantum coherences are propagated by means of non-local contribution of classical trajectories. In this way, we expect that our method would captures others quantum features which has no classical analogue.

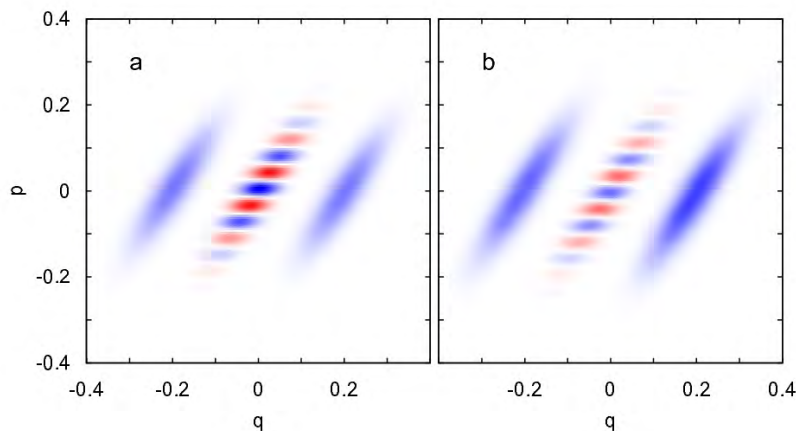


Figure 4.14: Schrödinger-cat states time-evolved in the Morse potential at time $t = 0.3$. The exact quantum calculation (panel a) as compare to semiclassical propagation from Wigner van Vleck propagator (panel a). Parameter values are $m = 0.5$, $D = 1$, $\alpha = 1.25$, $\hbar = 0.005$. The initial midpoint and separation of the Schrödinger-cat are $(q_0, p_0) = (0.3, 0)$, $d = 1$, respectively.

4.3.3 Propagation in the presence of classical chaos

Besides dynamical coherence effects, complex classical dynamics constitutes a major challenge for propagation schemas in molecular physics. The two one-dimensional models discussed in the preceding subsections as Morse potential are strongly anharmonic but remain integrable.

In order to test our semiclassical method also in the presence of chaos and to check its scalability towards higher dimensions, we consider a two-freedom system consisting of Morse oscillators coupled linearly through the positions, a standard model for complex molecular dynamics [CJ01], with a potential

$$V_{2\text{Morse}}(q_1, q_2) = V_{\text{Morse}}(q_1) + V_{\text{Morse}}(q_2) + cq_1q_2, \quad (4.24)$$

where $V_{\text{Morse}}(q_i)$, $i = 1, 2$ are Morse potentials, Eq. (3.32) and c is the coupling parameter. Starting from regular dynamics at $c = 0$, the system follows the Kolmogorov-Arnol'd-Moser scenario [LL92] with increasing c and becomes fully chaotic for $c \gg 1$. We here concentrate on the value $c = 0.3$, where phase space is mixed. As initial condition, we choose a two-dimensional minimum-uncertainty Gaussian $W(\mathbf{r}) = W(\mathbf{r}_1)W(\mathbf{r}_2)$, with $W(\mathbf{r}_i)$, $i = 1, 2$, as in Eq. (3.44), centered within a major chaotic subregion, see inset of Fig. 4.15. The

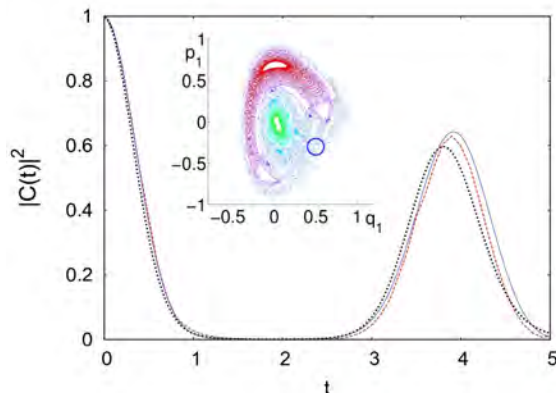


Figure 4.15: Autocorrelation function for two coupled Morse potentials (4.24) at $c = 0.3$. Parameter values are $m = 0.5$, $D = 1$, $a = 1.25$, $\hbar = 0.125$, the initial centroid is $(q_{10}, p_{10}, q_{20}, p_{20}) = (0.5, -0.3, 0.4322, 0)$, corresponding to a total energy $E = 0.5$. Inset: Poincaré surface of section at $p_2 = 0$ of the corresponding classical dynamics. Different initial conditions encoded by colors. The blue circle is the contour of the initial Gaussian enclosing a Planck cell.

Fig. 4.15 shows the autocorrelation function for first major revival of the probability. The exact quantum result (full line, blue color) is compared to semiclassical Wigner propagator (dashed line, red color), and classical propagation (dotted line, black color). Indeed, the semiclassical approach reproduces reasonably well the autocorrelation function, and shows a tendency to improve on the classical propagation. Evidencing the rôle of dynamical quantum effects in this system.

4.4 Perturbation theory and the semiclassical propagator.

A well-known that, any semiclassical approach based on second order in approximation must coincide with the quantum result for quadratic potentials. However, this situation is not evident from semiclassical Wigner-van Vleck propagator, and cannot be verified easily from a direct numerical implementation. Therefore, we analyze the asymptotic limits of weak anharmonicity, short time propagation and the classical limit for the Wigner propagator.

In follows, we shall consider a one-dimensional harmonic oscillator with small cubic anharmonicity, that is

$$H(p, q) = \frac{p^2}{2m} + \frac{m\omega^2}{2}q^2 + \epsilon q^3, \quad (4.25)$$

with m and ω denoting the mass and frequency of the oscillator, respectively. In order to obtain the expressions for the ingredients of the semiclassical Wigner van Vleck propagator, lets assume that in the regime of weak anharmonicity the cubic term is manifested as a perturbation, *i.e.*, $\epsilon \ll 1$. Therefore, the perturbation theory can be applied to obtain the equations of motion up to first order in approximation. Thus, the perturbed trajectories can be written as,

$$\begin{aligned} p_\epsilon(\tau) &= -m\omega q_0 \sin(\tau) + p_0 \cos(\tau) \\ &\quad - \epsilon \left(\frac{3p_0^2(\tau - \sin(\tau) \cos(\tau))}{2m^2\omega^3} + \frac{3p_0q_0 \sin^2(\tau)}{m\omega^2} + \frac{3q_0^2(\tau + \sin(\tau) \cos(\tau))}{2\omega} \right), \\ q_\epsilon(\tau) &= q_0 \cos(\tau) + \frac{p_0 \sin(\tau)}{m\omega} \\ &\quad - \epsilon \left(\frac{3p_0^2(\tau^2 - \sin^2(\tau))}{4m^3\omega^4} + \frac{3p_0q_0(\tau - \sin(\tau) \cos(\tau))}{2m^2\omega^3} + \frac{3q_0^2(\tau^2 + \sin^2(\tau))}{4m\omega^2} \right). \end{aligned} \quad (4.26)$$

where p_0, q_0 define the initial conditions in phase space, and the corresponding time scale as $\tau = \omega t$. To be precise with the notation, we have introduced the following phase-space vectors $\mathbf{r}_\epsilon''(\mathbf{r}', \tau) = (p_\epsilon(\tau), q_\epsilon(\tau))$ together with $\mathbf{r}' = (p_0, q_0)$. Moreover, we consider the vectors from perturbed trajectories

$$\mathbf{r}_{\epsilon\pm}''(\tau) = \mathbf{r}_\epsilon''(\mathbf{r}' \pm \tilde{\mathbf{r}}', \tau), \quad (4.27)$$

$$\tilde{\mathbf{r}}_\epsilon''(\mathbf{r}', \tilde{\mathbf{r}}', \tau) = (\mathbf{r}_{\epsilon+}'' + \mathbf{r}_{\epsilon-}'')/2, \quad (4.28)$$

$$\Delta\mathbf{r}_\epsilon''(\mathbf{r}', \tilde{\mathbf{r}}', \tau) = \tilde{\mathbf{r}}_\epsilon''(\mathbf{r}', \tilde{\mathbf{r}}', \tau) - \mathbf{r}_\epsilon''(\mathbf{r}', \mathbf{0}, \tau). \quad (4.29)$$

The previous equations denote the trajectory pairs with initial points displaced by $\tilde{\mathbf{r}}'$ from \mathbf{r}' , the corresponding centers and deviations of final midpoints trajectory which start in \mathbf{r}' , respectively. Particularly, the deviation takes the form,

$$\Delta p_\epsilon''(\mathbf{r}', \tilde{\mathbf{r}}', \tau) = \left(\frac{3\epsilon}{2\omega} \right) \begin{pmatrix} \tilde{p}' \\ \tilde{q}' \end{pmatrix}^T \begin{pmatrix} \frac{2\tau^3}{3} & \tau^2 \\ \tau^2 & 2(\tau - \frac{\tau^3}{3}) \end{pmatrix} \begin{pmatrix} \tilde{p}' \\ \tilde{q}' \end{pmatrix} + O(\epsilon^2, \tau^4) \quad (4.30)$$

$$\Delta q''(\mathbf{r}', \tilde{\mathbf{r}}', \tau) = \left(\frac{3\epsilon}{2m\omega^2} \right) \begin{pmatrix} \tilde{p}' \\ \tilde{q}' \end{pmatrix}^T \begin{pmatrix} \frac{\tau^4}{6} & \frac{\tau^3}{3} \\ \frac{\tau^3}{6} & 2(\tau^2 - \frac{\tau^4}{6}) \end{pmatrix} \begin{pmatrix} \tilde{p}' \\ \tilde{q}' \end{pmatrix} + O(\epsilon^2, \tau^5) \quad (4.31)$$

Is worthy of mentioning that the validity of the previous equations is restricted in time to $\tau \ll 2\pi$. At this point, we can proceed to compute the amplitude and phase factor associated to the semiclassical Wigner propagator. However, it is more convenient to express these quantities in terms of $\Delta \mathbf{r}''_\epsilon$. In practice, this corresponds to express the final argument of the propagator relative to the classical trajectory starting in \mathbf{r}' , instead of initial displacements $\tilde{\mathbf{r}}'$. To achieve we have used a simple transformations that diagonalize simultaneously the Eq. (4.30) and Eq. (4.31) which are basically a quadratic form. Followed to this, the semiclassical Wigner propagator is,

$$G_W(\mathbf{r}'', t, \mathbf{r}', 0) = 2\pi\hbar\beta [2\frac{t}{m}\Delta p''^2 - 12\Delta p''\Delta q'' + 12\frac{m}{t}\Delta q''^2]^{-1/4} \\ \times \left\{ \cos \left[\frac{2\beta}{3^{3/2}\hbar} (\Delta r''_+ - \Delta r''_-)^{3/2} \right] + \sin \left[\frac{2\beta}{3^{3/2}\hbar} (\Delta r''_+ + \Delta r''_-)^{3/2} \right] \right\}, \quad (4.32)$$

with $\beta = m^{3/4}\epsilon^{-1/2}t^{-5/4}$ and the deviation coordinates explicitly reads,

$$\Delta r''_- = (1 + \sqrt{3}) \sqrt{\frac{t}{m}} \Delta p'' - 2\sqrt{3\frac{m}{t}} \Delta q'', \\ \Delta r''_+ = (1 - \sqrt{3}) \sqrt{\frac{t}{m}} \Delta p'' + 2\sqrt{3\frac{m}{t}} \Delta q''. \quad (4.33)$$

Although this representation of the semiclassical propagator has been derived principally for the analysis of weak anharmonicity, it evidently diverges in limit $\epsilon \rightarrow 0$. This particular situation shows that in this limit the stationary points coalesce, and the stationary phase method breaks down. This difficulty can overcome by considering the uniform approximation method, it basically removes the singularities by taking into account a third order in approximation and frequently leading to Airy functions, This approach avoid a number of difficulties associated to the stationary phase method.

In order to obtain an uniform approximation for semiclassical Wigner propagator, we take into account that the action is manifestly odd-function for \mathbf{R} -variable, see Eq. (4.6). Moreover, we can uniquely reconstruct an effective action that contains only linear and cubic terms in the same variable \mathbf{R} . Thus, the semiclassical Wigner propagator can be evaluated in terms of Airy functions as follows,

$$G_W(\mathbf{r}'', t; \mathbf{r}', 0) = \frac{4\sqrt{3}}{\alpha^{2/3}} \text{Ai} \left(\frac{\Delta r''_-}{\alpha^{1/3}} \right) \text{Ai} \left(\frac{\Delta r''_+}{\alpha^{1/3}} \right), \quad (4.34)$$

with $\alpha = 3\epsilon\hbar^2 t^{5/2} m^{-3/2}$. From this representation can be recovered the short time approximation given by Eq. (4.32) for the semiclassical Wigner propagator, more precisely, to achieve this, we replace the Airy functions by the asymptotic representation for large negative values [Ae84],

$$\text{Ai}(-x) \rightarrow \pi^{-1/2} \left(\frac{3}{2} \right)^{1/4} x^{-3/8} \sin \left(\frac{2}{3} x^{3/2} + \frac{\pi}{4} \right). \quad (4.35)$$

together with a simple trigonometric property, *e.g.*,

$$\sin(x)\sin(y) = \frac{1}{2}(\cos(y-x) - \cos(x+y)). \quad (4.36)$$

On the other hand, The uniform approximation allows us to evaluate the asymptotic limits of interest as weak anharmonicity, short time propagation and the classical limit for the Wigner propagator, it is done by considering formally: $\lim_{\alpha \rightarrow 0}$ in the Eq. (4.34) with the help of property of Airy functions [VS04],

$$\lim_{\kappa \rightarrow 0} \kappa^{-1} \text{Ai}(x/\kappa) = \delta(x). \quad (4.37)$$

Thus, the propagator takes the form,

$$\begin{aligned} G_W(\mathbf{r}'', t; \mathbf{r}', 0) &= 4\sqrt{3}\delta(\Delta r''_-)\delta(\Delta r''_+), \\ &= \delta(\Delta \mathbf{r}''). \end{aligned} \quad (4.38)$$

Here we have considered the Eqs. (4.33) and the properties of the delta function. Moreover, by taking into account the dependence of α on parameters ϵ , \hbar and t , this includes the classical limit and $t \rightarrow 0$.

In follows we show the corresponding numerical applications accordingly to this section, the Fig. 4.4 shows a comparison in phase-space of the Wigner propagator from different versions previously discussed. However, in the panel a, we are include for comparison reasons the numerical result of the Wigner propagator based on phase-space path integral for the special case of cubic potential, it is considered in more detail in the chapter 7.

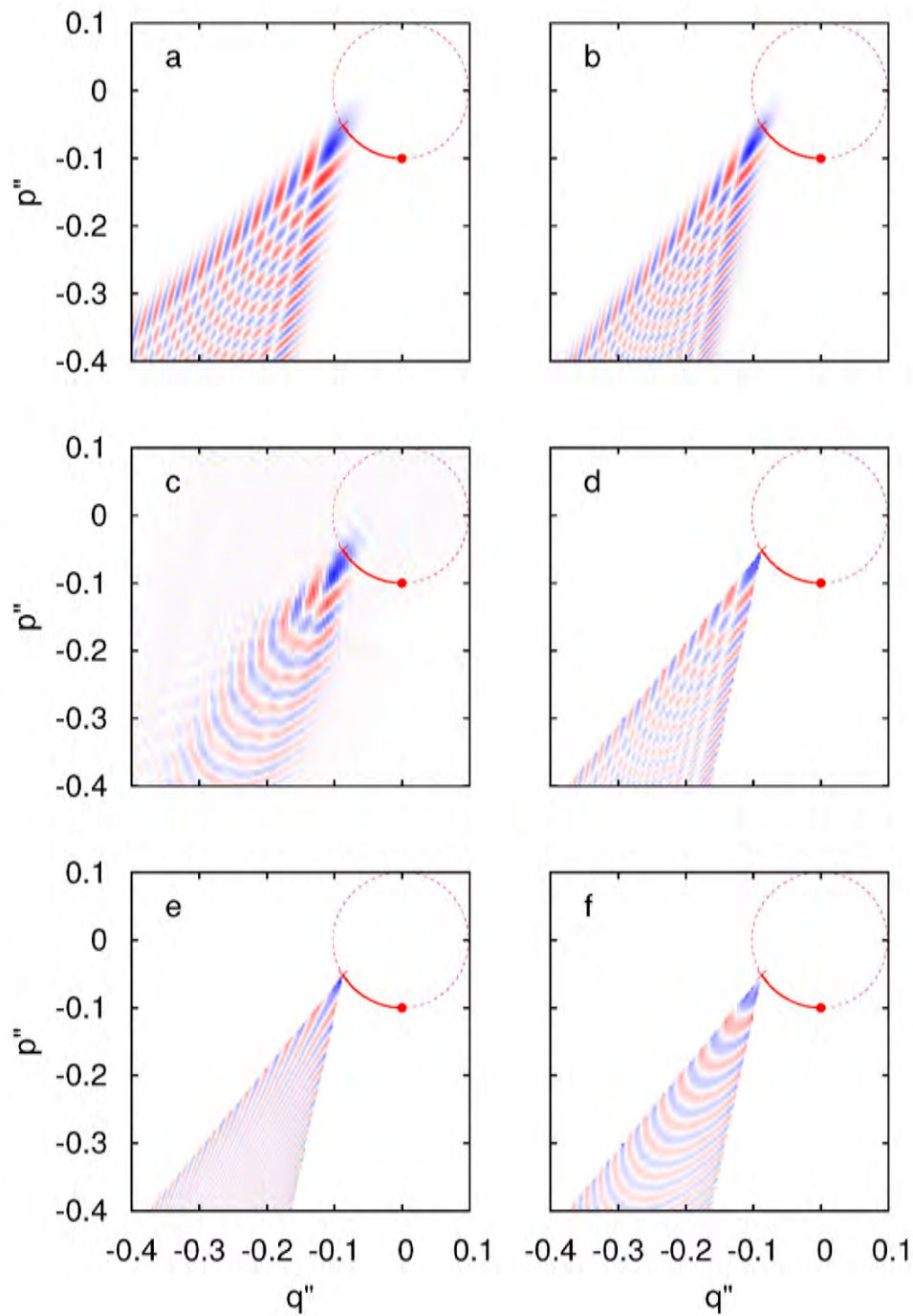


Figure 4.16: Different versions of the Wigner propagator for a harmonic oscillator in the regime of weak anharmonicity as a function of final phase-space coordinates (q'', p'') at time $\tau = \pi/3$. Wigner propagator from phase-space path integrals approach (Eq. (X)) (panel a), uniform approximation for short times (Eq. 4.34) (b), exact quantum calculation (Eq. (3.30)) (c), semiclassical approximation based on van Vleck approach (Eq. (4.32) (d)), and the contributions to Eq. (Eq. (4.32) corresponding to hyperbolic (cosine term) (e), and elliptic trajectory pairs (sine term) (f)). Parameters values are $\hbar = 0.01$, $\epsilon = 0.2$, $m = 1$, $\omega = 1$. The underlying classical trajectory (full line, red) has been launched at $(0, -0.1)$.

Chapter 5

Midpoints distribution and Random numbers

In this chapter, we shall address the discussion about importance of sampling methods in order to perform the semiclassical propagation from Wigner van Vleck approach. Furthermore, we describe a novel algorithms for sampling procedure which will allow us to obtain the corresponding exact midpoints distribution which entails the quantum initial state to be propagated directly in phase space.

One of the drawbacks of the semiclassical approximations is the dependence of the results on the initial parameters, thus it cannot define a criteria for the reliability of semiclassical calculations. In fact, several proposal have been considered in the past in order to formulate an approximation to the propagator as a phase-space integral over initial conditions of classical trajectories that evolve in time. Basically, the classical actions are associated to phases and the stability matrices are associated to amplitudes, however, from this approach the phases produce strong oscillations of the integrand, as a result of this, the semiclassical methods shows low convergence with respect to number of trajectories. In order to overcome these difficulties, a number of authors have considered alternative approximations, that in practice corresponds to a smoothing of the existing oscillations in all semiclassical approaches. For example, the linearization method, the stationary phase Monte-Carlo integration and integral-filtering techniques, they neglect the quantum fluctuations (strong oscillations) associated with highly non-classical paths. In one hand, it is well-known in the context of semiclassical propagation that the classical trajectories should be explore all admissible phase space for capturing quantum features. On the other hand, it becomes in a demanding and inefficient task. In order to surmount this inconvenient several methods have been developed. There are well-known methods, namely, the Monte-Carlo (MC) and MC-Metropolis shemas which have been plagued several branches of the physics, particularly the semiclassical approximations. Due to these methods are based on strategies for sampling a function in an optimal way. In practice a non-uniform distribution can be sampled analytically or from uniform distributions of a random numbers generator by applying an appropriate transformation. More compli-

cated distributions can be sampled by the acceptance-rejection method, which compares the desired distribution against a distribution which is similar or known analytically. This task usually requires a lot of samples from the random numbers generator in order to obtain an acceptable accuracy, particularly for high dimensional systems.

5.1 Generating Random Numbers.

In practice, many numerical simulations need a random numbers generator either for setting up initial configurations or for generating a new ones. In fact, such model does not exist in a computer program. A computer will always produce the same result if the input is the same. Then, a random numbers generator really means a pseudo random number generator that can generate a long sequence of numbers that imitate a given distribution. Although the pseudo random numbers generator are used frequently in computational physics, sometimes few attention has to be paid in it, and the numerical simulations could give wrong results. From computational point of view, the most important criteria for a good uniform random number generator are the following,

1. A good pseudo numbers generator should have a long period, which should be close to the range of the integers adopted.
2. A good pseudo numbers generator should have the best randomness, *i.e.*, there should only be a very small correlation among all the numbers generated in a long sequence. A simple test to the correlation function can illustrate the behavior associated to the pseudo random points, in principle, one can consider the correlation $\langle x_i x_{i+l} \rangle$ as a xy-plot of x_i and x_{i+l} . A good random numbers generator will have a very uniform distribution of the points for any $l \neq 0$. A poor generator may show stripes, lattices, or other inhomogeneous distributions.
3. A good pseudo number generator has to be very fast. In practice, we need a lot of random numbers in order to have good statistical results. Thus, the speed of the generator becomes in a very important factor, specially for molecular simulations where the high-dimensional spaces must be sampled.

5.2 Computing the exact midpoints distribution: Algorithms.

In the previous chapter, it was exposed in some detail an efficient algorithm in order to perform the semiclassical Wigner propagation. In fact, the main idea behind this algorithm is the sampling schema, and it could generate $N(N - 1)/2$ contributions of midpoints only by propagating N classical trajectories. Indeed, from this point of view the computational

effort is much less than the well-established Monte Carlo methods. On the other hand, the semiclassical Wigner propagation, in principle works for general quantum states, but the initial state should be represented in phase space. Here the question is, How could it be used the well-known sampling methods to find the midpoints distribution?.

In follows, we addressed this issue and discussion made for developing the algorithm, thats could be implemented easily,

5.2.1 Gaussian distributions.

Most of the numerical applications in the framework of semiclassical propagation are done by considering that the initial quantum state is represented by a Gaussian profile, in fact, there are several reasons to do that, namely, (i) many of those semiclassical approximations have been derived from Gaussian approaches, therefore, the sampling procedure is similar to well-known Monte-Carlo (MC) and MC-Metropolis methods where the initial state serves as a distribution function for sampling. (ii) From experimental point of view, the Gaussian states are much more accessible than any other. (iii) The sampling procedure is performed very fast by considering random points in phase space, where they follow some simple rules which are described in many of standard algorithms: as acceptance-rejection method, Box-Müller's or Ziggurat's algorithms for generating normal distributions (see Appendix C). In relation to that, we have derived an algorithm for computing the exact midpoints distribution in which those methods can be easily implemented for sampling the phase space.

In order to fix the notation and, also to introduce the spirit of the algorithm, lets start considering the one-dimensional case where $A(x)$ and $P(y)$ depicts the initial state and the desire midpoints distribution, respectively. We define the relation between both distributions as follows,

$$\begin{aligned} A(x) &= \int_{-\infty}^{\infty} \int_{-\infty}^{\infty} P(y)P(z)\delta(x - (y + z)/2)dydz, \\ &= 2 \int_{-\infty}^{\infty} P(y)P(2x - y)dy, \\ A\left(\frac{\alpha}{2}\right) &= 2(P * P)(\alpha). \end{aligned} \tag{5.1}$$

Where we have used $\alpha = 2x$, and the definition of convolution between two functions,

$$(f * g)(t) = \int f(\tau)g(t - \tau)d\tau. \tag{5.2}$$

Moreover, taking into account that a Fourier transform of a convolution is given by,

$$\mathcal{F}\{f * g\} = \sqrt{2\pi}\mathcal{F}\{f\}\mathcal{F}\{g\}. \tag{5.3}$$

Then, the Eq. (5.1) takes the form,

$$\begin{aligned}\mathcal{F}\left\{A\left(\frac{\alpha}{2}\right)\right\} &= 2\sqrt{2\pi}\mathcal{F}\{P * P\}, \\ &= 2\sqrt{2\pi}(\mathcal{F}\{P\})^2.\end{aligned}\tag{5.4}$$

Finally, we obtain explicitly the midpoints distribution by considering the inverse Fourier transform to the previous equation,

$$P(\alpha) = \mathcal{F}^{-1}\left\{\sqrt{\frac{\mathcal{F}\{A(\frac{\alpha}{2})\}}{2\sqrt{2\pi}}}\right\}.\tag{5.5}$$

It is worthy to mentioning that, for those cases where the Fourier transform can be applied analytically to the initial state, it will gives the equation for an exact midpoints distribution. For example, Gaussian states are the simplest. However, at this level of discussion, it is very premature to consider applications. In follows, we extend this method for two-dimensional case, in such a way, that it can be implemented directly in phase space as was done for numerical implementations.

Lets consider the procedure describe above, where $A(x_1, x_2)$ and $P(y_1, y_2)$ represents again an initial state and the midpoints distribution, repectively. Then we have,

$$\begin{aligned}A(x_1, x_2) &= \int_{-\infty}^{\infty} \int_{-\infty}^{\infty} \int_{-\infty}^{\infty} \int_{-\infty}^{\infty} P(y_1, y_2)P(z_1, z_2) \\ &\times \delta(x_1 - (y_1 + z_1)/2)\delta(x_2 - (y_2 + z_2)/2)dy_1dy_2dz_1dz_2, \\ &= 4 \int_{-\infty}^{\infty} \int_{-\infty}^{\infty} P(y_1, y_2)P(2x_1 - y_1)P(2x_2 - y_2)dy_1dy_2.\end{aligned}\tag{5.6}$$

Following a similar procedure to the one-dimensional case, we introduce a new variables as $\alpha_1 = 2x_1$ and $\alpha_2 = 2x_2$. Moreover, it can be assume that the sampling is done via bivariate distributions which are uncorrelated, *i.e.*, they are represented by two independent random variables as follows,

$$\begin{aligned}P(y_1, y_2) &= P(y_1)P(y_2), \\ P(z_1, z_2) &= P(z_1)P(z_2).\end{aligned}\tag{5.7}$$

As a consequence of replacing the Eqs. (5.7) into Eq. (5.6), and perform the integrations

over z_1, z_2 variables, we have simple expression for the midpoints distribution,

$$\begin{aligned}
 A\left(\frac{\alpha_1}{2}, \frac{\alpha_2}{2}\right) &= 4 \int_{-\infty}^{\infty} \int_{-\infty}^{\infty} P(y_1, y_2) P(z_1, z_2) \\
 &\quad \times \delta(x_1 - (y_1 + z_1)/2) \delta(x_2 - (y_2 + z_2)/2) dy_1 dy_2 dz_1 dz_2, \\
 &= 4 \int_{-\infty}^{\infty} \int_{-\infty}^{\infty} P(y_1, y_2) P(\alpha_1 - y_1) P(\alpha_2 - y_2) dy_1 dy_2, \\
 &= 4 \int_{-\infty}^{\infty} \int_{-\infty}^{\infty} P(y_1) P(\alpha_1 - y_1) P(y_2) P(\alpha_2 - y_2) dy_1 dy_2.
 \end{aligned} \tag{5.8}$$

In follows, the considerations about the convolution of two functions and the Fourier transform (see Eq. (5.2) and Eq. (5.3)) leads to the previous equation of two convolutions over α_1, α_2 . Then we have,

$$\begin{aligned}
 \mathcal{F}_{\alpha_1, \alpha_2} \left\{ A\left(\frac{\alpha_1}{2}, \frac{\alpha_2}{2}\right) \right\} &= 4 \left((P * P)(\alpha_1) \right) \left((P * P)(\alpha_2) \right), \\
 &= 8\pi \left(\mathcal{F}_{\alpha_1} \{ P(\alpha_1) \} \right)^2 \left(\mathcal{F}_{\alpha_2} \{ P(\alpha_2) \} \right)^2.
 \end{aligned} \tag{5.9}$$

Taking into account the inverse Fourier transform we obtain $P(\alpha_1, \alpha_2)$ as follows,

$$P(\alpha_1, \alpha_2) = \mathcal{F}_{\alpha_1}^{-1} \mathcal{F}_{\alpha_2}^{-1} \left\{ \sqrt{\frac{\mathcal{F}_{\alpha_1} \mathcal{F}_{\alpha_2} \{ A(\frac{\alpha_1}{2}, \frac{\alpha_2}{2}) \}}{8\pi}} \right\}. \tag{5.10}$$

Finally, it is the analytical expression for the midpoints distribution which entail the initial quantum state in phase space.

5.2.2 Example: Gaussian state.

Assume that a quantum system has a bounded energy spectrum, as is well-known, the ground state generally is described by a Gaussian function. Indeed, the Wigner function associated to this state can be calculated by taking the Weyl transform to it, as result of this, we obtain a normalized Gaussian function in phase space. For example, we consider the following Wigner function,

$$A(q, p) = \frac{ab}{\pi} \exp(-a^2 q^2 - b^2 p^2). \tag{5.11}$$

where a, b denotes the variances of the distribution function. Now performing the scaling into the Wigner state, it is,

$$A\left(\frac{q}{2}, \frac{p}{2}\right) = \frac{ab}{\pi} \exp\left(-\frac{a^2 q^2}{4} - \frac{b^2 p^2}{4}\right). \tag{5.12}$$

Particularly, we choose the symmetric Fourier transforms as follows,

$$\begin{aligned} h(\omega) = \mathcal{F}(f) &= \frac{1}{\sqrt{2\pi}} \int_{-\infty}^{\infty} e^{-ix\omega} f(x) dx, \\ f(x) = \mathcal{F}^{-1}(h) &= \frac{1}{\sqrt{2\pi}} \int_{-\infty}^{\infty} e^{ix\omega} h(\omega) d\omega. \end{aligned} \quad (5.13)$$

Finally, after simple mathematical manipulations involved in the Eq. (5.10), we arrive to an exact midpoints distribution for any Gaussian state in phase space.

$$P(q, p) = \frac{ab}{2\pi\sqrt{2}} \exp\left(-\frac{a^2 q^2}{2} - \frac{b^2 p^2}{2}\right). \quad (5.14)$$

Additionally, note that this result allow us to implement the sampling methods from normal distributions, in effect, our numerical applications were considered the Box-Müller (see AppendixC). On the other hand, the same approach exposed here can be extended for others initial distributions, in which, the Fourier transforms are relatively simple and the analytical calculations can be performed.

Chapter 6

Wigner propagator from phase-space path integrals

In this chapter we present the Wigner function propagator in terms of phase-space path integrals, and the semiclassical limit is considered from stationary phase method. In particular, the semiclassical limit leads to semiclassical Wigner van Vleck approach previously discussed. Briefly, we discuss the complex trajectories concept in this context and alternative to how they can be include into this formalism as an extension to the trajectory pairs.

6.1 Weyl propagator for small time step.

The path integrals formalism have been based in a particular way of thinking, *i.e.*, the full time evolution of quantum system is performed by a concatenation of small time steps of propagation. In fact, this mathematical treatment also can be extended to phase-space representation and applied to the Wigner propagator. In order to derive the Weyl propagator in in this framework, lets start dividing the full time of propagation as $\Delta t = t/N$, therefore, the evolution operator in an infinitesimal time step Δt takes the form $\hat{U}(\Delta t) = \exp\{-i\hat{H}\Delta t/\hbar\}$. Moreover, we assume that the Hamiltonian is given by $\hat{H} = \hat{p}^2/2m + V(\hat{q})$. So, the Weyl propagator reads,

$$\begin{aligned} U_W(\mathbf{r}, \Delta t) &= \int_{-\infty}^{\infty} \exp\left\{-\frac{i}{\hbar}\mathbf{p} \cdot \mathbf{y}\right\} \langle \mathbf{q} + \frac{\mathbf{y}}{2} | \hat{U}(t) | \mathbf{q} - \frac{\mathbf{y}}{2} \rangle d\mathbf{y}^{2f}, \\ &= \int_{-\infty}^{\infty} \exp\left\{-\frac{i}{\hbar}\mathbf{p} \cdot \mathbf{y}\right\} \langle \mathbf{q} + \frac{\mathbf{y}}{2} | \hat{I} - \frac{i\hat{H}\Delta t}{\hbar} \dots | \mathbf{q} - \frac{\mathbf{y}}{2} \rangle d\mathbf{y}^{2f}, \\ &= 1 - \frac{iH\Delta t}{\hbar} \dots, \\ &= \exp\left\{-\frac{i}{\hbar}H(\mathbf{r})\Delta t\right\} + O(t^2). \end{aligned} \tag{6.1}$$

Note that due to the Hamiltonian's structure, the Weyl correspondence between operators to c-numbers variables in phase space can be done simply by dropping the hat symbol to the operators, *e.g.* $T(\hat{p}) \rightarrow T(p)$, similarly for the potential function as follows $V(\hat{q}, t) \rightarrow V(q, t)$. The starting point in the process of building the path integrals, start always the infinitesimal propagator, thus, in order to obtain a representation to the Wigner propagator, we consider the Eqs. (3.10, 3.11) for a small time step, then by replacing the previous expression for the Weyl propagator given by Eq. (6.1). The Wigner propagator for a small time step is

$$G_W(\mathbf{r}_n, t_n; \mathbf{r}_{n-1}, t_{n-1}) = \frac{1}{(2\pi\hbar)^{2f}} \int_{-\infty}^{\infty} \exp\left\{-\frac{i}{\hbar}\Phi_n(\mathbf{R}_n, \mathbf{r}_n)\right\} d\mathbf{R}_n^{2f}, \quad (6.2)$$

where the phase factor is given by,

$$\Phi_n(\mathbf{R}_n, \mathbf{r}_n, \Delta t) = \Delta \mathbf{r}_n \wedge \mathbf{R}_n + \left\{H(\bar{\mathbf{r}}_n + \mathbf{R}_n/2) - H(\bar{\mathbf{r}}_n - \mathbf{R}_n/2)\right\} \Delta t. \quad (6.3)$$

In addition, we assume the discretization as follows, $\mathbf{r}_1 = \mathbf{r}'$, $\mathbf{r}_N = \mathbf{r}''$, $\Delta \mathbf{r}_n = \mathbf{r}_n - \mathbf{r}_{n-1}$, $\bar{\mathbf{r}}_n = (\mathbf{r}_n + \mathbf{r}_{n-1})/2$. Now, in order to build the finite-step version of the Wigner propagator we must consider the contribution of all infinitesimal propagators, in other words, taking into account the Eq. (3.26) where is manifested the Markovian property of the Wigner propagator. Thus, the Wigner propagator for finite-step version takes the form,

$$\begin{aligned} G_W(\mathbf{r}'', t; \mathbf{r}', 0) &= \frac{1}{(2\pi\hbar)^{2f}} \int_{-\infty}^{\infty} \prod_{k=1}^{N-1} d\mathbf{r}_k^{2f} G_W(\mathbf{r}_k, t_k; \mathbf{r}_{k-1}, t_{k-1}), \\ &= \int_{-\infty}^{\infty} \prod_{k=1}^{N-1} \frac{d\mathbf{r}_k^{2f}}{(2\pi\hbar)^{2f}} \int_{-\infty}^{\infty} \prod_{j=1}^N \frac{d\mathbf{R}_j^{2f}}{(2\pi\hbar)^{2f}} \exp\left\{-\frac{i}{\hbar}\Phi_n(\mathbf{R}_1 \cdots \mathbf{R}_N, \mathbf{r}_1 \cdots \mathbf{r}_N, \Delta t)\right\}. \end{aligned} \quad (6.4)$$

In addition, the phase of the propagator at this level reads,

$$\Phi_n(\mathbf{R}_1 \cdots \mathbf{R}_N, \mathbf{r}_1 \cdots \mathbf{r}_N, \Delta t) = \sum_{n=1}^N \Delta \mathbf{r}_n \wedge \mathbf{R}_n + \left\{H(\bar{\mathbf{r}}_n + \mathbf{R}_n/2) - H(\bar{\mathbf{r}}_n - \mathbf{R}_n/2)\right\} \Delta t. \quad (6.5)$$

Finally, the continuous version of the Wigner propagator is obtained by consider formally the $\lim_{N \rightarrow \infty}$ in the Eqs. (6.4, 6.5). Thus, the phase-space path integrals for the Wigner propagator reads,

$$G_W(\mathbf{r}'', t; \mathbf{r}', 0) = \frac{1}{(2\pi\hbar)^f} \int \int \mathcal{D}\mathbf{r}^{2f} \mathcal{D}\mathbf{R}^{2f} \exp\left\{-\frac{i}{\hbar}\Phi(\mathbf{R}, \mathbf{r})\right\}. \quad (6.6)$$

Where $\int \int \mathcal{D}\mathbf{r}^{2f} \mathcal{D}\mathbf{R}^{2f}$ denotes the measure associated to the infinite number of path integrations in phase space. On the other hand, the corresponding phase factor in the continuous limit is given by,

$$\Phi(\mathbf{R}, \mathbf{r}, t) = \int_0^t \left\{ \dot{\mathbf{r}}(\tau) \wedge \mathbf{R}(\tau) + H(\mathbf{r}(\tau) + \mathbf{R}(\tau)/2) - H(\mathbf{r}(\tau) - \mathbf{R}(\tau)/2) \right\} d\tau. \quad (6.7)$$

Moreover, we have the boundary conditions according to $\mathbf{R}(0) = \mathbf{r}'$ and $\mathbf{R}(t) = \mathbf{r}''$. In follows, we address the discussion about the semiclassical limit for the Wigner propagator from stationary phase method.

6.2 Semiclassical Limit.

The stationary phase method is a technique widely applied in the framework of semiclassical approximations. Principally, it allow to perform an integration procedure when phase factors are highly oscillatory (Fresnel integrals), in practice, most of semiclassical propagators are based under this schema. On the other hand, this mathematical tool plays an important role in path integrals formalims, basically it is considered in order to obtain the semiclassical limits, for example, it is well-known that the semiclassical limit of Feynman's path integrals leads to the van Vleck propagator. Similarly, the coherent state path integrals leads to semiclassical representation to the propagator in terms of complex trajectories [GJ94, BdAK⁺01].

So, we proceed to perform the stationary phase method to the Wigner propagator based on phase-space path integrals, therefore the stationary points are given by,

$$\frac{\partial\Phi(\mathbf{R}, \mathbf{r}, t)}{\partial\mathbf{R}} = 0, \quad \frac{\partial\Phi(\mathbf{R}, \mathbf{r}, t)}{\partial\mathbf{r}} = 0. \quad (6.8)$$

Where we obtain explicitly the following relations for \mathbf{R}, \mathbf{r} -variable as:

$$\dot{\mathbf{R}} = \mathbf{J} \left\{ \nabla H(\mathbf{r} + \mathbf{R}/2) - \nabla H(\mathbf{r} - \mathbf{R}/2) \right\}, \quad (6.9)$$

$$\dot{\mathbf{r}} = \frac{\mathbf{J}}{2} \left\{ \nabla H(\mathbf{r} + \mathbf{R}/2) + \nabla H(\mathbf{r} - \mathbf{R}/2) \right\}. \quad (6.10)$$

We introduce the new variables $\mathbf{r}_{\pm} = \mathbf{r} \pm \mathbf{R}/2$ into the previous equations, in such way, that we identify the trajectory pairs in phase space as follows,

$$\dot{\mathbf{r}}_{\pm} = \mathbf{J} \nabla H(\mathbf{r}_{\pm}). \quad (6.11)$$

In order to obtain the semiclassical limit, we focus on important aspects about the equivalence between phase factors involved in the semiclassical Wigner van Vleck propagator, and the Wigner propagator based on phase-space path integrals. Lets us consider a small time step for propagation, that is $\Delta t = t_{n-1} - t_n$ and the phase is given by Eq. (4.14) in the previous chapter. However, for this purpose a convenient notation is considered as follows, $\mathbf{r}'_{\pm} \rightarrow \mathbf{r}_{\pm, n-1}$, $\mathbf{r}''_{\pm} \rightarrow \mathbf{r}_{\pm, n}$ together with $\mathbf{r}'' \rightarrow \mathbf{r}_n$, $\mathbf{r}' \rightarrow \mathbf{r}_{n-1}$. Then we have,

$$\begin{aligned} S_{j\pm}(\mathbf{r}'', \mathbf{r}', \Delta t) &= \frac{1}{2}(\mathbf{r}_{n-1,+} - \mathbf{r}_{n-1,-} + \mathbf{r}_{n,+} - \mathbf{r}_{n,-}) \wedge (\mathbf{r}_n - \mathbf{r}_{n-1}) \\ &+ H\left(\frac{\mathbf{r}_{n-1} + \mathbf{r}_n + \mathbf{R}_n}{2}\right)\Delta t + H\left(\frac{\mathbf{r}_{n-1} + \mathbf{r}_n - \mathbf{R}_n}{2}\right)\Delta t. \end{aligned} \quad (6.12)$$

On the other hand, we know that the trajectories behave agree with the chord rule according to the Eq. (4.10) which can be solved for \mathbf{R} -variable and taking into account the latter notation, it reads,

$$\mathbf{R}_n = \frac{1}{2}(\mathbf{r}_{+, n-1} + \mathbf{r}_{+, n} - \mathbf{r}_{-, n-1} - \mathbf{r}_{-, n}). \quad (6.13)$$

Now, replacing the Eq. (6.13) into Eq. (6.12), and taking into account the corresponding text after Eq. (6.3) we have,

$$S_{j\pm}(\mathbf{R}_n, \mathbf{r}_n, \Delta t) = \mathbf{R}_n \wedge \Delta \mathbf{r}_n + H(\bar{\mathbf{r}}_n + \mathbf{R}_n/2)\Delta t + H(\bar{\mathbf{r}}_n - \mathbf{R}_n/2)\Delta t, \quad (6.14)$$

$$= \Phi_n(\mathbf{R}_n, \mathbf{r}_n, \Delta t). \quad (6.15)$$

Therefore, we conclude that those phases describe the same quantity, *i.e.*, the symplectic area enclosed by trajectory pairs plus the contribution associated to each trajectory through the Hamiltonian.

It is well-known from path integral formalism, that the propagation formally is given by a sum over all possible trajectories, however, in the semiclassical limit the classical trajectories contribute significantly [Sch81b, DCKB93], therefore, we replace $\int \mathcal{D}\mathbf{r} \rightarrow \sum_{j\pm}$, it is, in the semiclassical limit we have a sum over trajectory pairs. The derivation of the semiclassical propagator is described in the chapter 4. Note that it shows that in the semiclassical limit the the Wigner-van vleck propagator is recovered.

6.3 Complex trajectories.

The concept of complex trajectory has been referred by a number of authors in different contexts, in fact, many of the semiclassical approximations take into account this mathematical construction in order to overcome serious difficulties which arise from theoretical point of view. More precisely, the difficulties comes when the semiclassical methods aim to reproduce quantum phenomena which has no classical analogue. Perhaps, the most representative example with which the complex trajectories are found is the tunneling phenomena, it corresponds to a manifestation of the processes classically forbidden. The most simplest way to include the complex trajectories in the semiclassical approximations is by considering an extension to the complex plane, more precisely, this is accomplished by promoting the real trajectories to be complex. In this way, the concept of classical trajectory gets more general, and the time evolution takes place in the complex plane. According to the semiclassical limit previously discussed for Wigner propagator based on phase-space path integrals leads to Eq. (6.11). This equation only imposes the constrain that there are trajectory pairs, which are solutions to the Hamilton's equations and they contribute to the semiclassical propagation. But there is not restriction about their own nature, in fact, if we suppose that there are others kind of classical trajectories that are consistent with this requirements, in principle, they could be considered for semiclassical propagation. On the other hand, the Wigner van Vleck propagator imposes two additional constrains, specifically, they are given by the Eqs. (4.11), it means that, the initial phase-space point to be propagate must be located in the middle of the trajectory pairs, similarly for final phase-space point after propagation.

In order to introduce the complex trajectories in the semiclassical Wigner propagation, we take into account the previous discussion and introduce a new trajectory pairs, but in

this case being complex as follows,

$$\tilde{\mathbf{r}}_{\pm} = \mathbf{r}_{\pm} \pm i \tilde{\mathbf{R}}, \quad (6.16)$$

Note that, these complex trajectory pairs take into account that the midpoint always is real along of semiclassical propagation, in other words, the propagation start with a real phase-space point, then the trajectories follows a trip in a complex plane, but they finally give the contribution to the final phase-space point according to the expected in terms of trajectory pairs. In principle, those trajectories improve the semiclassical propagation, but here there is a price to be paid. This approach requires the solution of complex classical trajectories accordingly to

$$\tilde{\mathbf{r}}_{\pm} = \mathbf{J} \nabla H(\tilde{\mathbf{r}}_{\pm}). \quad (6.17)$$

In order to illustrate how the complex trajectory pairs can contribute strongly to the semiclassical Wigner propagation, we consider the double well potential (see section 3.4.2). The Fig. 6.1 shows a typical contribution due to midpoint trajectory based on complex trajectories pairs in phase space, more precisely, we have located the initial phase-space point close to the minimum, and the pair of complex trajectories also located inside of this well, it is indicated by the small dot (blue color) in the right well. In the panel b, we consider the same initial phase space point as panel a, but here we have considered one hundred complex trajectory pairs, they are shown in terms of their final phase-space coordinates (dots, red color). Note how most of the midpoint trajectories cross the barrier, although the trajectory pairs are located practically in the minimum of the well, In fact, in terms of classical mechanics those classical trajectories will never leave the well. In this way, the semiclassical Wigner propagation can be improve in the framework of complex trajectories.

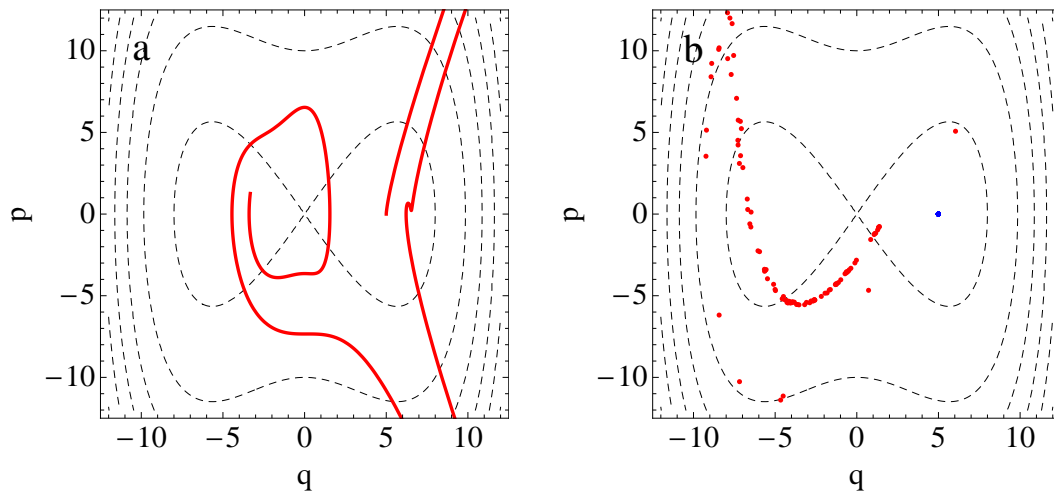


Figure 6.1: Phase space representation of the quartic double well (dashed lines, black). A typical midpoint trajectory based on complex trajectory pairs, the initial point is $(q', p') = (5, 0)$ and $\mathbf{r}'_{\pm} = (5, \pm 0.1)$, $\tilde{\mathbf{R}} = (5, 0.1)$ at time $t = 10$, (full line, red, panel a). Final coordinates of one hundred midpoint trajectories (dots, red, panel b) launched from right side (dot, blue) for the same initial conditions as panel a, except for $\tilde{\mathbf{R}}$ where the values have been choose randomness. Parameter values are $m = 1$, $\Delta = 1$.

Is worthy of mentioning that at the time of writting this part of thesis, we cannot be carry out the extesive numerical exploration supporting those ideas about the performance of semiclassical Wigner propagation from those complex trajectories, however, it is being object of study.

Chapter 7

Semiclassical Wigner propagator from phase-space path integrals

In this chapter we shall study a high order in approximation to the Wigner function propagator. More precisely, the uniform approximation method is considered in order to overcome the difficulties manifested in the semiclassical Wigner propagator based on van-Vleck approach. Also an analytical expression for this semiclassical propagator is derived in terms of Airy functions, and relevant applications are discussed.

7.1 Semiclassical Wigner propagator.

Although this semiclassical approximation to the Wigner propagator has been worked previously in the reference [TDS03, San05], we here consider the derivation of this propagator as a relevant issue in order to present this thesis more clearly, at the same time, it serves as support for the discussion about analytical solution to this propagator.

We start restricting the discussion to one-dimensional systems with the Hamiltonian given by $\hat{H} = \hat{p}^2/2m + \hat{V}(\hat{q})$. Thus, the Weyl correspondence allows us to replace operators by c-numbers in a simple way, *i.e.*, $\hat{p} \rightarrow p$, $\hat{q} \rightarrow q$, therefore the Hamiltonian in Weyl representation is $H = p^2/2m + V(q)$. On the other hand, the small time step version for phase factor of the Wigner function propagator is given by Eq. (6.3). Then we have,

$$\Phi_n(\mathbf{R}_n, \mathbf{r}_n, \Delta t) = -\left(\Delta q_n - \frac{\Delta t}{m}\bar{p}_n\right)P_n + \Delta p_n Q_n + \left(V(\bar{q}_n + Q_n/2) - V(\bar{q}_n - Q_n/2)\right). \quad (7.1)$$

together with the discretization given by $\Delta \mathbf{r}_n = \mathbf{r}_n - \mathbf{r}_{n-1}$, $\bar{\mathbf{r}}_n = (\mathbf{r}_n + \mathbf{r}_{n-1})/2$. By introducing a simple transformation $\mathbf{r}_n \rightarrow \mathbf{r}_n + \tilde{\mathbf{r}}_n$, and considering a Taylor expansion of the potential function up to third order around $\bar{q}_n \pm Q_n/2$, Also, we identify a couple of equations as

follows,

$$\begin{aligned}\Delta\tilde{q}_n - \frac{\Delta t}{m}\tilde{p}_n &= 0, \\ \Delta\tilde{p}_n + V'(\tilde{q}_n)\Delta t &= 0.\end{aligned}\tag{7.2}$$

Taking into account the continuous limit *e.g.*, $\Delta t \rightarrow 0$, $(\tilde{p}_n, \tilde{q}_n)$ satisfies the Hamilton's equations, therefore we denote them as $(p_n^{\text{cl}}, q_n^{\text{cl}})$ and defines the classical trajectory \mathbf{r}^{cl} . Moreover, the phase factor explicitly reads,

$$\Phi_n(\mathbf{R}_n, \mathbf{r}_n, \Delta t) = (\Delta q_n - T''(p_n^{\text{cl}})\tilde{p}_n\Delta t)P_n + (\Delta p_n + V''(q_n^{\text{cl}})\tilde{q}_n\Delta t)Q_n\tag{7.3}$$

$$+ \frac{1}{24}V'''(q_n^{\text{cl}})Q_n^3.\tag{7.4}$$

The integration over Q_n, P_n can now performed, and the small time step propagator Eq. (6.2) reads,

$$\begin{aligned}G_{WPI}(\mathbf{r}''_n, t_n; \mathbf{r}'_{n-1}, 0) &= \delta\left(\Delta q_n - \frac{\Delta t}{m}p_{n-1}\right)\left(\frac{V'''(q_n^{\text{cl}})\hbar^2\Delta t}{8}\right)^{-1/3} \\ &\times \text{Ai}\left[\left(\frac{V'''(q_n^{\text{cl}})\hbar^2\Delta t}{8}\right)^{-1/3}(\Delta p_n + V''(q_n^{\text{cl}})q_{n-1}\Delta t)\right].\end{aligned}$$

Now, by introducing the new set of variables as follows,

$$\begin{aligned}\check{p}_n &\equiv \left(mV''(q_n^{\text{cl}})\right)^{-1/4}p_n, & \check{q}_n &\equiv \left(mV''(q_n^{\text{cl}})\right)^{1/4}q_n, \\ \check{\tau}_n &\equiv \left(\frac{1}{mV''(q_n^{\text{cl}})}\right)^{3/4}\frac{V'''(q_n^{\text{cl}})\hbar^2}{8}\Delta t.\end{aligned}$$

We have that the small time step version for Wigner propagator is,

$$G_{WPI}(\mathbf{r}''_n, t_n; \mathbf{r}'_{n-1}, 0) = \delta(\check{q}_n - (\mathbb{M}_n\check{\mathbf{r}}_{n-1})_{\check{q}})\check{\tau}_n^{-1/3}\text{Ai}\left[\check{\tau}_n^{-1/3}(\check{p}_n - (\mathbb{M}_n\check{\mathbf{r}}_{n-1})_{\check{p}})\right],\tag{7.5}$$

together with,

$$\mathbf{M}_n = \begin{pmatrix} \cos\phi_n & -\sin\phi_n \\ \sin\phi_n & \cos\phi_n \end{pmatrix}\tag{7.6}$$

where \mathbf{M}_n is the stability matrix of the classical trajectory and $\phi_n = \arctan\left(\sqrt{\frac{V'''(q_n^{\text{cl}})\Delta t}{m}}\right)$. If $V''(q_n^{\text{cl}}) > 0$ it corresponds to elliptic case, otherwise, $V''(q_n^{\text{cl}}) < 0$ is the hyperbolic case. Now we take advantage of the Fourier-space where the calculations becomes simpler. To achieve this the Fourier transform is applied to Eq. (7.5), then by evaluation of continuous limit in Fourier-space the Wigner propagator takes the form,

$$G_{WPI}(\gamma'', t; \gamma', 0) = \exp\left(\frac{-i}{3}\int_0^t dt'(\sigma(t')\mathbf{M}(t')\gamma')_{\beta}^3\right)\tag{7.7}$$

with

$$\sigma(t) = \left(\frac{1}{mV''(q^{cl}(t))} \right)^{3/4} \frac{V'''(q^{cl}(t))\hbar^2}{8}, \quad (7.8)$$

and the continuous version for stability matrix as follows,

$$\mathbf{M}(t) = \begin{pmatrix} \cos(\phi(t)) & -\sin(\phi(t)) \\ \sin(\phi(t)) & \cos(\phi(t)) \end{pmatrix}, \quad (7.9)$$

together with,

$$\phi(t) = \int_0^t \sqrt{\frac{V''(q^{cl}(t'))}{m}} dt', \quad (7.10)$$

Finally, by considering the inverse Fourier transform and reordering the terms, the semiclassical Wigner propagator based on phase-space path integrals reads,

$$\begin{aligned} G_{WPI}(\mathbf{r}'', t; \mathbf{r}', 0) &= \frac{1}{(2\pi)^2} \int_{-\infty}^{\infty} \exp\left\{ -i(a\alpha^3 + [b\alpha^2 - \{(\mathbf{M}^{-1}(t)\mathbf{r}'')_{p''} - p'\}]\beta \right. \\ &\quad \left. + [c\beta^2 + \{(\mathbf{M}^{-1}(t)\mathbf{r}'')_{q''} - q'\}]\alpha + d\beta^3) \right\} d\alpha d\beta. \end{aligned} \quad (7.11)$$

Here the coefficients a, b, c, d are given explicitly:

$$\begin{aligned} a &= \frac{1}{3} \int_t^{t_0} \sigma(t') \sin^3(\phi(t')) dt', \\ b &= \int_t^{t_0} \sigma(t') \sin^2(\phi(t')) \cos(\phi(t')) dt', \\ c &= \int_t^{t_0} \sigma(t') \sin(\phi(t')) \cos^2(\phi(t')) dt', \\ d &= \frac{1}{3} \int_t^{t_0} \sigma(t') \cos^3(\phi(t')) dt', \end{aligned} \quad (7.12)$$

This representation has been already done in reference [TDS03]. But, few is known about this semiclassical approach. In fact, one part of this thesis aims contribute by studying numerical applications to this propagator. On the other hand, we made a relevant contribution to the formalism with the derivation of an analytical form to this approach.

7.2 Analytical expression for the Wigner propagator.

An additional step can be done for Wigner propagator based on phase-space path integrals, more precisely the Eq. (7.11) the aim is obtain an analytical expression in terms of the Airy functions. Lets start introducing a coordinate transformations as follows,

$$\beta = y_1 - \lambda_1 x_1, \quad \alpha = x_1, \quad \text{with} \quad 3d\lambda_1 = c. \quad (7.13)$$

After this, another transformation is introduced,

$$y_1 = y_2 - \lambda_2 x_2, \quad x_1 = x_2, \quad (7.14)$$

where λ_2 is defined as:

$$\lambda_2 = \left(\frac{2b_1^3}{-27a_1d_1^2 + \sqrt{118b_1^3d_1^3 + 729a_1^2d_1^4}} \right)^{1/3} - \left(\frac{-9a_1d_1^2 + \sqrt{12b_1^3d_1^3 + 81a_1^2d_1^4}}{18d_1^3} \right)^{1/3}, \quad (7.15)$$

where a_1, b_1, d_1 reads,

$$a1 = a + \frac{2c^3}{27d^2} - \frac{bc}{3d}, \quad b1 = b - \frac{2c^2}{3d}, \quad d1 = d. \quad (7.16)$$

Additionally, there are two new transformations, which are described by,

$$x_2 = x_3 - \lambda_3 y_3, \quad y_2 = y_3, \quad \text{with} \quad \lambda_3 = \frac{c_1}{2b_1}, \quad (7.17)$$

and the second one is,

$$x_3 = \frac{y_4 - x_4}{2\lambda_4}, \quad y_3 = \frac{y_4 + x_4}{2}, \quad (7.18)$$

then, a relationship between the new coefficients and older as follows

$$\text{with} \quad \lambda_4 = \left(\frac{b_3}{3d_3} \right)^{1/2}, \quad d_3 = d_2 - \frac{c_2^2}{4b_2}, \quad b_3 = b_2.$$

Hence, taking into account the corresponding Jacobian factors associated to the each transformations introduced before. Then by replacing all quantities in Eq. (7.11), and some algebraic manipulations, it is straightforward to obtain an intermediate representation to the semiclassical propagator in terms of new variables ξ, χ ,

$$G_{WPI}(\mathbf{r}'', t; \mathbf{r}', 0) = -\frac{1}{8\pi^2\lambda_4} \int_{-\infty}^{\infty} \exp\left\{-i[\Lambda x_4^3 + \Lambda y_4^3 + (\chi + \xi)x_4 - (\chi - \xi)y_4]\right\} dx_4 dy_4 \quad (7.19)$$

which explicit reads,

$$\begin{aligned} \xi(t) &= -\frac{1}{2\lambda_4(t)} \left\{ \left[(\mathbf{M}^{-1}(t)\mathbf{r}'')_{q''} - q' \right] + f(t) \left[(\mathbf{M}^{-1}(t)\mathbf{r}'')_{p''} - p' \right] \right\}, \\ \chi(t) &= -\frac{\lambda_3(t)}{2} \left\{ \left[(\mathbf{M}^{-1}(t)\mathbf{r}'')_{q''} - q' \right] + f(t) \left[(\mathbf{M}^{-1}(t)\mathbf{r}'')_{p''} - p' \right] \right\}, \\ &\times -\frac{1}{2} \left[(\mathbf{M}^{-1}(t)\mathbf{r}'')_{p''} - p' \right]. \end{aligned}$$

The last expressions explicitly shows the time-dependence, also we define a new new function as $f(t) = \lambda_1(t) + \lambda_2(t)$. Furthermore, the parameter $\Lambda(t)$ is related to the coefficients $a(t), b(t), c(t), d(t)$ as follows,

$$\Lambda(t) = \frac{d(t)}{8} \left[\frac{9d^2(t)\lambda_2^2(t) + 12b(t)d(t) - 4c^2(t)}{9d^2(t)\lambda_2^2(t) + 3b(t)d(t) - c^2(t)} \right]. \quad (7.20)$$

By considering an integral representation for the Airy functions [VS04],

$$\text{Ai}(z) = \frac{1}{\pi} \int_0^\infty \cos\left(\frac{t^3}{3} + zt\right) dt, \quad (7.21)$$

the Eq. (7.19) is analytically integrated, then the Wigner propagator reads,¹

$$G_{WPI}(\mathbf{r}'', t; \mathbf{r}', 0) = -\frac{1}{2\lambda_4 \sqrt[3]{9\Lambda(t)^2}} \text{Ai}\left(\frac{\chi(t) + \xi(t)}{\sqrt[3]{3\Lambda(t)}}\right) \text{Ai}\left(\frac{\chi(t) - \xi(t)}{\sqrt[3]{3\Lambda(t)}}\right). \quad (7.22)$$

7.2.1 Asymptotic limits $t \rightarrow 0, \hbar \rightarrow 0$.

In order to test the analytical solution given by Eq. (7.22), we check the asymptotic limits $t \rightarrow 0, \hbar \rightarrow 0$. Indeed, the coefficients $a, b, c, d, \sigma(t)$ in those limits vanish, *i.e.* $a = b = c = d = \sigma(t) = 0$. Moreover, the variables χ and ξ take the form,

$$\lim_{a,b,c,d \rightarrow 0} \chi = \frac{1}{4}(A - B), \quad (7.23)$$

$$\lim_{a,b,c,d \rightarrow 0} \xi = -\frac{1}{4}\sqrt{3}(A + B), \quad (7.24)$$

together with,

$$\lim_{a,b,c,d \rightarrow 0} \lambda_4 = \frac{2}{\sqrt{3}}, \quad (7.25)$$

$$\lim_{a,b,c,d \rightarrow 0} \Lambda = 0. \quad (7.26)$$

In this limit, the Eq. (7.22) reads,

$$G_{WPI}(\mathbf{r}'', 0; \mathbf{r}', 0) = -4\sqrt{3}\delta\left((1 + \sqrt{3})A - (1 - \sqrt{3})B\right) \delta\left((1 - \sqrt{3})A - (1 + \sqrt{3})B\right). \quad (7.27)$$

Here we have considered the property of the Airy function (see Eq. (4.37)). Also, it can be fully simplify by considering that the Dirac delta [Ae84] is represented by,

$$\delta(x) = \frac{1}{2\pi} \int_{-\infty}^{\infty} e^{itx} dt, \quad (7.28)$$

¹I enjoyed a lot of inspiring discussions with Leonardo Pachón and particularly because this equation is a result of our collaboration.

and using the reflection symmetry property of the δ -function the Eq. (7.27) can be written

$$G_{WPI}(\mathbf{r}'', 0; \mathbf{r}', 0) = -\frac{\sqrt{3}}{16\pi^2} \int_{-\infty}^{\infty} \exp\left\{-\frac{i}{4}[(1-\sqrt{3})A - (1+\sqrt{3})B]t\right\} \quad (7.29)$$

$$\times \exp\left\{-\frac{i}{4}[(1+\sqrt{3})A - (1-\sqrt{3})B]t'\right\} dt dt'. \quad (7.30)$$

By introducing the following transformations,

$$t = \frac{-(3+\sqrt{3})y - \sqrt{3}(x+y)}{6(1+\sqrt{3})}, \quad (7.31)$$

$$t' = \frac{-(1-\sqrt{3})y + (1+\sqrt{3})x}{4\sqrt{3}}, \quad (7.32)$$

into Eq. (7.29), we obtain that,

$$G_{WPI}(\mathbf{r}'', 0; \mathbf{r}', 0) = \int_{-\infty}^{\infty} \exp\left\{-\frac{i}{4}[xA - yB]\right\} \frac{dx dy}{64\pi^2}. \quad (7.33)$$

where we have considered that the Jacobian of the transformation is equal to $-1/(4\sqrt{3})$. Again we have used the Eq. (7.28) and the reflection symmetry property of the δ -function. Then the Eq. (7.33) can be fully simplify to

$$G_{WPI}(\mathbf{r}'', 0; \mathbf{r}', 0) = \delta(A)\delta(B), \quad (7.34)$$

or in terms of the phase-space coordinates,

$$\begin{aligned} G_{WPI}(\mathbf{r}'', 0; \mathbf{r}', 0) &= \delta((\mathbf{r}'')_{q''} - q')\delta((\mathbf{r}'')_{p''} - p') \\ &= \delta(\mathbf{r}'' - \mathbf{r}'). \end{aligned} \quad (7.35)$$

Note taht the Eq. (7.35) was considered when $t \rightarrow 0$, and $\mathbf{M}(t) \rightarrow \mathbf{I}$, it being \mathbf{I} the identity matrix.

7.2.2 Harmonic oscillator.

The previous Wigner propagator is easily calculated for simple case of quadratic potentials, it is straightforward shows that $\sigma(t) = 0$, therefore the coefficients take the value $a = b = c = d = 0$, it implies that the Eq. (7.35) is reduced as follows,

$$G_{WPI}(\mathbf{r}'', t; \mathbf{r}', 0) = \delta((\mathbf{M}^{-1}(t)\mathbf{r}'')_{q''} - q') \quad (7.36)$$

$$\delta((\mathbf{M}^{-1}(t)\mathbf{r}'')_{p''} - p'). \quad (7.37)$$

Moreover, $V'' = m\omega^2$ (harmonic oscillator), then $\phi(t) = \omega t$ and

$$\mathbf{M}(\phi(t)) = \begin{pmatrix} \cos\omega t & -\sin\omega t \\ \sin\omega t & \cos\omega t \end{pmatrix}, \quad (7.38)$$

Then, semiclassical Wigner propagator reduces to

$$G(\mathbf{r}'', t; \mathbf{r}', 0) = \delta(p \cos \omega t + m\omega q \sin \omega t - p_0) \quad (7.39)$$

$$\delta\left(q \cos \omega t - \frac{p}{m\omega} \sin \omega t - q_0\right). \quad (7.40)$$

This expression coincides with the classical propagation as is expected.

7.2.3 Semiclassical Wigner propagator and the asymptotic limits.

In follows, we study the asymptotic limits of the Wigner propagator previously derived, more precisely, the Eq. (7.22) is evaluated for large negative values accordingly to Eqs. (4.35) and Eq. (4.36). After additional simplifications the semiclassical Wigner propagator is given by,

$$G_{WVV}(\mathbf{r}'', t; \mathbf{r}', 0) = -\frac{(\chi^2 - \xi^2)^{-1/4}}{4\pi\lambda_4\sqrt{3\Lambda}} \left\{ \sin\left(\frac{2(\tilde{\xi}^{3/2} + \tilde{\chi}^{3/2})}{\sqrt{3\Lambda}}\right) + \cos\left(\frac{2(\tilde{\chi}^{3/2} - \tilde{\xi}^{3/2})}{\sqrt{3\Lambda}}\right) \right\}, \quad (7.41)$$

where $\tilde{\chi} = \xi - \chi$ and $\tilde{\xi} = -\xi - \chi$. Note that through these variables the dependence of the relevant quantities of the propagator. We here identify the cosine function with the contribution of hyperbolic points, in contrast to the sine function which corresponds to the contribution of elliptic points. They are the extrema of the action in the semiclassical Wigner propagator based on van Vleck's approach. In addition, a similar discussion have presented in section 4.4 for the corresponding asymptotic limits of $t \rightarrow 0$, $\hbar \rightarrow 0$ in which this propagator becomes spurious and diverge.

7.2.4 Path-integral approach for weak cubic nonlinearity.

In this section we consider again the case of harmonic oscillator with a small cubic anharmonicity, in fact, a relevant discussion has been presented in the section 4.4 from semiclassical propagator based on van Vleck approximation. However, we here follows a different approach, it is in terms of phase-space path integrals in order to obtain an analytical expression for the propagator. Assuming that the trajectory is close to the minimum, the linearized flow is elliptic. Then $\partial^3 V(q)/\partial q^3 \equiv V''' = m\omega^2/q_{\min} = \text{const}$, moreover, one can assume that $(V''/T'')^{1/2} \approx \omega = \text{const}$. In consequence $\sigma = (\hbar^2/8)(m\omega)^{-3/2}V''' = (\hbar^2/8)\sqrt{\omega/m}/q_{\min}$, and the stability matrix corresponds to a rotation by $\tau = \omega t$,

$$\mathbf{M}(t) = \begin{bmatrix} \cos \tau & -\sin \tau \\ \sin \tau & \cos \tau \end{bmatrix}, \quad (7.42)$$

and the phase of the Fourier transformed propagator for this system (see Eq. (7.7)) reduces to

$$\begin{aligned} \tilde{G}_{\text{WPI}}(\boldsymbol{\gamma}'', t; \boldsymbol{\gamma}', 0) &= \delta[\boldsymbol{\gamma}'' - \mathbf{M}(t)\boldsymbol{\gamma}'] \\ &\times \exp\left[\frac{-i\sigma}{3\omega} \int_0^\tau d\tau' (\alpha' \sin \tau' + \beta' \cos \tau')^3\right]. \end{aligned} \quad (7.43)$$

Then, introducing a new coordinates in a reference frame $\bar{\rho} = (\bar{\eta}, \bar{\xi})$ rotating by $\tau/2$ with respect to ρ ,

$$\bar{\eta} = \eta \cos \frac{\tau}{2} - \xi \sin \frac{\tau}{2}, \quad \bar{\xi} = \eta \sin \frac{\tau}{2} + \xi \cos \frac{\tau}{2}, \quad (7.44)$$

Then the propagator after inverting the Fourier transform takes the form,

$$\begin{aligned} G_{\text{WPI}}(\bar{\rho}'', t; \bar{\rho}', 0) &= \pi \sqrt{f(s)} \\ &\times \left[\frac{\sigma s^3}{3\omega} f(s) \right]^{-1/3} \text{Ai} \left\{ - \left[\frac{\sigma s^3}{3\omega} f(s) \right]^{-1/3} \bar{\rho}_- \right\} \\ &\times \left[\frac{\sigma s^3}{3\omega} f(s) \right]^{-1/3} \text{Ai} \left\{ - \left[\frac{\sigma s^3}{3\omega} f(s) \right]^{-1/3} \bar{\rho}_+ \right\}, \end{aligned} \quad (7.45)$$

together with $f(s) = 3s^{-2} - 1$, $s = \sin(\tau/2)$ and

$$\bar{\rho}_- = \left(\bar{\eta} - \sqrt{f(s)} \bar{\xi} \right) / 2, \quad \bar{\rho}_+ = \left(\bar{\eta} + \sqrt{f(s)} \bar{\xi} \right) / 2. \quad (7.46)$$

This analytical expression for the Wigner propagator can be evaluated numerically without major difficulties, in particular we explore the time evolution of the quantum-spot for the case of weak cubic anharmonicity in the next section.

7.3 Numerical applications.

We here consider numerical applications to Wigner propagator based on phase-space path integrals. Particularly, we illustrate the usefulness of the semiclassical formula given by Eq. (7.11) in the context of wave packets dynamics. To achieve this, we start focus on time evolution of quantum-spot for exploring the capability of the Wigner propagator to resolve phase-space structures. Indeed, the Fig. 7.1 shows the quantum-spot in a Morse potential for strong nonlinearity, here surprisingly this approach deviates significantly from classical trajectory, it is more evident when the propagator evolve in the weak part of the potential. Is worthy of mentioning that this particular situation is manifested due to the shape of the potential, in fact, we have performed some numerical experiments on other molecular potential as Posch-Teller model (no shown here) confirm that for a more symmetric shape of the potential, the propagator follows much better the classical trajectory. On the other hand, we observe that this approach can reproduce qualitatively important quantum features along time evolution, it is, the nodelines structures that emerge in phase-space, moreover, this method certainly overcome the difficulties that inherent to the semiclassical propagation based on van Vleck approach. Namely, the caustics problem in phase-space and lack of norm-conservation. Other relevant characteristic that comes with the uniform approximation is the smooth penumbra outside of classical skeleton, in contrast to the semiclassical Wigner propagator (the van Vleck's approach) that appears as a cut in phase space, it is due to caustics. On the other hand, this method has its own limitations, more precisely, when the

nonlinearity is already considerable this propagator does not reproduce the curved nodelines and therefore fails, this situation is illustrate in the Fig. 7.3 where we have considered long time propagation. In order to compare both semiclassical approaches, the same figure contains the corresponding semiclassical calculations, Indeed, the interference pattern in phase space are quiet different.

Related to localized initial states, we compute the time evolution of the same state as the previous numerical applications, we recommend see sections 3.6, 4.3. In the Fig 7.2 shows the propagation of the Gaussian initial state, note that the wave packet moves practically as initial state without change the shape, it can be explained easily it is clear that the initial state cover a phase-space area bigger than the propagator, then the oscillations associated to the propgator are damped out by this state. As a complementary test of the performance of our semiclassical method, the Fig. 7.4 shows the autocorrelation function as the previous applications. Although this Wigner propagator has some difficulties to reproduce the quantum behavior, it is remarkable good.

Finally, we consider an application to the section 7.2.4, where we have discussed the cubic oscillator with weak nonlinearity. This particular case corresponds to an analytical solution to the semiclassical Wigner propagator base on phase-space path integrals, the Fig. 7.5 shows the quantum spot as a time-evolved propagator in terms of the final phase-space coordinates at several times. Note that, for short time of propagation $\tau \ll 1$ the quantum-spot appears as quasi-one-dimensional (panel a) pointing in the negative p-direction if $V''' > 0$, its oscillatory pattern scales with time as τ^3 illustrated in the panels b, c, d.

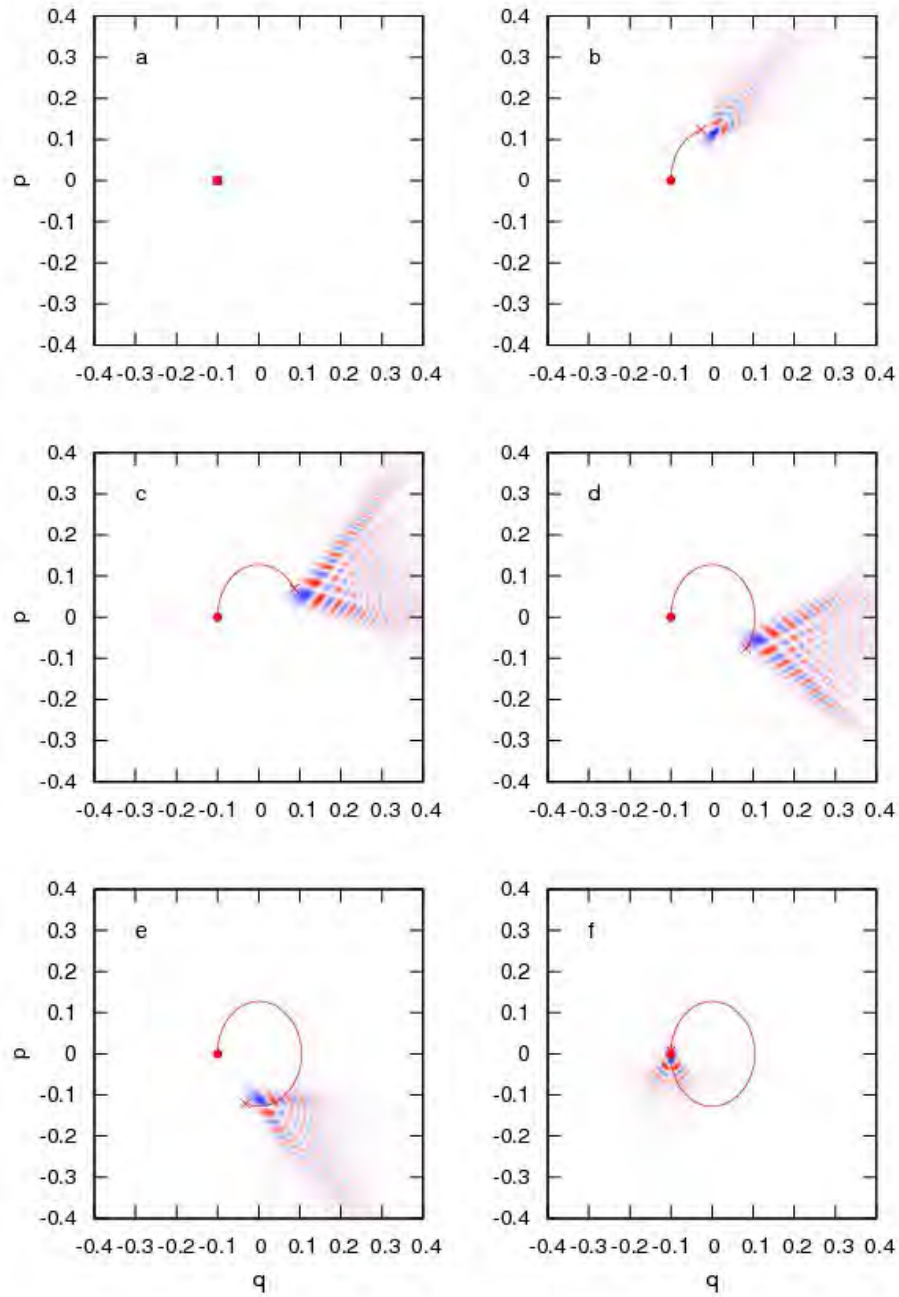


Figure 7.1: Time evolution of the Wigner propagator in the Morse potential from semi-classical approximation at times, $t = 0$ (panel a), 0.5072 (b), 1.0144 (c), 1.5216 (d), 2.0288 (e), 2.536 (f). The underlying classical trajectory has been launched at $\mathbf{r}_0 = (-0.1, 0)$. Parameter values are $D = 1$, $\alpha = 1.25$, $\hbar = 0.005$. Color code ranges from red (negative) through white (zero) through blue (positive).

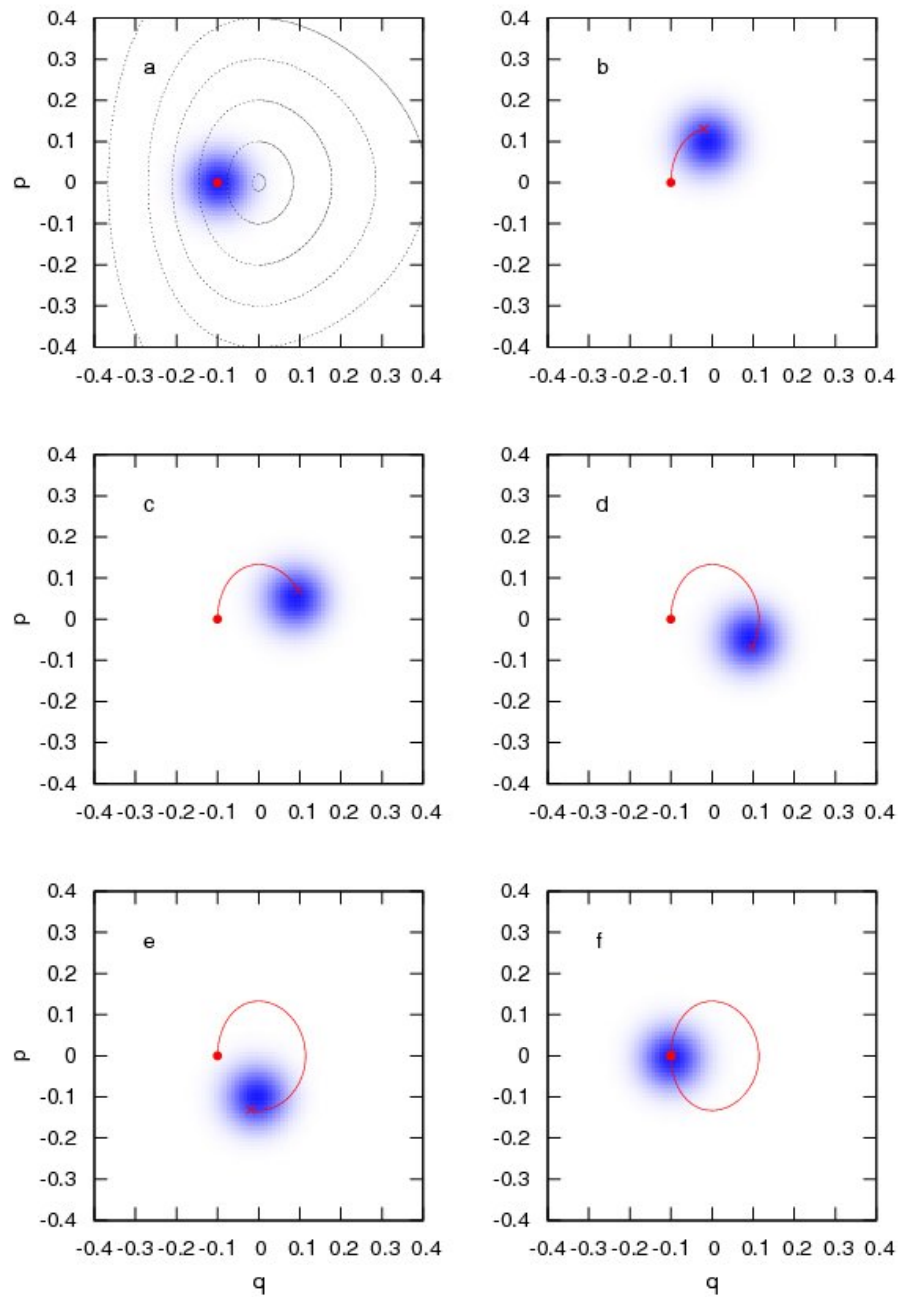


Figure 7.2: Time evolution of an initial Wigner function (Gaussian state) in the Morse potential for the semiclassical approximation based on path integrals at times $t = 0$ (panel a), 0.5072 (b), 1.0144 (c), 1.5216 (d), 2.0288 (e), 2.536 (f). In panel a, some contour lines of the potential are shown superimposed. The underlying classical trajectory has been launched at $\mathbf{r}_0 = (-0.1, 0)$. Parameter values are $D = 1$, $\alpha = 1.25$, $\hbar = 0.005$.

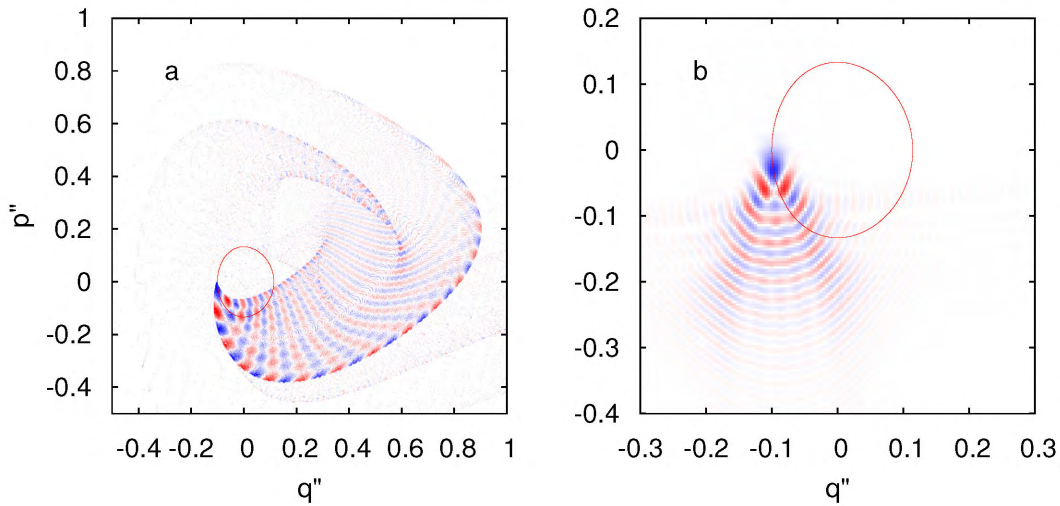


Figure 7.3: Time-evolved quantum spot from semiclassical Wigner-van Vleck propagator Eq. (??) (panel a) as compared with semiclassical approximation for Wigner propagator based on phase-space path integrals Eq. (7.11) (panel b) at time $t = 10$. The classical trajectory underlying with initial point $(q', p') = (-0.1, 0)$ is superimposed. Parameter values are $D = 1$, $\alpha = 1.25$, $\hbar = 0.005$.

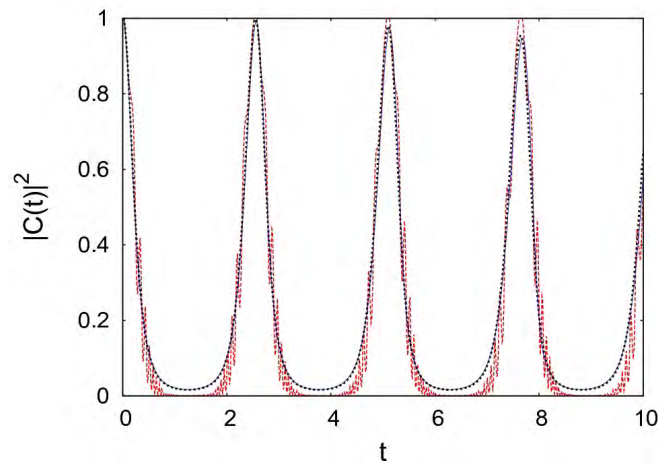


Figure 7.4: Autocorrelation function for an initial Gaussian state in the Morse potential, the semiclassical Wigner propagator based on phase-space path integrals (dashed line, red color) compared with the exact quantum result (full line, blue color) and classical calculations (dotted line, black color). Parameter values are $m = 0.5$, $D = 1$, $\alpha = 1.25$, $\hbar = 0.005$.

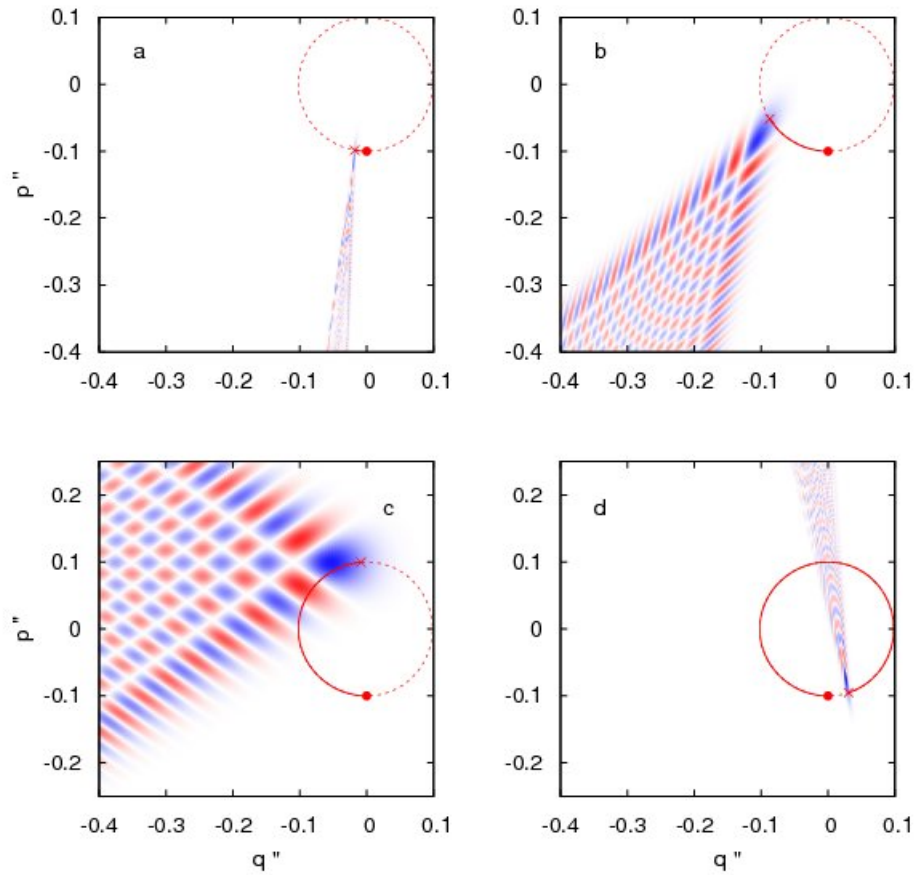


Figure 7.5: Time evolution of the Wigner propagator in the semiclassical approximation based on phase-space path integration as a function of final phase-space coordinates (q'', p'') for a potential with constant cubic anharmonicity $\sigma(t) = \text{const}$ at times $t = \pi/18$ (panel a), $t = \pi/3$ (b), $t = \pi$ (c), $t = 2\pi - 0.3$ (d). The underlying classical trajectory has been launched at $(q', p') = (0, -0.1)$. Parameters value are $m = 1$, $\omega = 1$, $\hbar = 1$, $\epsilon = 0.2$. Color code ranges from red (negative) through white (zero) through blue (positive).

Chapter 8

Semiclassical Wigner propagator and tunneling.

This chapter is dedicated to the tunneling phenomenon in terms of semiclassical Wigner propagator. Mainly, we focus on numerical applications for quartic double well potential, and the performance of the semiclassical method is tested in terms of autocorrelation function as well as the capability to resolve phase-space structures.

The tunneling is the most striking quantum phenomenon and the interest on it is renewed constantly. Recent experiments have confirmed theoretical predictions about chaos-assisted tunneling and dynamical tunneling [*Det. all00*, *Het. all01*, *DASR01*]. Besides, the tunneling has been considered practically in the framework of almost all semiclassical approximations, more precisely, from semiclassical approaches that are based on classical trajectories. Although these methods have been applied successfully in most applications, the tunneling continues being the hardest task to reproduce, it is due to this phenomenon corresponds to a manifestation of classically forbidden process. In order to overcome theoretical difficulties, and at the same time to obtain a better performance of the semiclassical approximations, a variety of proposals have been developed. The most widespread proposal in the semiclassical methods is the analytical extension to the complex plane. In this way, the classical trajectories becomes complex and the contribution to the semiclassical propagation is improved [*JdA97*, *BL98*, *RdAB04*, *dAVG09*]. However, a small group of semiclassical approaches have been formulated in terms of real trajectories and have avoided the complex trajectories. Surprisingly those methods have shown that the real trajectories are sufficient to account correctly of quantum tunneling [*JdA07*, *VH02*, *Nov05*, *ZP05*]. In spite of this, the theoretical discussion remain open and there are not conclusive results that indicate what kind of trajectories are necessary to capture the tunneling phenomenon.

8.1 Semiclassical description of tunneling.

Although the vast literature about Wigner representation few works have been dedicated to study in some extend the tunneling phenomenon in terms of Wigner functions [MS96, MS97a, MS97b], and almost nothing from semiclassical approach. In follows, we shall consider particularly the quartic double well potential (see section 3.4.2), in order to fix ideas about how the tunneling from semiclassical Wigner propagator takes place. Indeed, the Fig. 3.4.2) illustrates this situation according to the trajectory-pairs construction underlying our semiclassical method.

Although of the vast literature about Wigner representation, certainly, few works have been dedicated to study in some extend the tunneling phenomenon in terms of Wigner functions [MS96, MS97a, MS97b], and almost nothing from semiclassical approach. In follows we shall consider particularly the double-well potential (see section 3.4.2) in order to fix ideas about how takes place the tunneling from semiclassical Wigner propagator. Indeed, the Fig. 8.1 illustrates this situation according to the trajectory-pairs construction underlying our semiclassical method.

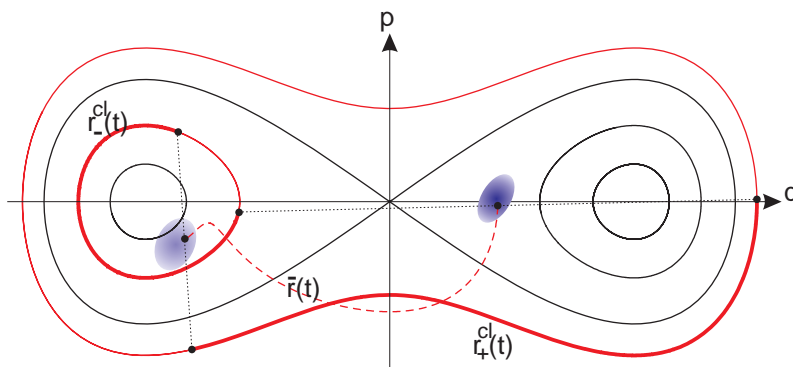


Figure 8.1: Semiclassical description of coherent tunneling in terms of trajectory pairs, in the framework of the Wigner van Vleck propagator. A wave packet initially prepared near the right minimum of a double-well potential (blue patch) can be transported along a non-classical midpoint path $\bar{\mathbf{r}}(t)$ (dashed red line) into the opposite well if the two classical orbits $\mathbf{r}_{\pm}^{\text{cl}}(t)$ (full red lines) underlying this path through $\bar{\mathbf{r}}(t) = (\mathbf{r}_{+}^{\text{cl}}(t) + \mathbf{r}_{-}^{\text{cl}}(t))/2$ are sufficiently separated initially, e.g., $\mathbf{r}_{+}^{\text{cl}}$ on the same side but above the barrier, $\mathbf{r}_{-}^{\text{cl}}$ within the opposite well. Other contours of the potential and the separatrix are indicated by black curves.

Note that we have restricted ourselves to consider only real trajectories in phase space, according to the semiclassical Wigner propagator based on van Vleck approach. In this way, the Wigner formalism is close to classical mechanics, it means that the semiclassical description of the tunneling is completely clear in terms of pure classical concepts. In particular, this approach takes advantage of non-local contribution of the classical trajectories in order to reproduce quantum features that cannot be captured from others semiclassical approaches.

In follows, we consider the numerical applications from semiclassical Wigner propagator in a double well potential. The Fig. 8.2 shows several snapshots of time evolution of localized initial state, a characteristic pattern in phase space emerges along of evolution, taking positive as well as negative values. This effect, it is in agreement with the Wigner representation, since only admissible Wigner function that always is positive defined is the Gaussian state. In order to resolve phase-space structures the Fig. 8.3 shows the naked Wigner propagator for semiclassical approximation based trajectory pairs and the exact quantum calculations. Here, is much more evident how the propagator defines a fine pattern in phase space.

The performance of semiclassical Wigner propagator is compare to the quantum results and pure classical propagation, note that our semiclassical method reproduces important quantum features as it is shown in the autocorrelation function of the Fig. 8.4. In the same figure, the inset shows the non-conservation norm associated to the semiclassical Wigner propagator, as a consequence of this we need constantly re-normalize the state along of time evolution. This disadvantage is inherent to the semiclassical Wigner propagator due to the non-conservation probability along the caustics, and it can be overestimates the calculations in the autocorrelation function as is shown in the second revival. However, the performance of the method is surprisingly good.

Now we focus on tunneling regime, as is well-known any initial state located into one well, always it will gets tunnel according to quantum description, however, the tunneling time strongly depends of number of tunneling doublets, and it can be approximates as the inverse of first doublet for the double well potential [Raz03, Ank07]. Moreover, it generally corresponds to long times scales in order to see coherent tunneling, *i.e* when the probability density oscillates periodically. In our case, we cannot consider long times due to the semiclassical approximations breaks down as is expected. Therefore, to study tunneling phenomenon we consider an initial localized state prepared just below of the barrier top, and the tunneling takes place along the time evolution of this wave packet. The Fig. 8.5 shows the quantum results as compare to semiclassical Wigner propagation, indeed the fine fringes in the quantum result are reaching out in to opposite well and they are strongly marked in contrast to semiclassical propagation method where they are almost suppressed as is shown in the same figure. It is a manifestation of the quantum phenomenon that cannot be easily captured by the semiclassical approaches. Although the semiclassical Wigner propagator reproduces at least qualitatively some quantum features, we test the performance of the method by considering the autocorrelation function. The Fig. 8.6 shows the quantum result as compare to the semiclassical Wigner propagation and classical calculations. The semiclassical Wigner propagator reproduces the revival but exaggerates their amplitude. This significant deviation surprises as it underestimates the quantum effects. A possible explanation for this behavior in the autocorrelation function, also for resolving phase-space structures come from the non-conservation probability at caustics.

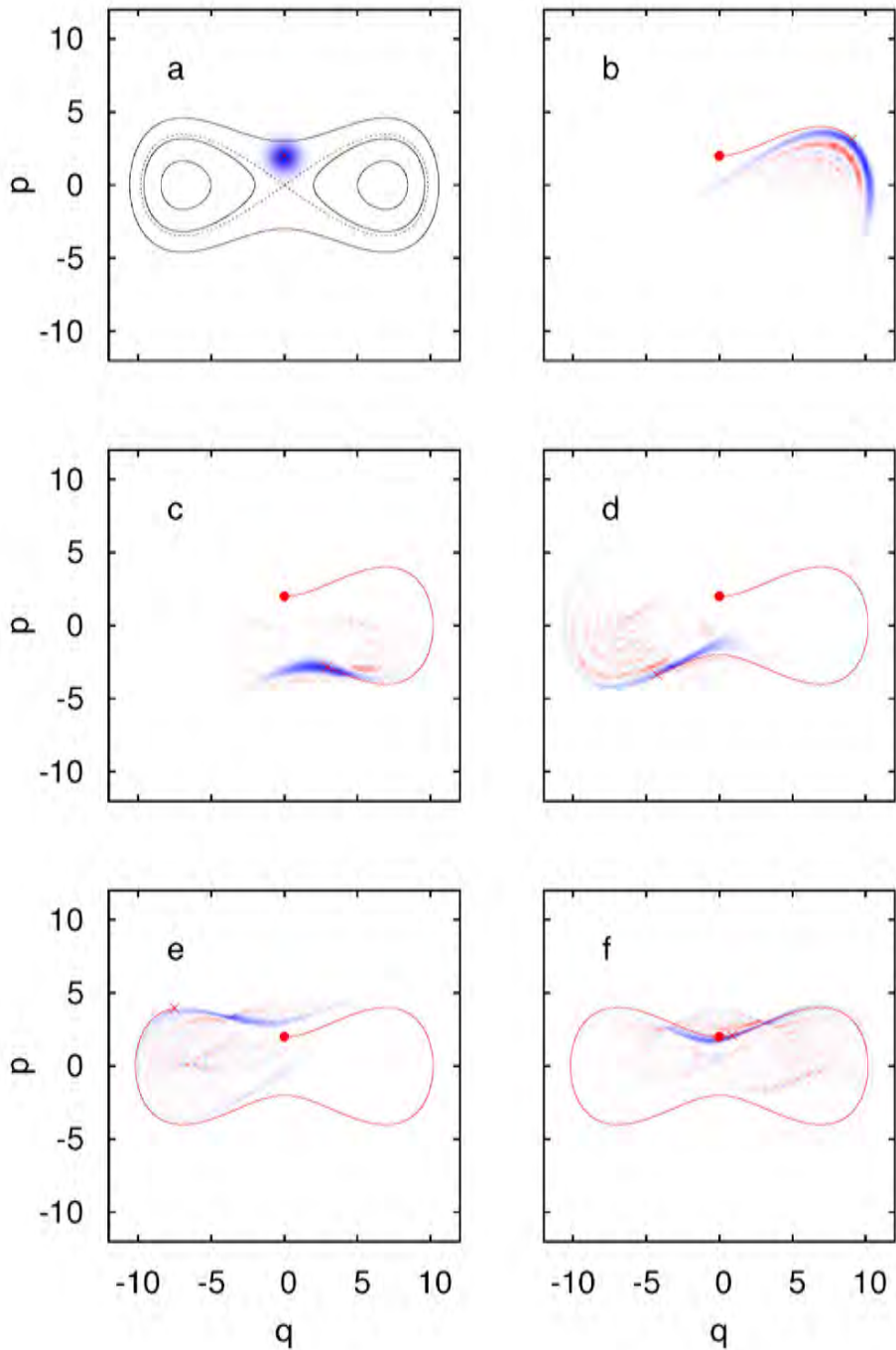


Figure 8.2: Time evolution of initial Gaussian state in the quartic double well (contour lines in panel a) from semiclassical Wigner propagator at times $t = 0$ (panel a), $t = 3$ (b), $t = 6$ (c), $t = 9$ (d), $t = 12$ (e), $t = 15$ (f). The full red line is the classical trajectory the initial state $(q_0, p_0) = (0, 2)$. Parameter values are $m = 1$, $\Delta = 6$.

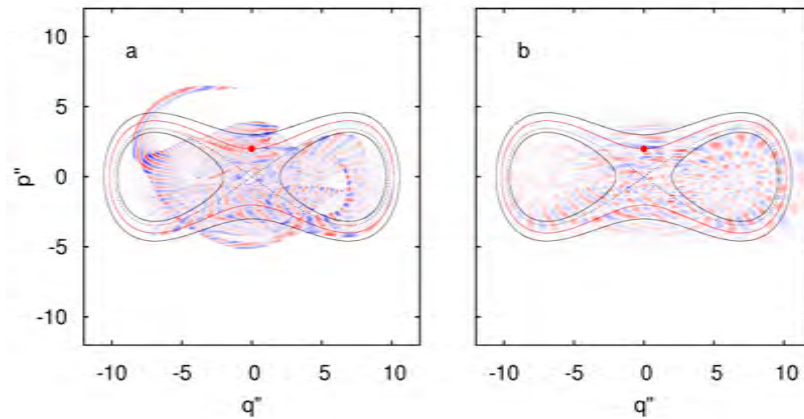


Figure 8.3: Time-evolved semiclassical propagator of the Wigner function (panel a) and the corresponding exact quantum propagator (panel b) for the quartic double well at time $t = 15$ with energy $E = 1.0026$. Parameter values are $m = 1$, $\Delta = 6$.

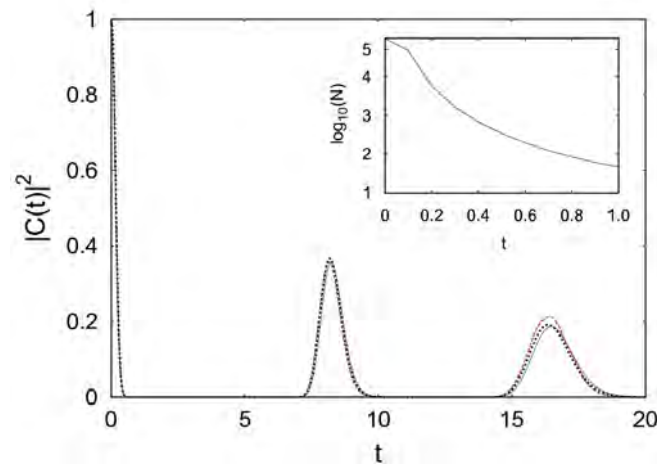


Figure 8.4: Autocorrelation function for a Gaussian initial state in a quartic double well at an energy $E = 1.0026$ above the barrier top, the semiclassical approximation based on Wigner van Vleck propagator (dashed line, red color) as compare to an exact quantum result (full line, blue color) and classical calculation (dotted line, black color). The initial Gaussian state is $(q_0, p_0) = (0, 2)$. The inset shows non-conservation norm along time evolution, where N denotes the integral of the Wigner function over all phase space. Parameter values are $m = 1$, $\Delta = 6$.

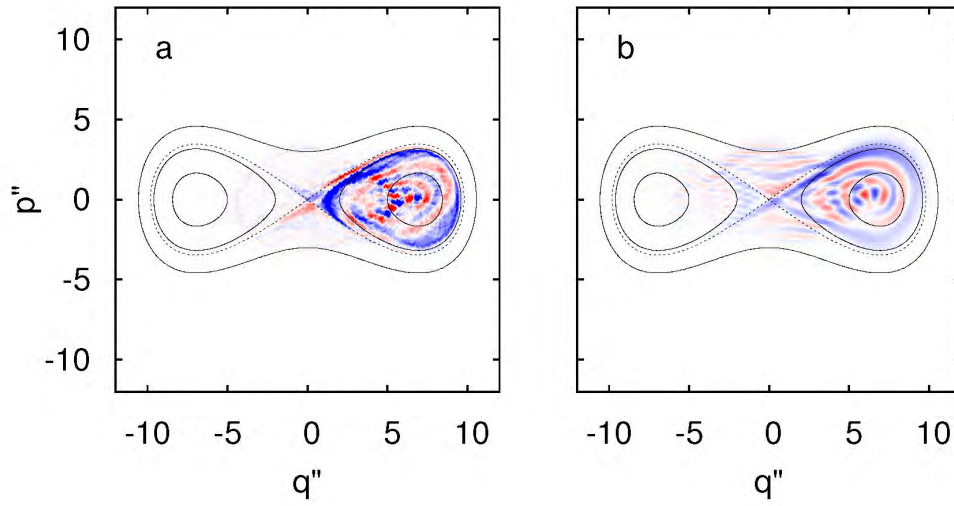


Figure 8.5: Time-evolved state, initially prepared as Gaussian state at time $t = 5$ in the quartic double well, semiclassical approximation based on Wigner van Vleck propagator (panel a) and the corresponding exact quantum calculation (panel b) with energy $E = -0.958$. Parameter values are $m = 1$, $\Delta = 6$.

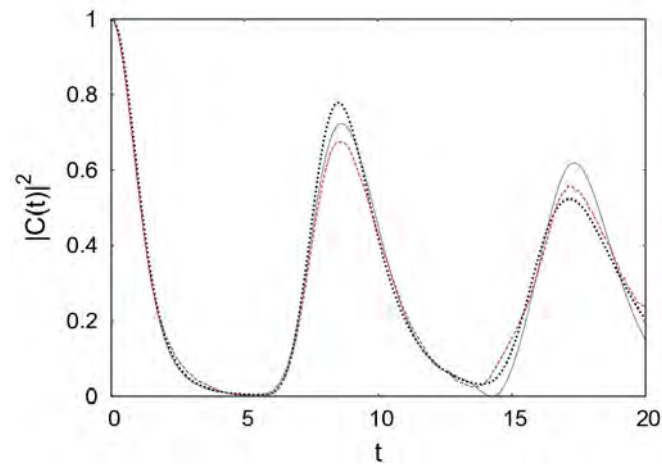


Figure 8.6: Autocorrelation function for a Gaussian initial state in a quartic double well at an energy $E = -0.958$ below the barrier top, the semiclassical approximation based on Wigner van Vleck propagator (dashed line, red color) as compare to exact quantum result (full line, blue color) and the classical calculation (dotted line, black color). The initial Gaussian state is $(q_0, p_0) = (2, 0)$. Parameter values are $m = 1$, $\Delta = 6$.

Chapter 9

Conclusions and perspectives.

- To date, little is known about semiclassical Wigner propagation, thus, this thesis contributes to fill the gap in quantum dynamics in phase space from Wigner representation, more precisely, in terms of Wigner function propagator. At the same time, we have been discussed important theoretical aspects about advantages and disadvantages associated with a particular semiclassical approximation to the Wigner propagator. Namely, the van Vleck approach and the uniform approximation. On the other hand, a relevant discussion was considered due to the failure of stationary-phase method in the asymptotic limits of weak anharmonicity, short time propagation, and the classical limit of the propagator.
- In this work a variety of numerical applications have been considered, principally, we have focussed on the wave packet dynamics and tunneling phenomena, in order to test the performance of the semiclassical approximations to the Wigner propagator. Moreover, it is attempted to establish those schemas of propagation in the scientific community, more precisely, the approach based on trajectory pairs due to it can be generalized to high-dimensional phase space.
- In this thesis, an efficient numerical algorithm is proposed in order to perform the semiclassical Wigner propagation. In practice, the numerical implementation of this algorithm is straightforward and it is not required for additional methods such as the filtering-techniques of classical trajectories. Also, the semiclassical Wigner propagator together with this algorithm or an approach like Monte-Carlo Metropolis algorithms can be applied directly to *ab-initio* molecular dynamics simulations.
- Although the approximation based on phase-space path integrals approach, it allows to overcome the caustics and normalization problem manifested in the Wigner van Vleck propagator, it tends to fail at strong nonlinearity. Therefore, the numerical applications considered in this work serves a support and motivation for novel semiclassical approaches, which aim to integrate the robust structure of the trajectory pairs together with a uniform approximation in order to improve the accuracy in semiclassical

propagation.

- In this thesis, the concept trajectory pairs is discussed as a powerful tool in order to capture important quantum features in phase space. In principle, this formalism is based on non-local contribution of classical trajectories and it offers a comprehensive description of quantum phenomena from semiclassical point of view.
- This thesis also contributes to establish the mathematical formalism of Wigner function propagator, at the same time, it serves as starting point for novel semiclassical approximations in phase space. Moreover, other semiclassical methods could be combined to the Wigner representation leading to a powerful semiclassical approximation.
- Numerical applications are presented in the framework of wave packet dynamics, and the semiclassical propagation of quantum effects as well as tunneling and quantum coherences. However, there are much more to learn and explore with these semiclassical approximations to the Wigner function propagator. To mention few of them, the studying incoherent processes like dephasing and dissipation quantum, as well as, the quantum evolution of classically chaotic systems and stochastic processes, from semiclassical description.

Appendix A

Weyl Formalism.

The Wigner function as well the Wigner propagator have a mathematical structure in phase space which can be understood in terms of Weyl formalism. In this appendix the Weyl representation and its properties are studied.

Definition: Lets $u, v \in \text{Re}$ and \hat{p}, \hat{q} operators of momentum and position, respectively, The displacement operator is defined as:

$$\hat{T}(u, v) := \int_{-\infty}^{\infty} \exp\left\{\frac{i}{\hbar}(u\hat{p} + v\hat{q})\right\} dudv. \quad (\text{A.1})$$

Proposition: Lets be $\hat{T}(u, v)$ a displacement operator, then the composition rule for two displacement operators reads:

$$\hat{T}(u, v)\hat{T}(u', v') = \exp\left\{\frac{i}{2\hbar}(uv' - u'v)\right\}\hat{T}(u + u', v + v'). \quad (\text{A.2})$$

Proof:

$$\begin{aligned} \hat{T}(u, v)\hat{T}(u', v') &= \exp\left\{\frac{i}{\hbar}(u\hat{p} + v\hat{q})\right\}\exp\left\{\frac{i}{\hbar}(u'\hat{p} + v'\hat{q})\right\} \\ &= \exp\left\{\frac{1}{2}\left[\frac{i}{\hbar}(u\hat{p} + v\hat{q}), \frac{i}{\hbar}(u'\hat{p} + v'\hat{q})\right]\right\}\exp\left\{\frac{i}{\hbar}((u + u')\hat{p} + (v + v')\hat{q})\right\} \\ &= \exp\left\{\frac{i}{2\hbar}(uv' - u'v)\right\}\hat{T}(u + u', v + v'). \end{aligned} \quad (\text{A.3})$$

Proposition: Lets be $\hat{T}(u, v)$ a displacement operator, then the inverse displacement operator is given by $\hat{T}^{-1}(-u, -v)$.

Proof: Using Eq. (A.3) and the considering that the commutator for \hat{p}, \hat{q} operators is zero, also changing $u' \rightarrow -u, v' \rightarrow -v$, is straightforward shows that,

$$\begin{aligned} \hat{T}(u, v)\hat{T}^{-1}(-u, -v) &= \hat{T}(0, 0) \\ &= 1 \end{aligned} \quad (\text{A.4})$$

Proposition: The unitary displacement operator is given by $\hat{T}(u, v)$.

Proof:

$$\begin{aligned}\hat{T}^{-1}(u, v) &= \hat{T}(-u, -v) \\ &= \{(\hat{T}(-u, -v))^\dagger\}^\dagger \\ &= \hat{T}^\dagger(u, v)\end{aligned}\tag{A.5}$$

Proposition: The trace operation for displacement operator is equal to $2\pi\hbar\delta(u)\delta(v)$.

Proof:

$$\begin{aligned}\text{Tr}[\hat{T}(u, v)] &= \int_{-\infty}^{\infty} \langle q_1 | \hat{T}(u, v) | q_1 \rangle dq_1 \\ &= \int_{-\infty}^{\infty} \langle q_1 | \left\{ \exp\left(\frac{iv\hat{q}}{2\hbar}\right) \exp\left(\frac{iu\hat{p}}{\hbar}\right) \exp\left(\frac{iv\hat{q}}{2\hbar}\right) \right\} | q_1 \rangle dq_1 \\ &= \int_{-\infty}^{\infty} \langle q_1 | \left\{ \exp\left(\frac{iv\hat{q}}{2\hbar}\right) | p_1 \rangle \langle p_1 | \exp\left(\frac{iu\hat{p}}{\hbar}\right) | p_2 \rangle \langle p_2 | \exp\left(\frac{iv\hat{q}}{2\hbar}\right) \right\} dq_1 dp_1 dp_2 \\ &= \int_{-\infty}^{\infty} \exp\left(\frac{ivq_1}{\hbar}\right) \exp\left(\frac{iup_1}{\hbar}\right) dq_1 dp_1 \\ &= 2\pi\hbar\delta(u)\delta(v)\end{aligned}\tag{A.6}$$

Definition: Lets be $u, v, p, q \in \text{Re}$ and \hat{p}, \hat{q} operators of position and momentum, respectively, Then the operator $\hat{d}(p, q)$ is defined as:

$$\hat{d}(p, q) := (2\pi\hbar)^{-1} \int_{-\infty}^{\infty} \exp\left\{\frac{i}{\hbar}(up + vq)\right\} \hat{T}(-u, -v) dudv.\tag{A.7}$$

Proposition: The operator $\hat{d}(p, q)$ is hermitian.

Proof:

$$\begin{aligned}\hat{d}(p, q) &= (2\pi\hbar)^{-1} \int_{-\infty}^{\infty} \exp\left\{\frac{i}{\hbar}(up + vq)\right\} \hat{T}(-u, -v) dudv \\ &= (2\pi\hbar)^{-1} \int_{-\infty}^{\infty} \exp\left\{\frac{-i}{\hbar}(up + vq)\right\} \hat{T}^\dagger(u, v) dudv \\ &= \text{changing } u' \rightarrow -u, v' \rightarrow -v \\ &= \left\{ (2\pi\hbar)^{-1} \int_{-\infty}^{\infty} \exp\left\{\frac{i}{\hbar}(up + vq)\right\} \hat{T}(-u, -v) dudv \right\}^\dagger \\ &= \hat{d}^\dagger(p, q).\end{aligned}\tag{A.8}$$

Proposition: The operator $\hat{d}(p, q)$ is normalized in phase space.

Proof:

$$\begin{aligned}
\hat{d}(p, q) &= (2\pi\hbar)^{-1} \int_{-\infty}^{\infty} \hat{d}(p, q) dpdq & (A.9) \\
&= (2\pi\hbar)^{-2} \int_{-\infty}^{\infty} \exp\left\{\frac{i}{\hbar}(up + vq)\right\} \hat{T}(-u, -v) dudvdpdq \\
&= \int_{-\infty}^{\infty} \delta(u)\delta(v)\hat{T}(-u, -v)dudv \\
&= \hat{T}(0, 0) = 1.
\end{aligned}$$

Proposition: The operator $\hat{d}(p, q)$ has trace operation equal to 1.

Proof: Using the Eq. (A.6), we easily obtain,

$$\begin{aligned}
Tr[\hat{d}(p, q)] &= (2\pi\hbar)^{-2} \int_{-\infty}^{\infty} \exp\left\{\frac{i}{\hbar}(up + vq)\right\} Tr[\hat{T}(-u, -v)] dudv & (A.10) \\
&= (2\pi\hbar)^{-1} \int_{-\infty}^{\infty} \exp\left\{\frac{i}{\hbar}(up + vq)\right\} (2\pi\hbar)\delta(-u)\delta(-v)dudv \\
&= 1. & (A.11)
\end{aligned}$$

Proposition: Lets be $\hat{d}(p, q)$ and $\hat{d}(p', q')$ two operators, then the composition rule for these operators is given by $\frac{2}{\pi\hbar} \int_{-\infty}^{\infty} \hat{d}(\mathbf{r}'') \exp\left\{\frac{i}{\hbar}\Delta_3(\mathbf{r}'', \mathbf{r}', \mathbf{r})\right\}$.

Proof: The operator $\hat{d}(p, q)$ is defined by Eq. (A.7),

$$\begin{aligned}
\hat{d}(p, q)\hat{d}(p', q') &= (2\pi\hbar)^{-1} \int_{-\infty}^{\infty} \exp\left\{\frac{i}{\hbar}[u_1p_1 + v + 1q_1 + up + vq]\right\} \\
&\quad \hat{T}(-u_1, -v_1)\hat{T}(-u, -v)dudvdu'dv', & (A.12)
\end{aligned}$$

Moreover, the composition rule for operator $\hat{T}(p, q)$ and the Eq. (A.2),

$$\begin{aligned}
\hat{d}(p, q)\hat{d}(p', q') &= (2\pi\hbar)^{-2} \int_{-\infty}^{\infty} \exp\left\{\frac{i}{\hbar}\left[u_1\left(p_1 + \frac{v}{2}\right) + v_1\left(q_1 + \frac{u}{2}\right) + up + vq\right]\right\} \\
&\quad \hat{T}(-u - u_1, -v - v_1)dudvdu'dv', & (A.13)
\end{aligned}$$

Now, by introducing a change of variables as follows: $u = 2(q_2 - q_1), v = 2(p_1 - p_2), u_1 = u_2 - 2(q_2 - q_1), v_1 = v_2 - 2(p_1 - p_2)$, we have

$$\hat{d}(p, q)\hat{d}(p', q') = \frac{2}{\pi\hbar} \int_{-\infty}^{\infty} \hat{d}(p_2, q_2) \exp\left\{\frac{2i}{\hbar}[p_2q_1 - q_2p_1 + p_1q - q_1p + pq_2 - qp_2]\right\} dp_2dq_2. \quad (A.14)$$

A convenient notation has introduced, where $\mathbf{r} = (p, q)$ defines a vector in phase space, also the symplectic product between two vectors is given by $\mathbf{r}^t \mathbf{J} \mathbf{r}''$ where \mathbf{J} is the unitary symplectic matrix, and $\Delta_3(\mathbf{r}'', \mathbf{r}', \mathbf{r}) := 2(\mathbf{r}'' \wedge \mathbf{r}' + \mathbf{r}' \wedge \mathbf{r} + \mathbf{r} \wedge \mathbf{r}'')$. We can rewrite the last equation in such a way as:

$$\hat{d}(\mathbf{r})\hat{d}(\mathbf{r}') = \frac{2}{\pi\hbar} \int_{-\infty}^{\infty} \hat{d}(\mathbf{r}'') \exp\left\{\frac{i}{\hbar}\Delta_3(\mathbf{r}'', \mathbf{r}', \mathbf{r})\right\} d\mathbf{r}''.$$
(A.15)

Definition: Lets be $\hat{A}(\hat{p}, \hat{q})$ an arbitrary operator, then the Weyl transform for \hat{A} is defined as:

$$A(p, q) := Tr[\hat{A}\hat{d}(p, q)].$$
(A.16)

Definition: Lets be $\hat{A}(\hat{p}, \hat{q})$ operator expressed in terms of $\hat{d}(p, q)$ operator, then the Weyl symbol of $\hat{A}(p, q)$ is,

$$\hat{A}(\hat{p}, \hat{q}) := \int_{-\infty}^{\infty} A(p, q)\hat{d}(p, q)dpdq.$$
(A.17)

Proposition: Lets be \hat{A} an arbitrary operator, then the Weyl transform in position representation is given by $(2\pi\hbar)^{-1} \int_{-\infty}^{\infty} \exp\left\{\frac{-ipu}{2}\right\} < q + \frac{u}{2} | \hat{A} | q - \frac{u}{2} > du$.

Proof: By taking into account the trace operation in position representation for q_1 variable,

and using the definition for \hat{d} operator.

$$\begin{aligned}
A(p, q) &= Tr[\hat{A}\hat{d}(p, q)] \\
&= \frac{1}{2\pi\hbar} \int_{-\infty}^{\infty} \langle q_1 | \hat{A} | \exp\left\{\frac{i}{\hbar}(up + vq)\right\} \hat{T}(-u, -v) dq_1 dudv \\
&= \frac{1}{2\pi\hbar} \int_{-\infty}^{\infty} \langle q_1 | \hat{A} | \exp\left\{\frac{i}{\hbar}(up + vq)\right\} \exp\left(\frac{-iv\hat{q}}{2\hbar}\right) \exp\left(\frac{-iu\hat{p}}{\hbar}\right) \exp\left(\frac{-iv\hat{q}}{2\hbar}\right) | q_1 \rangle dq_1 dudv \\
&= \frac{1}{2\pi\hbar} \int_{-\infty}^{\infty} \exp\left\{\frac{i}{\hbar}(up + vq)\right\} \langle q_1 | \hat{A} | q_2 \rangle \langle q_2 | \exp\left(\frac{-iv\hat{q}}{2\hbar}\right) \\
&\quad | p_2 \rangle \langle p_2 | \exp\left(\frac{-iu\hat{p}}{\hbar}\right) | p_1 \rangle \langle p_1 | \exp\left(\frac{-iv\hat{q}}{2\hbar}\right) | q_1 \rangle dq_1 dq_2 dp_1 dp_2 dudv \\
&\quad \text{then, applying the } \hat{q}, \hat{p} \text{ operators and performing the integral on } p_2. \\
&= \frac{1}{2\pi\hbar} \int_{-\infty}^{\infty} \exp\left\{\frac{i}{\hbar}v(q - q_2/2 - q_1/2)\right\} \langle q_1 | \hat{A} | q_2 \rangle \\
&\quad \exp\left(\frac{-iup}{\hbar}\right) \exp\left\{\frac{-ip_1}{\hbar}(u + q_2 - q_1)\right\} dq_1 dq_2 dp_1 dudv \\
&\quad \text{Then, performing the integrals on } v, p_1, q_1, q_2 \text{ we find a conditions as} \\
&\quad \delta\left(q - \frac{q_2}{2} - \frac{q_1}{2}\right) \text{ and } \delta(u + q_2 - q_1). \\
&\quad \text{Thus, we have } q_1 = q + u/2, q_2 = q - u/2. \\
&= \int_{-\infty}^{\infty} \exp\left(\frac{-iup}{\hbar}\right) \langle q + \frac{u}{2} | \hat{A} | q - \frac{u}{2} \rangle du.
\end{aligned} \tag{A.18}$$

Proposition: Lets be \hat{A} an arbitrary operator. Then the Weyl transform in momentum representation is given by $(2\pi\hbar)^{-1} \int_{-\infty}^{\infty} \exp\left\{\frac{-iqu}{2}\right\} \langle p + \frac{u}{2} | \hat{A} | p - \frac{u}{2} \rangle du$.

Proof: (The same as before.)

Proposition: Lets be $\hat{A}_1(\hat{p}, \hat{q}), \hat{A}_2(\hat{p}, \hat{q})$ two arbitrary operators. Then the Weyl transform of the product of these operators is given by

$$A(\mathbf{r}) = \frac{1}{(\pi\hbar)^2} \int_{-\infty}^{\infty} A_1(\mathbf{r}') A_2(\mathbf{r}'') \exp\left\{\frac{i}{\hbar}\Delta_3(\mathbf{r}'', \mathbf{r}', \mathbf{r})\right\} d\mathbf{r}' d\mathbf{r}'' \tag{A.19}$$

Proof: Starting with the definition of the Weyl transform, *i.e.* Eq. (A.16), moreover, by introducing the operator given in Eq. (A.17) and Eq. (A.15) we have,

$$\begin{aligned}
A(\mathbf{r}) &= Tr[\hat{A}_1(\hat{p}, \hat{q}) \hat{A}_2(\hat{p}, \hat{q}) \hat{d}(\mathbf{r})] \\
&= \int_{-\infty}^{\infty} A_1(\mathbf{r}') A_2(\mathbf{r}'') Tr[\hat{d}(\mathbf{r}'') \hat{d}(\mathbf{r}') \hat{d}(\mathbf{r})] d\mathbf{r}' d\mathbf{r}'' \\
&= \frac{1}{(\pi\hbar)^2} \int_{-\infty}^{\infty} A_1(\mathbf{r}') A_2(\mathbf{r}'') \exp\left\{\frac{i}{\hbar}\Delta_3(\mathbf{r}'', \mathbf{r}', \mathbf{r})\right\} d\mathbf{r}' d\mathbf{r}'' .
\end{aligned} \tag{A.20}$$

Proposition: Lets be $\hat{A}_1(\hat{p}, \hat{p}), \hat{A}_2(\hat{p}, \hat{p}), \hat{A}_3(\hat{p}, \hat{p})$ three arbitrary operators . Then the Weyl transform for the product of these operators is given by

$$A(\mathbf{r}) = \frac{1}{(\pi\hbar)^2} \int_{-\infty}^{\infty} A_1(\mathbf{r}_1)A_2(\mathbf{r}_2)A_3(\mathbf{r}_3)exp\left\{-\frac{2i}{\hbar}(\mathbf{r}_3 \wedge \mathbf{r} + \mathbf{r}_1 \wedge \mathbf{r}_2)\right\}\delta(\mathbf{r}_3 - \mathbf{r} + \mathbf{r}_1 - \mathbf{r}_2)d\mathbf{r}_1d\mathbf{r}_2d\mathbf{r}_3 \quad (\text{A.21})$$

Proof: By considering the Weyl transform for two operators, it can be proof for case of three operators as follows, we rewritte $A_{12} = A_1A_2$. Then using the Eq. (A.19) we have

$$\begin{aligned} A(\mathbf{r}) &= \frac{1}{(\pi\hbar)^2} \int_{-\infty}^{\infty} A_{12}(\mathbf{r}_0)A_3(\mathbf{r}_3)exp\left\{-\frac{i}{\hbar}\Delta_3(\mathbf{r}_0, \mathbf{r}_3, \mathbf{r})\right\}d\mathbf{r}_0d\mathbf{r}_3 \\ &= \frac{1}{(\pi\hbar)^4} \int_{-\infty}^{\infty} A_1(\mathbf{r}_1)A_2(\mathbf{r}_2)A_3(\mathbf{r}_3)exp\left\{-\frac{i}{\hbar}(\Delta_3(\mathbf{r}_0, \mathbf{r}_3, \mathbf{r}) + \Delta_3(\mathbf{r}_1, \mathbf{r}_2, \mathbf{r}_0))\right\}d\mathbf{r}_0d\mathbf{r}_1d\mathbf{r}_2d\mathbf{r}_3 \end{aligned}$$

After some algebraic manipulations for the simpletic product, the integral on \mathbf{r}_0 .

$$= \frac{1}{(\pi\hbar)^2} \int_{-\infty}^{\infty} A_1(\mathbf{r}_1)A_2(\mathbf{r}_2)A_3(\mathbf{r}_3)exp\left\{-\frac{2i}{\hbar}(\mathbf{r}_3 \wedge \mathbf{r} + \mathbf{r}_1 \wedge \mathbf{r}_2)\right\}\delta(\mathbf{r}_3 - \mathbf{r} + \mathbf{r}_1 - \mathbf{r}_2)d\mathbf{r}_1d\mathbf{r}_2d\mathbf{r}_3. \quad (\text{A.22})$$

Appendix B

Simplified action for Wigner-van Vleck propagator.

The main ingredient of the semiclassical Wigner van Vleck propagator is the term associated to the action, which contains all information about trajectory pairs. In this appendix an alternative way to compute numerically the action is shown. In particular, we follow the notation introduced in reference [TDS03].

Basically, our objective is to find an alternative expression to compute the integral (see Eq. (B.1)) that cannot be solved analytically for general Lagrangian function of the classical system, however, it is possible to rewrite this integral in such a way that it only depends on the Lagrangian along of each trajectory, and the classical information of the initial and final points in phase space.

$$S_{j\pm}(\mathbf{r}'', \mathbf{r}', t) = \int_0^{tf} \dot{\bar{\mathbf{r}}}_j(t) \wedge \mathbf{R}_j(t) - H_{j+}(\mathbf{r}_{j+}) + H_{j-}(\mathbf{r}_{j-}) dt. \quad (\text{B.1})$$

Although the derivation is shown for one-dimensional system, the generalization to high dimensional phase spaces is straightforward by following the same approach.

Lets start considering the chord rule,

$$\bar{\mathbf{r}}(t) = \frac{\mathbf{r}_{j-} + \mathbf{r}_{j+}}{2}. \quad (\text{B.2})$$

Additionally, the vector $\mathbf{R}(t)$ in phase space is defined as:

$$\mathbf{R}_j(t) = \mathbf{r}_{j+}(t) - \mathbf{r}_{j-}(t). \quad (\text{B.3})$$

The first step consist in split the integral in two contributions, one part can be associated to the reduced action, and it corresponds to the symplectic area between classical trajectories,

$$A_j = \int_0^{tf} \dot{\bar{\mathbf{r}}}_j(t) \wedge \mathbf{R}_j(t) dt, \quad (\text{B.4})$$

the second part is given by A_1 , which is defined as,

$$A_1 = \int_0^{tf} -H_{j_+}(\mathbf{r}_{j_+}) + H_{j_-}(\mathbf{r}_{j_-}) dt, \quad (\text{B.5})$$

In follows, we rewrite the vectors in phase space explicitly,

$$\begin{aligned} \frac{d\bar{\mathbf{r}}_j(t)}{dt} &= \frac{\dot{\mathbf{r}}_{j_-}(t) + \dot{\mathbf{r}}_{j_+}(t)}{2}, \\ &= \frac{1}{2} \begin{pmatrix} \dot{p}_{j_-} + \dot{p}_{j_+} \\ \dot{q}_{j_-} + \dot{q}_{j_+} \end{pmatrix}. \end{aligned} \quad (\text{B.6})$$

together with,

$$\begin{aligned} \mathbf{R}_j(t) &= \mathbf{r}_{j_+}(t) - \mathbf{r}_{j_-}(t), \\ &= (p_{j_+} - p_{j_-}, q_{j_+} - q_{j_-}). \end{aligned} \quad (\text{B.7})$$

After simple manipulations with the symplectic product, the integral reads,

$$\int_0^{tf} \dot{\bar{\mathbf{r}}}_j \wedge \mathbf{R}_j dt = I_1 + I_2 + I_3 + I_4. \quad (\text{B.8})$$

Here, we have defined each term of the integral explicitly as follows,

$$I_1 = \frac{1}{2} \int_0^{tf} [\dot{p}_{j_-} q_{j_-} - \dot{q}_{j_-} p_{j_-}] dt, \quad (\text{B.9})$$

$$I_2 = -\frac{1}{2} \int_0^{tf} [\dot{p}_{j_+} q_{j_+} - \dot{q}_{j_+} p_{j_+}] dt, \quad (\text{B.10})$$

$$I_3 = -\frac{1}{2} \int_0^{tf} [\dot{p}_{j_-} q_{j_+} + \dot{q}_{j_+} p_{j_-}] dt, \quad (\text{B.11})$$

$$I_4 = \frac{1}{2} \int_0^{tf} [\dot{p}_{j_+} q_{j_-} + \dot{q}_{j_-} p_{j_+}] dt. \quad (\text{B.12})$$

Note that, the symplectic product reads,

$$\dot{\bar{\mathbf{r}}}_j \wedge \mathbf{R}_j = \frac{1}{2} [\dot{p}_{j_-} q_{j_-} - \dot{q}_{j_-} p_{j_-} + \dot{q}_{j_-} p_{j_+} + \dot{p}_{j_+} q_{j_-} - \dot{p}_{j_-} q_{j_+} - \dot{p}_{j_+} q_{j_+} - \dot{q}_{j_+} p_{j_-} + \dot{q}_{j_+} p_{j_+}] \quad (\text{B.13})$$

By introducing the some transformations in the integrand and noting that j_{\pm} indices are mixed in a convenient way,

$$\frac{d}{dt}(p_{j_{\pm}} q_{j_{\mp}}) = \dot{p}_{j_{\pm}} q_{j_{\mp}} + \dot{q}_{j_{\mp}} p_{j_{\pm}}, \quad (\text{B.14})$$

$$\frac{d}{dt}(p_{j_{\pm}} q_{j_{\pm}}) = \dot{p}_{j_{\pm}} q_{j_{\pm}} + \dot{q}_{j_{\pm}} p_{j_{\pm}}. \quad (\text{B.15})$$

These transformations (B.14) gives the integrals I_3 and I_4 ,

$$I_3 = -\frac{1}{2} \int_0^{t_f} [\dot{p}_{j-} q_{j+} + \dot{q}_{j+} p_{j-}] dt, \quad (\text{B.16})$$

$$= -\frac{1}{2} \int_0^{t_f} \left[\frac{d}{dt} (p_{j-} q_{j+}) - \dot{q}_{j+} p_{j-} + \dot{q}_{j+} p_{j-} \right] dt, \quad (\text{B.17})$$

$$= -\frac{1}{2} \int_0^{t_f} \left[\frac{d}{dt} (p_{j-} q_{j+}) \right] dt, \quad (\text{B.18})$$

$$= -\frac{1}{2} [p_{j-}(t_f) q_{j+}(t_f) - p_{j-}(0) q_{j+}(0)]. \quad (\text{B.19})$$

$$I_4 = \frac{1}{2} \int_0^{t_f} [\dot{p}_{j+} q_{j-} + \dot{q}_{j-} p_{j+}] dt, \quad (\text{B.20})$$

$$= \frac{1}{2} \int_0^{t_f} \left[\frac{d}{dt} (p_{j+} q_{j-}) - \dot{q}_{j-} p_{j+} + \dot{q}_{j-} p_{j+} \right] dt, \quad (\text{B.21})$$

$$= \frac{1}{2} \int_0^{t_f} \left[\frac{d}{dt} (p_{j+} q_{j-}) \right] dt, \quad (\text{B.22})$$

$$= \frac{1}{2} [p_{j+}(t_f) q_{j-}(t_f) - p_{j+}(0) q_{j-}(0)]. \quad (\text{B.23})$$

An analogous procedure is done for the integrals I_1 , I_2 by introducing the transformation (B.15),

$$I_{1,2} = \int_0^{t_f} [\dot{p}_{j\pm} q_{j\pm} - \dot{q}_{j\pm} p_{j\pm}] dt, \quad (\text{B.24})$$

$$= \int_0^{t_f} \left[\frac{d}{dt} (p_{j\pm} q_{j\pm}) - \dot{q}_{j\pm} p_{j\pm} - \dot{q}_{j\pm} p_{j\pm} \right] dt, \quad (\text{B.25})$$

$$= \int_0^{t_f} \left[\frac{d}{dt} (p_{j\pm} q_{j\pm}) - 2\dot{q}_{j\pm} p_{j\pm} \right] dt. \quad (\text{B.26})$$

we get a simple expressions the integrals as follows,

$$I_1 = -\frac{1}{2} [p_{j+}(t_f) q_{j+}(t_f) - p_{j+}(0) q_{j+}(0)] \quad (\text{B.27})$$

$$+ \int_0^{t_f} \dot{q}_{j+} p_{j+} dt \quad (\text{B.28})$$

$$I_2 = \frac{1}{2} [p_{j-}(t_f) q_{j-}(t_f) - p_{j-}(0) q_{j-}(0)] \quad (\text{B.29})$$

$$- \int_0^{t_f} \dot{q}_{j-} p_{j-} dt \quad (\text{B.30})$$

Finally, an expression for the action given by Eq. (B.1) reads,

$$\begin{aligned}
 S_{j_{\pm}}(\mathbf{r}'', \mathbf{r}', t) &= \frac{1}{2}[p_{j_-}(t_f)q_{j_-}(t_f) - p_{j_-}(0)q_{j_-}(0)] & (B.31) \\
 &\quad - \frac{1}{2}[p_{j_+}(t_f)q_{j_+}(t_f) - p_{j_+}(0)q_{j_+}(0)] \\
 &\quad - \frac{1}{2}[p_{j_-}(t_f)q_{j_+}(t_f) - p_{j_-}(0)q_{j_+}(0)] \\
 &\quad + \frac{1}{2}[p_{j_+}(t_f)q_{j_-}(t_f) - p_{j_+}(0)q_{j_-}(0)] \\
 &\quad + \int_0^{t_f} \dot{q}_{j_+} p_{j_+} - H_{j_+}(\mathbf{r}_{j_+}) dt \\
 &\quad - \int_0^{t_f} \dot{q}_{j_-} p_{j_-} - H_{j_-}(\mathbf{r}_{j_-}) dt
 \end{aligned}$$

The last two terms that are associated to the Poincaré-Cartan invariants (B.31), which can be rewritten in terms of the classical actions along of each trajectory j_{\pm} ,

$$S_{j_+} = \int_0^{t_f} \dot{q}_{j_+} p_{j_+} - H_{j_+}(\mathbf{r}_{j_+}) dt, \quad (B.32)$$

$$= \int_0^{t_f} L_{j_+} dt. \quad (B.33)$$

$$S_{j_-} = - \int_0^{t_f} \dot{q}_{j_-} p_{j_-} - H_{j_-}(\mathbf{r}_{j_-}) dt, \quad (B.34)$$

$$= - \int_0^{t_f} L_{j_-} dt. \quad (B.35)$$

Therefore, the numerical calculation of the action is much more efficient if we compute the individual actions S_{\pm} along each classical trajectory and the symplectic area by an evaluation of only the initial and final phase-space points according to Eq. (B.31).

Appendix C

Box Müller Method.

Although there is much literature about sampling methods and possibly there are many others which could be faster than this. In follows, we derive the method Box-Müller which has used in our numerical implementations. Moreover, it offers to reader a complementary information about how can it be implemented other methods for sampling in the semiclassical propagation.

Lets start considering that we have two stochastic variables U_1, U_2 that follow a uniform distribution *i.e.*, $U_1, U_2 \in [0, 1)$, we are interested in generate a Gaussian distribution as follows,

$$P(x, y) = \frac{ab}{2\pi} \exp\left\{ -\frac{a^2(x - x_0)^2}{2} - \frac{b^2(y - y_0)^2}{2} \right\} dx dy. \quad (\text{C.1})$$

By introducing a new variables as $\bar{x} = a(x - x_0)$ and $\bar{y} = b(y - y_0)$, we have,

$$P(\bar{x}, \bar{y}) = \frac{1}{2\pi} \int_{-\infty}^{\infty} \int_{-\infty}^{\infty} \exp\left\{ -\frac{\bar{x}^2}{2} - \frac{\bar{y}^2}{2} \right\} d\bar{x} d\bar{y}. \quad (\text{C.2})$$

Since this density is radially symmetric, it is natural to consider polar coordinates, therefore $\bar{x} = R\cos(\theta)$ and $\bar{y} = R\sin(\theta)$. Clearly, the θ variable is uniformly distributed in the interval $[0, 2\pi]$ and it may be sample as,

$$\theta = 2\pi U_2. \quad (\text{C.3})$$

On the other hand, the radial function takes the form,

$$\begin{aligned} f(R) &= \frac{1}{2\pi} \int_0^{2\pi} \int_0^R r \exp\left\{ -\frac{r^2}{2} \right\} d\theta dr, \\ &= 1 - \exp\left\{ -\frac{R^2}{2} \right\}. \end{aligned} \quad (\text{C.4})$$

Therefore, we solve the simple function equation and we get

$$R = \sqrt{-2\ln(s)}, \quad (\text{C.5})$$

where $s = 1 - U_1$, Finally, the bivariate distribution function is sampled as,

$$\begin{aligned}x &= x_0 + \frac{1}{a}\sqrt{-2\ln(s)}\cos(\theta), \\y &= y_0 + \frac{1}{b}\sqrt{-2\ln(s)}\cos(\theta).\end{aligned}\tag{C.6}$$

Thus, we can generate exactly the quantum initial state in phase space from random points that are uniformly distributed, and by adjusting the factors a, b in the Gaussian function according to the midpoints distribution.

Bibliography

- [Ae84] M. Abramowitz and I. A. Stegun (eds.). *Pocketbook of Mathematical Functions*. Harri Deutsch, Thun, 1984.
- [Ank07] J. Ankerhold. Quantum tunneling in complex systems: The semiclassical approach. 2007.
- [BdAK⁺01] M. Baranger, M. A. M. de Aguiar, F. Keck, H. J. Korsch, and B. Schellhaass. Semiclassical approximations in phase space with coherent states. *J. Phys. A: Math. Gen.*, **34**:7227, 2001.
- [Ber19] M. V. Berry. Quantum scars of classical closed orbits in phase space. *Proc. R. Soc. A*, **423**, (1989), 219.
- [Ber37] M. V. Berry. Semi-classical mechanics in phase space: a study of Wigner's function. *Phil. Trans. R. Soc. A.*, **287**, (1977), 237.
- [Ber01] M. V. Berry. Chaos and the semiclassical limit of quantum mechanics (is the moon there when somebody looks?). *Scientific perspectives on divine action, Vatican Observatory CTNS publications*, **39**, (2001).
- [BHW01] B. Li B. Hu, Q. Jie and S. Wang. General initial value form of the semiclassical propagator. *Phys. Rev. A.*, **63**:044102, 2001.
- [BL98] M. Boiron and M. Lombardi. *J. Chem. Phys.*, 108:3431, 1998.
- [CB94] G. Campolieti and P. Brumer. Semiclassical propagation: Phase indices and the initial-value formalism. *Phys. Rev. A*, **50**:997, 1994.
- [CJ01] E. Ziemniak C. Jung. *Chaos. Number 38 in Applied Mathematical Sciences. Springer, New York, 2nd edition*, **11**, (2001).
- [CZC05] D. Fairlie C. Zachos and T. Curtright. Quantum mechanics in phase space. *World Scientific, Singapore*, (2005).
- [DASR74] W. H. Oskay D. A. Steck and M. G. Raizen. Observation of Chaos-Assisted tunneling between islands of stability. *Science*, **293**, (2001), 274.

- [DASR01] W. H. Oskay D. A. Steck and M. G. Raizen. *Science*, 293:274, 2001.
- [dAVG09] M. A. M. de Aguiar, S. A. Vitiello, and A. Grigolo. *arXiv:0908.1875v1 [quant-ph]*, 2009.
- [DCKB93] S. V. Lawande D. C. Khandekar and K. V. Bhagwat. *Path-integral methods and their applications*. World Scientific, New York, 1993.
- [Det. all00] C. Dembowski and *et. all.* *Phys. Rev. Lett*, 84:867, 2000.
- [Eft33] A. Eftekharzadeh. The classical and commutative limits of noncommutative quantum mechanics: A superstar Wigner-Moyal equation. *Braz. J. Phys.*, **35**, (2005), 333.
- [EJH48] R. C. Brown E. J. Heller. Errors in the Wigner approach to quantum dynamics. *J. Chem. Phys.*, **75**, (1981), 1048.
- [Fai81] D. B. Fairlie. The formulation of quantum mechanics in terms of phase space functions. *Proc. Camb. Phil. Soc.*, **60**, (1964), 581.
- [GC06] Y. Guang-Can. Semiclassical propagator and van vleck determinant in a mixed position-momentum space. *Chin. Phys.*, **15**:919, 2006.
- [GJ94] F. Grossmann and A. L. Xavier Jr. From coherent state path integrals to a semiclassical initial value representation of the quantum mechanical propagator. *J. Chem. Phys*, **100**:4377, 1994.
- [Gla66] Roy J. Glauber. Coherent and incoherent states of the radiation field. *Phys. Rev.*, **131**, (1963), 2766.
- [Gro05] H.J. Groenewold. On the principles of elementary quantum mechanics. *Physica*, **12**, (1946), 405.
- [Gro99] F. Grossmann. A hierarchy of semiclassical approximations based on Gaussian wavepackets. *Comments At. Mol. Phys.*, **34**:141, 1999.
- [Gro26] F. Grossmann. Long-time and unitary properties of semiclassical initial value representations. *J. Chem. Phys.*, **120**, (2004), 26.
- [Gut43] M. C. Gutzwiller. Periodic orbits and classical quantization conditions. *J. Math. Phys.*, **12**, (1970), 343.
- [Gut91] M. C. Gutzwiller. Energy spectrum according to classical mechanics. *J. Math. Phys.*, **11**, (1970), 1791.
- [Hel89] E. J. Heller. Wigner phase space method: analysis for semiclassical applications. *J. Chem. Phys.*, **65**, (1976), 1289.

- [Hel23] E. J. Heller. Cellular dynamics: a new semiclassical approach to time-dependent quantum mechanics. *J. Chem. Phys.*, **94**, (1991), 2723.
- [Het. all01] W. K. Hensinger and *et. all.* *Nature*, 412:52, 2001.
- [HK84] M. F. Herman and E. Kluk. A semiclassical justification for the use of non-spreading wavepackets in dynamics calculations. *Chem. Phys.*, **91**:27, 1984.
- [HWL61] M. O. Scully H. W. Lee. The Wigner phase-space description of collision processes. *J. Found. Phys.*, **13**, (1983), 61.
- [JdA97] A. L. Xavier Jr. and M. A. M. de Aguiar. *Phys. Rev. Lett*, 79:3323, 1997.
- [JdA07] L-D. C. Jaubert and M. A. M. de Aguiar. *Phys. Scr*, 75:363, 2007.
- [JPD35] M. Springborg J. P. Dahl. The Morse oscillator in position space, momentum space, and phase space. *J. Chem. Phys.*, **88**, (1988), 4535.
- [JVLH32] M. I. Haftel J. V. Lill and G. H. Herling. Semiclassical limits in quantum-transport theory. *Phys. Rev. A*, **39**, (1989), 5832.
- [Kan13] Y. Kano. A new phase-space distribution function in the statistical theory of the electromagnetic field. *J. Math. Phys.*, **6**, (1965), 1913.
- [Kap98] L. Kaplan. Semiclassical Dynamical Localization and the Multiplicative Semiclassical Propagator. *Phys. Rev. Lett.*, **81**:3371, 1998.
- [Kay94a] K. Kay. Integrals expressions for the semiclassical time-dependent propagator. *J. Chem. Phys.*, **100**:4377, 1994.
- [Kay94b] K. Kay. Numerical study of semiclassical initial value methods for dynamics. *J. Chem. Phys.*, **100**:4432, 1994.
- [Kay05] K. Kay. Semiclassical initial value treatments of atoms and molecules. *Annu. Rev. Phys. Chem.*, **56**:255, 2005.
- [Ken96] A. Kenfack. Negativity of the Wigner function as an indicator of non-classicality. *J. Opt. B: Quantum Semiclass. Opt.*, **6**, (2004), 1396.
- [Lee47] Hai-Woong Lee. Theory and application of the quantum phase-space distribution functions. *Phys. Rep.*, **259**, (1995), 147.
- [Lee95] H. Lee. Wigner trajectories of a Gaussian wave packet perturbed by a weak potential. *J. Found. Phys.*, **22**, (1992), 995.
- [Lib30] R. L. Libof. Quantum billiard chaos. *Phys. Lett. A.*, **269**, (2000), 230.
- [Lit 7] R. G. Littlejohn. The van Vleck formula, Maslov theory, and phase space geometry. *J. Stat. Phys.*, **68**, (1992), 7.

- [LL92] A. J. Lichtenberg and M. A. Lieberman. Regular and chaotic dynamics. *Number 38 in Applied Mathematical Sciences. Springer, New York, 2nd edition*, **12**, (1992).
- [LM07] J. Liu and W. H. Miller. *J. Chem. Phys.*, 126:234110, 2007.
- [LR87] R. G. Littlejohn and J. M. Robbins. New way to compute Maslov indices. *Phys. Rev. A*, **36**:2953, 1987.
- [LS82] H. W. Lee and M. O. Scully. Wigner phase space description of a Morse oscillator. *J. Chem. Phys.*, 77, 1982.
- [Mas72] V. P. Maslov. Théorie des perturbations et méthodes asymptotiques. *Dunod, Paris*, (1972).
- [Mas81] V. P. Maslov. Semiclassical approximation in quantum mechanics. *Reidel, Boston*, (1981).
- [MH21] M. O. Scully E. P. Wigner M. Hillery, R. F. O’Connell. Distribution functions in physics: Fundamentals. *Phys. Rep.*, **106**, (1984), 121.
- [MH17] W. P. Schleich M Hug, C. Menke. How to calculate the Wigner function from phase space. *J. Phys. A: Math. Gen.*, **31**, (1988), L217.
- [Mor57] P. M. Morse. Diatomic molecules according to the wave mechanics II. Vibrational levels. *Phys. Rev.*, **34**, (1929), 57.
- [Moy99] J. E. Moyal. Quantum mechanics as a statistical theory. *Proc. Cambridge Phil. Soc.*, **45**, (1949), 99.
- [MS96] M. S. Marinov and B. Segev. *Phys. Rev. A*, 54:4762, 1996.
- [MS97a] M. S. Marinov and B. Segev. *Found. Phys*, 27:113, 1997.
- [MS97b] M. S. Marinov and B. Segev. *Phys. Rev. A*, 55:3580, 1997.
- [Nov05] M. Novaes. *J. Math. Phys*, 46:102102, 2005.
- [PC45] F. Zachariasen P. Carruthers. Quantum collision theory with phase-space distributions. *Rev. Mod. Phys.*, **55**, (1983), 245.
- [PS $et. al.$ 01] H. Lignier P. Szriftgiser and *et. al.* Experimental study of quantum chaos with cold atoms. *Communications in Nonlinear Science and Numerical Simulation*, **8**, (2003), 301.
- [Raz19] M. Razavy. Wigner trajectories in quantum tunneling. *Phys. Lett. A.*, **212**, (1996), 119.
- [Raz03] M. Razavy. Quantum theory of tunneling. *World Scientific*, 2003.

- [RdAB04] A. D. Ribeiro, M. A. M. de Aguiar, and M. Baranger. *Phys. Rev. E*, 69:066204, 2004.
- [RFO21] E. P. Wigner R. F. O’Connell. Some properties of a non-negative quantum-mechanical distribution function. *Phys. Lett. A.*, **85**, (1981), 121.
- [RFO45] E. P. Wigner R. F. O’Connell. Quantum-mechanical distribution functions: Conditions for uniqueness. *Phys. Lett. A.*, **83**, (1981), 145.
- [RPF65] A. R. Hibbs R. P. Feynman. Quantum mechanics and path integrals. *New York: McGraw-Hill*, (1965).
- [San05] L. Sandoval. Propagador semiclásico de la función de Wigner. *Master’s thesis, Universidad Nacional de Colombia*, (2005).
- [Sch81a] L. S. Schulman. Techniques and applications of path integration. *John Wiley and Sons*, (1981).
- [Sch81b] L. S. Schulman. *Techniques and Applications of Path Integration*. Wiley, New York, 1981.
- [Sch96] F. E. Schroeck. Quantum optics on phase space. *Kluwer Academic Publishers, Boston, London*, (1996).
- [Sch01] W. P. Schleich. Quantum optics in phase space. *WILEY-VCH Verlag, Berlin*, (2001).
- [SEC04] Francisco Soto-Eguibar and Pierre Claverie. Time evolution of the Wigner function. *J. Math. Phys.*, **24**, (1983), 1104.
- [SLS78] K. Möhring S. Levit and U. Smilansky. Focal points and the phase of the semiclassical propagator. *Ann. Phys.*, **114**:223, 1978.
- [Sta09] J. Stanek. Wigner function for the radial equation of the Coulomb problem in Langer space. *J. Phys. A: Math. Gen.*, **39**, (2006), 209.
- [Sud77] E. C. G. Sudarshan. Equivalence of semiclassical and quantum mechanical descriptions of statistical light beams. *Phys. Rev. Let.*, **10**, (1963), 277.
- [TAO79] F. H. Molzahn T. A. Osborn. Moyal quantum mechanics: The semiclassical Heisenberg dynamics. *Annals Phys.*, **241**, (1995), 79.
- [TDS03] C. Viviescas T. Dittrich and L. Sandoval. Semiclassical propagator of the Wigner function. *Phys. Rev. Let.*, **96**, (2006), 070403.
- [Tra11] C. Trahan. A new method for wave packet dynamics: Derivative propagation along quantum trajectories. *J. Chem. Phys.*, **118**, (2003), 9911.

- [TW04] M. Thoss and H. Wang. Semiclassical description of molecular dynamics based on Initial-Value Representation methods. *Ann. Rev. Phys. Chem.*, **55**:299, 2004.
- [VH02] T. V. Voorhis and E. J. Heller. *Phys. Rev. Lett*, 66:050501, 2002.
- [Viv00] C. Viviescas. Propagador de la función de Wigner. *Master's thesis, Universidad Nacional de Colombia*, (2000).
- [Vle78] J. H. Van Vleck. The correspondence principle in the statistical interpretation of quantum mechanics. *Proc. Nat. Acad. Sci. U.S.A.*, **14**, (1928), 178.
- [VM07] C. Venkataraman and W. H. Miller. Chemical reaction rates using the semiclassical van vleck initial value representation. *J. Chem. Phys.*, **126**:094104, 2007.
- [VS04] O. Vallée and M. Soares. *Airy Functions and Applications to Physics*. Imperial College Press, London, 2004.
- [Wey27] H. Weyl. Gruppentheorie und Quantenmechanik. *Z. Phys.*, **46**, (1927).
- [Wey31] H. Weyl. The theory of groups and quantum mechanics. *Dover, New York*, (1931).
- [Wig49] E. P. Wigner. On the quantum correction for thermodynamic equilibrium. *Phys. Rev.*, **40**, (1932), 749.
- [WKH*et. al.*52] H. Häffner W. K. Hensinger and *et. al.* Dynamical tunnelling of ultracold atoms. *Nature*, **412**, (2001), 52.
- [ZP05] D. H. Zhang and E. Pollak. *Phys. Rev. Lett*, 93:140401, 2005.